Investigation of Fiber Optic Sensor based on Surface Plasmon Resonance for Sensing Applications

A Thesis

submitted in fulfillment of the requirements for the award of the degree of

DOCTOR OF PHILOSOPHY

in

Electronics and Communication Engineering

By

Sarbjit Singh

(Reg. No: 901506002)

Supervised by

Dr. R. S. Kaler
Sr. Professor (ECED)

Dr. Siddharth Sharma
Associate Professor (BTD)

Department of Electronics and Communication Engineering,

Thapar Institute of Engineering & Technology,

(Deemed to be University), Patiala-147004, India

01st July, 2020

Under the inspiration of Almighty GOD, the present thesis is dedicated to my Parents

Certificate

I, **Sarbjit Singh** hereby certify that the work, which is being presented in this thesis, entitled **Investigation of Fiber Optic Sensor based on Surface Plasmon Resonance for Sensing Applications** submitted to **Thapar Institute of Engineering and Technology, Patiala**, in partial fulfillment of the requirement for the award of the degree of **Doctor of Philosophy** in the **Electronics and Communication Engineering,** is an authentic record of my own research work carried out during the period July, 2015-May, 2019, under the supervision of **Dr. R.S. Kaler** and **Dr. Siddharth Sharma**.

The research work presented in this thesis has not been submitted elsewhere for the award of any other degree or diploma of any other institute or university.

Date: 01st July, 2020

Sarbjit Singh

This is to certify that above statement made by the candidate is correct to the best of our knowledge.

Dr. R.S. Kaler
Senior Professor (ECE)

Dr. Siddharth Sharma
Associate Professor (BTD)

Abstract

Surface plasmon resonance together with optical fiber technology has emerged as an encouraging application of optical bio-sensing in the present circumstances. It has made a significant contribution to certain measures in medical diagnosis. This technique permits the instant and extremely sensitive recognition of biological samples, with utilizations in medical diagnostics, ecological monitoring, and agriculture science etc. Surface plasmon resonance is most sought after technique with wide spread uses in the recognition of molecular biology interactions but certain modifications are necessary for both refractive index (RI) sensitivity and in-vivo uses for many scientific applications.

Sensors manufactured using optical fiber offer significant advantages over traditional platforms, such as simple manufacturing process, small size and possibility for in situ and remote measurements. In present scenario, surface plasmon resonance technology has been incorporated into optical fiber for sensing applications. SPR technology is basically an optical phenomenon and involves the coating of metallic nanostructure materials of SPR nobel metals e.g. gold, silver, copper etc on optical fiber core. SPR has turn out as most important optical bio-sensing technique in the field of bio-chemistry and medicine science. The research presented in this thesis focuses on the optical fiber sensor based on surface plasmon resonance (SPR) technique for sensing applications. Metallic nanostructure material, when embedded on the core of fiber may be designed to support plasmonic resonance phenomenon and is usually perceptive to the sensing sample refractive index (RI). In the sensing region, various types of analyte such as glucose etc are used to test the sensing performance of the sensor. In case of angular interrogation and wavelength interrogation type of sensor, the identification of distinct refractive index (RI) may be accomplished by measuring resonant dip angle shift θ_{RDA} and resonant wavelength shift λ_{reson} of spectral intensity from TM-reflectance curve. Factors contributing to the analyte refractive index (RI) sensitivity are investigated methodically through modeling, simulating process and

theoretical explanation. The refractive index (RI) sensitivity of optical sensing system may be customized through designing a applicable metallic structure with optimized parameters. This thesis highlights the basic theory and concepts of SPR technology. Fiber optic sensor with multilayer structure based on two-dimensional (2D) material and SPR nobel metal *Au* is proposed for achieving high sensitivity for glucose (i.e. sensing analyte) sensing. Multilayer stack consists of stack of four layers i.e. fiber core-*Au* metal-2D material graphene-sample layer. We have shown the use of a new type of 2D material, graphene in the sensing region for glucose sensing. 2D materials are the material consisting of single layer of atoms. It is worthwhile to mention here that optoelectronics using 2D material is interested subject of research in the present scenario. Therefore such types of material show extreme behaviour with properties which are observable at nanoscale dimensions but not observable at bulkscale (macro-scale).

Different properties of active metals have also been studied and investigated in order to search the best suitable combination of noble metal, thickness and 2D material. The parameters related with plasma wavelength λ_{plasma} and collision wavelength $\lambda_{collision}$ are carefully studied and chosen. The well known Drude-Lorentz model has been considered for dielectric constant of SPR active metals and oxides metals. The effect of dielectric constant ε_{metal} on the resonant shift has been examined as the plasmonic resonance phenomenon is exhibited by the active metal with negative real dielectric constant. The aforesaid design is simulated with multiple iterations in order get better shift of reflectance curve in response with the refractive index of glucose. It is analysed that the proposed sensor design of SPR sensor utilizing 2D material, *Au* film and graphene film exhibit extreme sensitivity, $S_n \approx 198°/RIU$.

Several parameters related with metal diffraction grating based SPR sensors are explored. It is analysed from the study of wave polarization techniques such as TM-polarization and TE-polarization that metallic gratings are highly sensitive to the incident electromagnetic (EM) wave polarization and only TM-polarization is

associated with the excitation of surface plasmon politrons (SPPs). Using metal grating in the structure explore the advantage that the momentum component of the diffracted wave in parallel to the interface and the propagation constant of surface plasmons (SPs) are matched. The impact of sensor system parameters such as operating wavelength, the grating period *T*, type of nobel metal, and the RI of sensing sample n_{sense} on the refractive index (RI) sensitivity are systematically studied. In accordance with the above observation, bimetallic diffraction grating (*Au & Al*) based SPR sensor is reported. By carrying out the simulation analysis, the resonant impact of bimetallic diffraction grating on the sensing enhancement is observed. The incident optical wave at metal grating is partly returned back and partly divided into sequences of diffracted waves or diffraction orders. It is observed that for the proposed geometry of the sensor, enhanced sensitivity is attained if -1^{st} diffraction order of metallic grating is used to excite the surface plasmon waves (SPW).

Active metal nanoparticles (NPs) have several benefits in a plethora of sensing applications. Gold nanorods (AuNRs) are sensitive to both refractive index (RI) change & nanorods (NRs) shape and their size. Circular AuNPs distinctively exhibit a unique intense absorption belt which does not exist in spectrum of the bulk scale gold. This intense absorption belt appears when the frequency of applied light photon is resonant with the combined oscillation of a free electron of nanoparticles (NPs). Consequently, the absorbance & peak wavelength of the NPs are perceptive to refractive index (RI) of the surrounding sample.

Based on the study, the SPR sensor based on nanoparticle employing *Au* NR array is reported and its performance is observed with the help FEM simulation technique. It is analysed from the simulation results that the resonant wavelength λ_{reso} rises with rise in RI of the anlayte. The value of *R-square,* co-efficient of determination was calculated as 98.78 % & it is extremely high. Further results conclude that when the radius of circular AuNR is 60*nm* then the enhanced sensitivity, $S_{AuNR} \approx 2200$*nm/RIU*

is presented by proposed geometry of the sensor for analyte recognition. Enhanced sensitivity and high *R-square,* co-efficient of determination (COD) are attained after geometric optimization.

These sensors offer numerous advantages in bio-medical science, food processing, chemical species recognition & agriculture science. The study suggests that fiber optic sensor with SPR technology is beneficial for creating perfect sensing design. The research outcomes of the thesis have been published in various Science Citation Index (SCI) international referred journals as per publications list in the next section.

Publication Lists

The following publications have been derived from the work contributed in this thesis:

Manuscripts Published in SCI Journal

1. Sarbjit Singh, R.S. Kaler, Siddharth Sharma, "A Novel Two-Dimensional Material Based Optical Fiber Surface Plasmon Resonance Sensor for Sensing of Organic Compounds in Infrared Spectrum Window," ***Journal of Communication Technology and Electronics***, vol. 63, Issue 11, pp. 1269-1275, 2018. **SCI IF: 0.51**
2. Sarbjit Singh, R.S. Kaler, Siddharth Sharma, "Resonance Effect of Bimetallic Diffraction Grating on the Sensing Characteristics of Surface Plasmon Resonance Sensor with COMSOL Multiphysics," ***Journal of Nanoelectronics and Optoelectronics,*** Volume 14, Number 5, pp. 669–674, 2019. **SCI IF: 1.069.**
3. Sarbjit Singh, R.S. Kaler, Siddharth Sharma, "FEM simulation analysis of fiber optic surface plasmon resonance sensor based on array of circular gold nanorod," ***Optik - International Journal for Light and Electron Optics***, Volume 183, pp. 508-512, 2019. **SCI IF: 1.914.**

Acknowledgement

First of all, I am obliged to the Almighty **Dhan Dhan Shri Guru Granth Sahib Ji** and I bow before Him for his myriad blessings and granting me the spirit and courage to accomplish the PhD research work.

Most importantly, my special thanks to our Hon'ble Director Dr. Prakash Gopalan and Dr. Rafat Siddique, Dean (RSP) for providing me such a golden opportunity to undertake PhD. I would like to express my sincere, deep and truthful gratitude to my PhD Supervisors, **Dr. R.S. Kaler**, Senior Professor, ECED and **Dr. Siddharth Sharma**, Associate Professor, BTD, TIET, Patiala. Once again, I am thankful to both my supervising souls for their invaluable guidance and encouragement.

I am also thankful to the doctoral committee members, Dr. Alpana Agarwal (Head of the Department), Dr. Hardeep Singh (Associate Professor, ECED), Dr. Amit Mishra (Assistant Professor, ECED), Dr. Neeraj Kumar (Associate Professor, CSED) for their consistent help and support.

Finally, I would like to express my deep and truthful gratitude towards my parents **Sardar Gurmukh Singh** and **Sardardni Gurbachan Kaur** for their love, attachment, and sacrifices in every step of my life. Finally large thanks to my wife **Sarabjeet Kaur**, my brother **Harpreet Singh**, my sister **Manpreet Kaur** for having faith in me and supporting me at each and every step. Without their support, I would not have completed my PhD research work. Finally, lots of love to my little daughter **Gursimran Kaur**.

TIET, Patiala **Sarbjit Singh,**

India.

Table of Contents

Title **Page No.**

Abstract.....ii

Publications Lists…….....vi

Acknowledgement……..……..…….....vii

Table of Contents.....viii

List of Figures xi

List of Tables.....xiv

Symbols and Abbreviations Lists.....xv

Chapter 1 Introduction 1

1.1 Introduction 1

1.2 Fiber Optic Sensors 2

1.2.1 Intensity Modulated Fiber Optic Sensors 4

1.2.2 Frequency modulated Fiber Optic Sensors 5

1.2.3 Phase Modulated Fiber Optic Sensors 6

1.2.4 Polarization modulated Fiber Optics Sensors 6

1.3 Plasmons and Surface Plasmons 7

1.3.1 Significance of Maxwell Equations 8

1.3.2 SPR Nobel Metal for Plasmon Excitation 9

1.3.3 *p*-polarization and *s*-polarization 10

1.3.3.1 TM-wave or *p*-Polarization 10

1.3.3.2 TE-wave or *s*-Polarization 13

1.4 Surface Plasmon Resonance 13

1.4.1 Otto Configuration 15

1.4.2 Kretschmann Configuration 17

1.4.3 Fundamental Concept of SPR and Sensor Characteristics 18

1.4.3.1 Fundamental Concept of SPR 18

1.4.3.2 Sensor Characteristics 18

Chapter 2	**Literature Survey**	21
2.1	Introduction	21
2.2	Multilayer with Gold-Graphene Layer Combination based SPR Sensor	22
2.3	Resonant Impact of Metal Diffraction Grating Design on Sensing Performance	28
2.4	Circular Gold Nanorod Design Based SPR Sensor	31
2.5	Gaps Identified in Present Study	36
2.6	Problem Formulation	37
2.7	Research Objectives	39
2.8	Research Methodology	39
2.9	Major Contribution of Thesis	40
3.0	Outline of Thesis	41
Chapter 3	**2D Material Based SPR Sensor**	43
3.1	Introduction	43
3.2	Theory	45
3.3	COMSOL 2-dimensional Modeling	47
3.4	Results and Discussions	48
3.5	Outcomes of the Proposed Sensor Design	57
Chapter 4	**Bimetallic Diffraction Grating Based SPR Sensor**	58
4.1	Introduction	58
4.2	Theoretical Explanation	60
4.3	Grating Results and Discussion	62
4.4	Outcomes of the Proposed Sensor Design	67
Chapter 5	**Optical Fiber Sensor Based on SPR utilizing Circular AuNR array**	68
5.1	Introduction	68

5.2 Circular AuNR Based SPR Sensor 70
5.3 Results and Discussions 72
5.4 Outcomes of the Proposed Sensor Design 78
Chapter 6 Conclusions, Recommendations and Scope for Future Research 79
6.1 Conclusions 79
6.2 Recommendations 80
6.3 Scope for Future Research 82
References 84
Publications Copies 100

List of Figures

Figure No.	Title	Page No.
1.1	Optical sensing system structure	2
1.2	Operation of extrinsic sensor	3
1.3	Operation of intrinsic sensor	3
1.4	Black body sensor	5
1.5	Exponential decay of SPW field intensity in active metal and dielectric medium.	14
1.6	Relationship between surface plasmon wave propagation constant and propagation constant of light signal in dielectric	15
1.7	Otto configuration schematic representation	16
1.8	Kretschmann configuration schematic representation	17
3.1	Sensor structure with 2D material (Graphene) and SPR active metal *Au*	46
3.2	Surface magnetic field distribution for different RI values of glucose (a) 1.3337 (b) 1.3447 (c) 1.3508 (d) 1.3603	52
3.3	Relationship between TM reflectance and angle of incident (*deg*) for various RI of Glucose for (a) *Au*-thin film of 60*nm* thickness and graphene-thin film of 10*nm* thickness (b) *Au*-thin film of 50*nm* thickness and graphene-thin film of 10*nm* thickness.	53
3.4	Relationship between the full-width half maximum (*deg*) and various RI of Glucose.	55
3.5	Relationship between the SPR resonant angle (*deg*) and various RI of glucose.	56

3.6 Sensitivity (*Deg/RIU*) variation with various RI values of glucose (a) *Au* thin film of 60*nm* thickness and graphene thin film of 10*nm* thickness (b) *Au* thin film of 50*nm* thickness and graphene thin film of 10*nm* thickness 57

4.1 General design of multiple metallic grating based SPR sensor 61

4.2 Metallic grating unit cell (a) Schematic (b) 3D layout (c) 2D ref. index Re(y). 61

4.3 Field distribution for glucose refractive indices (a) 1.3337 (b) 1.3447 (c) 1.3508 and (d) 1.3603 respectively 65

4.4 TM Reflectivity variation with angle of incidence for -1^{st} diffraction order with *Au=60nm* and *Al*=20*nm*. 65

4.5 Sensitivity variation with glucose refractive index for *Au=60nm* and *Al=20nm.* 66

4.6 TM Reflectivity variation with angle of incidence for -1^{st} diffraction order with *Au*=50*nm* and *Al*=10*nm.* 66

4.7 Sensitivity variation with glucose refractive index for *Au*=50*nm* and *Al*=10*nm*. 66

5.1 Schematic representation of circular AuNRs based SPR Sensor 71

5.2 (a) Normalized plot of surface electric field for AuNR (*radius=20nm*) (b) surface magnetic field for AuNRs (*radius=20nm and spacing=200nm*) (c) normalized plot for surface electric field for 2-AuNRs (*radius=20nm and spacing = 200nm*) 73

5.3 (a) Relationship between maximal surface magnetic field and AuNR radius at 1200*nm*, 1300*nm* (b) Relationship between minimal surface magnetic field and AuNR radius at 1200*nm*, 1300*nm* 74

5.4 Graph of electric field norm and arc length with AuNR (a) radius=20*nm* (b) radius=30*nm* (c) radius=50*nm* (d) Polar plot showing far-field pattern 76

5.5 (a) Relationship between Resistive Losses and Radius of AuNRs for E-field Strength, E_0=1$V.m^{-1}$ and E_0=2$V.m^{-1}$ (b) Relationship between Resonant Wavelength, λ_{reso} and Sensing Medium RI 77

List of Tables

Table No.	Title	Page No.
2.1	A brief of concluded results of various researchers/investigators in relation with multilayer surface plasmon resonance sensor	24
2.2	A brief of concluded results of various researchers/investigators in relation with metallic grating surface plasmon resonance sensor	30
2.3	A brief of concluded results of various researchers/investigators in relation with metallic NR sensor based on SPR technology	34
3.1	Plasma wavelength (λ_{plasma}) and collision wavelength ($\lambda_{collision}$) of SPR active metals and oxide metal	47
3.2	Resonant angle, θ_R (degree) and FWHM (degree) for various RI of sample glucose	54

Symbols and Abbreviations List

Measurement Units:

μm: micro-meter (10^{-6})

nm: nano-meter (10^{-9})

Universal Physical Constants:

c: Velocity of light in a vacuum ($3x10^{8} m.s^{-1}$)

e: Electronic charge

μ_0: Free space permeability

ε_0: Free space permittivity

m_e: Mass of electrons

Physical Symbols:

E: Electric field

H: Magnetic field

μ: Permeability

ε_d: Dielectric material dielectric constant

ε_{metal}: Metal Dielectric constant

ε_{prism}: Prism Dielectric constant

σ_g:Graphene electrical conductivity

k_g:Graphene thermal conductivity

ω: Frequency

k_0: Incident light wave vector

λ_0: Wavelength of incident light

n: refractive index

f_n: Natural frequency

λ_{plasma}: Plasma wavelength

$\lambda_{collision}$: Collision wavelength

τ_e: Avg. collision time of free electrons

f_{ilp} : Incident Light Photon Frequency

Chemical Symbols:

Au: Gold (ω dependent)

Ag: Silver (ω dependent)

Al: Aluminum (ω dependent)

Cu: Copper (ω dependent)

Pt: Platinum (ω dependent)

Pd: Palladium (ω dependent)

Abbreviations:

ATR: Attenuated Total Reflection

AuNRs: Gold Nanorods

AgNRs: Silver Nanorods

COD: Coefficient of Determination

2D: 2-dimensional

3D: 3-dimensional

EM: Electromagnetic

EMI: Electromagnetic Interference

EW: Evanescent Wave

FDTD: Finite-difference time-domain method

FEM: Finite-element method

FOS: Fiber Optic sensor

FO SPR: Fiber Optic Surface Plasmon Resonance

FM-FOS: Frequency Modulated fiber Optic Sensor

GPAI: Glass prism-air interface

GSPRS: Grating Based Surface Plasmon Resonance Sensor

GNRA: Gold Nanorod Array

IM-FOS: Intensity Modulated Fiber Optic Sensor

IR: Infrared

LSP: Localized surface plasmon

LSPR: Localized surface plasmon resonance

MDI: Metal-dielectric interface

MDM: Metal-dielectric-media

MMF: Multimode fiber

MNP: Metal Nanoparticle

NP: Nanoparticle

PCS: Plastic clad silica

PM-FOS: Phase Modulated Fiber Optic Sensor

PML: Perfect matched layers

POC: Point of Care

POLM-FOS: Polarization Modulated Fiber Optic Sensor

RI: Refractive index

RIU: Refractive index unit

SD: Standard Deviation

SMF: Single Mode Fiber

SNR: Signal to Noise ratio

SP: Surface plasmon

SPP: Surface plasmon polariton

SPR: Surface plasmon resonance

SWs: Surface Waves

SPW: Surface Pasmon Wave

SNR: Signal to Noise ratio

TE: Transverse electric

TEM: Tranverse electromagnetic

TIR: Total internal reflection

TM: Transverse magnetic

TMDC: Transition metal dichalogenide

WM-FOS: Wavelength modulated fiber optic sensor

Chapter 1
Introduction

1.1 Introduction

In the last three decades of optical technology, optical sensing instrumentation has made considerable advancements. With a view to attain enhanced performance, range of optical sensing platforms, data processing and detection methods have been developed [1]. The field of fiber optic sensing has shown a significant expansion of interest in the last few decades. Now a day the scientist and researchers in electronic industry have the constant requirements for optical devices which enable them to carry out accurate and reliable data measurements in distinct sensing environment [2]. A wide range of instrumentation and circuitry is available in industry and recently all these things have been replaced by development of FO sensing instrumentation which do offer unique advantages to make it excellent or indeed the only economical solution to few sensing requirements. However, in order to compete with well established sensing instrumentation on a huge scale, FO sensing devices must have the capability to show better response in terms of accuracy, convenience use, cost etc. In addition to this, such type of devices must present those additional advantages which make the retraining of engineer to adopt this innovative technology worthwhile.

The motivation behind carrying out the research in fiber optic sensing is that fiber optic sensing systems have significantly greater advantages over conventional sensing systems like faster response, low-cost fabrication, very light weight, highly sensitive and non-reactive to electromagnetic interference. Therefore, fiber optic sensing entices more interest of investigators and application engineers for their exclusive and vital characteristics. Sensors based on optical sensing are commonly used to perceive the physical and chemical properties like sensing of organic compounds such as glucose, sucrose, glycerol etc determination of pH, refractive index of liquid solution, micro-

bending, strains, vibrations, accelerations, temperatures, pressures, pipeline condition monitoring etc. These advantages make the optical sensing better than conventional sensing. In addition to these, optical sensors exhibit higher sensitivity and greater dynamic range. They are intrinsically free from RF field interference and present better isolation properties [2].

Aforesaid two reasons solely account for motivation behind extensive research in these sensing systems being realized by the some of the fiber sensing technology industries. They are safe to use in biologically and chemically hazardous areas-there being no currents flowing and no risk of spark [2]. Moreover there has been a tremendous effort towards the development of optical biosensors and biochips worldwide and recent advances have demonstrated that such devices hold tremendous potential for applications in numerous important areas including sensing of organic compounds, medical diagnostics, environmental toxins detection and food defense and security [3].

1.2 Fiber Optic Sensors

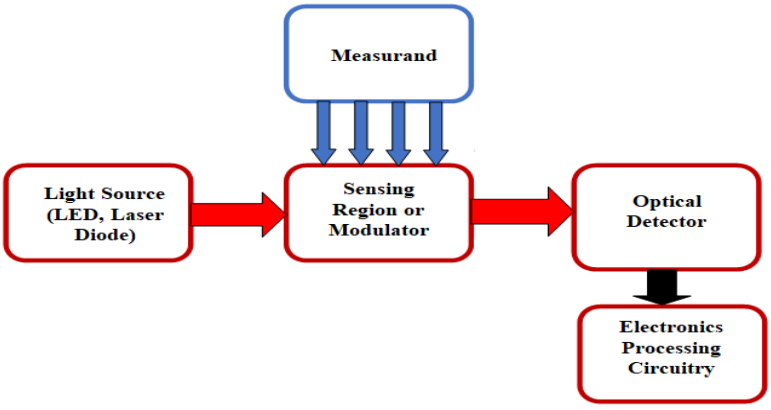

Figure 1.1: Optical Sensing System Structure

Figure 1.1 shows the block diagram for optical sensing system structure. LED or laser light source at the input side, is used to incident the light at a proper wavelength. Measurand is the quantity which we want to measure and it is applied to the sensing region or modulator. The response optical signal is detected at the optical detector and at the final stage the signal is processed using electronics processing circuitry. Fiber optic sensors may be categorized in three types: sensing position, principle of

operation, and usage in application. On the basis of sensing position, fiber optic sensor can be classified as extrinsic or intrinsic. The general schematic, representing the operation of extrinsic sensor is shown in Figure 1.2. In an extrinsic sensor as depicted by below Figure, the light passes through the fiber and the sensing process takes place in external optical device. While in intrinsic FOS, some physical properties of the fiber are changed. The general schematic representing the operation of intrinsic sensor is shown in Figure 1.3. Perturbations act upon the fiber and in response to it optical fiber alters certain light characteristic in fiber [4].

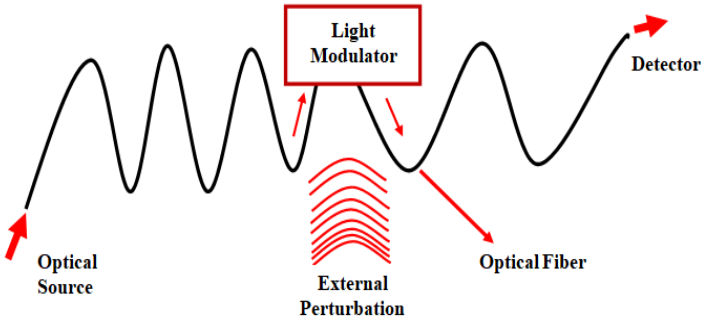

Figure 1.2: Operation of Extrinsic Sensor

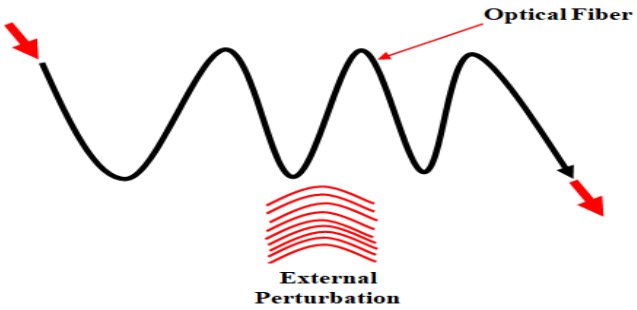

Figure 1.3: Operation of Intrinsic Sensor

From the application point of view, FOS may be categorized as below:

- Physical sensors: These sensors are used for the measurement of physical properties such as temperature, stress, etc.
- Chemical sensors: Used for pH measurement, gas analysis, spectroscopic studies, etc.

- Bio-medical sensors: Used in bio-medical applications like measurement of blood flow, glucose content etc.

According to the modulation-demodulation technique, several FO sensor categories are elucidated below:

- Intensity based Fiber Optic Sensor
- Frequency Modulated Fiber Optic Sensor
- Phase Modulated Fiber Optic Sensor
- Polarization Modulated Fiber Optic Sensor

Owing to outside perturbations, these parameters may be susceptible to change. Therefore, by identifying the parameter changes, the outside perturbations can be detected [4].

1.2.1 Intensity Modulated Fiber Optic Sensors (IM-FOS)

These type of fiber optic sensors are related with the intensity of the signal which has some attenuation. The IM-FOS employs multimode fibers (MMF) having large core diameter. These types of sensors also require more light [4]. There are several ways to induce the attenuation in the optical signal and once the signal is attenuated its intensity is being measured at the detector side. Microbending loss, signal attenuation, and evanescent fields are certain ways that results change in intensity of optical signal propagated in optical fiber. One simplest type of IM-FOS is microbend sensor, in which attenuation of the optical signal is achieved by certain mechanical periodic microbends. Guided mode energy is being spread in to radiation mode and light signal intensity gets reduced [6], resulting in intensity modulation. This sensor offers some useful benefits such as low cost, ease of implementation and multiplexing. But because of slight fluctuations in the intensity of optical wave may results in wrong reading, until and unless a reference optical system is used [5].

Evanescent wave sensor is another example of IM-FOS. It utilizes the light signal which escapes from fiber core and moves to fiber clad. Evanescent wave sensor is most popularly useful in chemical science for detecting chemicals. Detection is

achieved by the incidence of light source wavelength and resonance wavelength is being detected at the detector side. Due to this light intensity gets reduced and this change in light intensity results in the chemical concentration measurement [7].

1.2.2 Frequnecy Modulated Fiber Optic Sensors (FM-FOS)

FM-FOS utilizes changes in the light wavelength (i.e. frequency) for detection of species. Several types of FM-FOS are black body sensor, fluorescence FO sensors, and the Bragg grating FO sensor. Fluorescent FO sensors are useful in medical and chemical applications as well as in sensing other species such as temperature humidity and viscosity [8]. Another type of WM-FOS (wavelength modulated FOS) is the blackbody sensor. Figure 1.4 shows the general schematic of black body sensor.

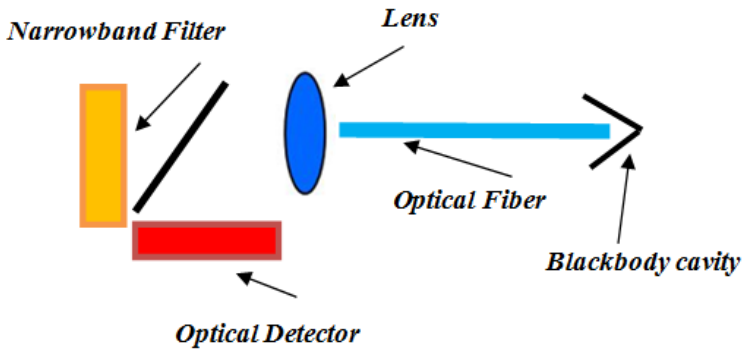

Figure 1.4: Black Body sensor

Blackbody cavity position is towards the end of optical fiber cable. Extremely high temperature of the cavity makes it to glow and it behaves as a light source. The arrangement of optical detectors with narrow band filters is used to estimate the profile of the blackbody curve. The commercial application of this type of sensor is to compute temperature to within a few degrees centigrade under powerful radio frequency fields [9]. Bragg grating sensor is another type of WM-FOS in which brag gratings in the fiber are created by making periodic modulation of RI inside the fiber core of SMF. A strong pattern of ultraviolet light energy is used to create refraction index periodic changes. These variations in RI so formed, are responsible for making of interference patterns which acts as grating. As per the equality condition of brag

wavelength and center wavelength, optical fiber is being fed with signal from laser source. The light signal propagates through the grating and portion of the signal is reflected back at bragg wavelength. The response of the sensor shows the bragg grating to be an useful optical filter [9].

1.2.3 Phase Modulated Fiber Optic Sensors (PM-FOS)

PM-FOS uses optical interferometers to measure the phase change of the light signal. There are several types of optical interferometers such as Mach-Zehnder, Michelson, Fabry-Perot, Sagnac, Polarimetric, and grating interferometers. The basic concept of using interferometers in sensors is that this device divides the light signal in two parts. Out of these two divided parts, one part of the optical signal is subjected to sensing environment where it undergoes a phase shift. The second part of the optical signal is considered as a reference signal and is isolated from the sensing environment. Once the light signals are added, they interfere with each other [10]. Michelson interferometers provide better performance in terms of sensitivity and it requires less number of optical components. Folded Mach–Zehnder interferometer is called as Michelson and vice versa. On the other hand, for the Michelson interferometer, reflection mirror needs to be of excellent quality [11].

1.2.4 Polarization Modulated Fiber Optic Sensors (POLM-FOS)

Polarization is defined as the direction of the electric field vector of field intensity. Many polarization states of light field exist such as linear polarization, elliptical polarization, and circular polarization. If the direction of the E-field vector follow the same path while light propagation then this type of polarization falls in linear type. On the other hand if during light propagation, the E-field vector direction changes then this polarization fall in elliptical polarization type and E-field vector makes an elliptical shape. Therefore, in POLM-FOS outside perturbation (i.e. analyte) may be measured by detecting alteration in output polarization position [11].

1.3 Plasmons and Surface Plasmons

The nobel metals have a negatively charged free electrons in an equally charged positive ion background arrangement. The collections of negatively charged free electrons and positive ions may be compared with the plasma of particles because it has extremely dense collections of charged particles with the conditions of quasi-neutrality. Because positive ions have infinitely large mass as compared to negative charged free electrons. So to fulfil the condition for quasi-neutrality, the free electrons can move from one point to another point in perpetually constant positive background. The free electrons in the metal are like electron gas having high density of about $10^{23} cm^{-3}$. As described in Jellium model [12], a positive constant background charge can replace these positive ions. Still, the overall charge density in the conductor stays at zero. Free electrons density is decreased locally, when outside electric field is applied to the conductor, as a result, electrons may start moving and the negatively charged free electrons start getting attracted towards the positive ion background. Hence, free electrons begin approaching the positive area and get accumulated in greater density than required for the local charge neutrality. So the coulomb repulsion produces movement in opposite direction as that of moving free electrons. The combined effect of these two forces i.e. repulsive restoring force & attractive driving force, results in oscillations among the free electrons. These longitudinal density fluctuations are called as plasma oscillations and these oscillations propagate through the entire volume of the metal. The frequency of plasma oscillations, ω_{plasma} is expressed as given below [13],

$$\omega_{plasma} = \sqrt{\frac{4\pi n e^2}{m_0}} \qquad (1.1)$$

In the above equation, *n* represents density of free electrons, *e* represents the charge on electrons and m_0 represents the mass of electrons. The coherent oscillations of free electrons or propagation of electron density waves on metal-dielectric interface are called as Surface Plasmon, also a SP wave or a SP mode. Surface plasmons are

accompanied by longitudinal (TM-polarized) electric field. The longitudinal electric field decays exponentially in metal as well as in dielectric media. Due to this exponentially decays of field intensity, the field has its maximum at metal-dielectric interface itself. So being TM- polarized and exponential decay of electric field are the two crucial properties of surface plasmon for TM excitation.

1.3.1 Significance of Maxwell Equations

Surface plasmon polaritons are propagating excitations that exist when optical energy couples with combined oscillations of electrons at the interface between metal and dielectric [14]. Plasmon politrons are grouped longitudinal charge oscillations which are created by an external excitation and can be described by the Bose-Einstein data [15]. The metal interaction with electromagnetic field can be illustrated by adopting Maxwell's Equations. The Maxwell's equations concerning the material are [16]:

$$\vec{\nabla} \times \vec{E} = -\frac{\partial \vec{B}}{\partial t}, \quad (1.2)$$

$$\vec{\nabla} \times \vec{H} = -\vec{J} + \frac{\partial \vec{D}}{\partial t}, \quad (1.3)$$

$$\vec{\nabla} \cdot \vec{D} = -\rho_{ext}, \quad (1.4)$$

$$\vec{\nabla} \cdot \vec{B} = 0 \quad (1.5)$$

where ρ_{ext} is the external charge density and $\vec{J}$ is the external current density. The constitutive relations for linear, isotropic and nonmagnetic media are given as [17]:

$$\vec{D} = \varepsilon_0 \varepsilon_d \vec{E} \quad (1.6)$$

$$\vec{B} = \mu_0 \mu_r \vec{H} \quad (1.7)$$

Maxwell's Equations can be modified for nonmagnetic isotropic media and under the conditions that (ρ_{ext} = 0, $\vec{J}$ = 0). Therefore under the assumptions that there are no free charges $\nabla \cdot E = 0$, no currents $\nabla \cdot B = 0$, and for non-magnetic media, $\mu = 1$, we obtained the generalized wave equation as given below [16]:

$$\mu_0 \frac{\partial^2 \vec{D}}{\partial t^2} = \nabla^2 \vec{E} \qquad (1.8)$$

where ε_0 and μ_0 are the electric permittivity and the magnetic permeability of vacuum, ε_d is the dielectric function of the medium and μ_r is relative permeability. In this case Maxwell's equations reduce to vector wave equations and the solutions will be propagating waves as given in above equations. The wave equation can be solved only if we know the exact relation existing between the displacement vector **D** and the electric field **E**, that is if we know the behavior with frequency of the dielectric function of the material.

1.3.2 SPR Nobel Metal for Plasmon excitations

Metals with negative real and less positive imaginary dielectric constant have shown their capability of supporting plasmonic phenomenon. Gold, silver, aluminum, copper are most widely used SPR nobel metals. The Drude model [18] assumes that the free electrons can interact. In other words, we can say that Drude model considers that electrons in a metal are essentially free and can be forced to oscillate when an electromagnetic wave of frequency ω is incident upon them. Electrons-ions interactions are considered presenting an effective e^- mass, m_e. Electrons and external electric field interactions are depicted by the equation [18]:

$$m_e \ddot{e_d} + m_e \gamma_{collision} \dot{e_d} = -eE_0 e^{-j\omega t} \qquad (1.9)$$

where e_d is the electrons displacement and $\gamma_{collision}$ is the electrons collision frequency. In this equation, Collision frequency, $\gamma_{collision} \propto \frac{v_f}{l_m}$, where v_f is the Fermi velocity and l_m mean free length.

Equation (1.9) can modified and rewritten by using $e_d = e_{d0} e^{-j\omega t}$ and obtained dielectric function is expressed as [18]:

$$\varepsilon_d(\omega) = 1 - \frac{\omega_{plasma}^2}{\omega^2 + j\gamma_{collision}\omega} \qquad (1.10)$$

The parameter $\omega_{plasma} = \frac{ne^2}{\varepsilon_0 m}$ is the plasma frequency, *n* is the number of free electrons and $\gamma_{collision}$ is the collision frequency. This frequency is inversely proportional to the conductivity of the metal as given by the expression, $\gamma_{collision} = \frac{ne}{m_e \sigma}$. For the condition, $\frac{\omega}{\gamma_{collision}} \gg 1$, the dielectric function has the modified form [18]:

$$\boldsymbol{\varepsilon_d(\omega) = 1 - \frac{\omega_{plasma}^2}{\omega^2}} \qquad (\mathbf{1.11})$$

Metal dielectric constant turns to be negative and has complex number RI under the condition $\omega < \omega_{plasma}$ and field travels up to some depth. Metal dielectric constant turns to be positive number and has a real number RI under the condition $\omega > \omega_{plasma}$ and metal has dielectric characteristics. Plasma frequency, ω_{plasma} and collision frequency, $\gamma_{collision}$ for the most common SPR metals used in the sensor design are adopted from ref [19].

1.3.3 *p*-polarization and *s*-polarization

Electromagnetic fields must satisfy the Maxwell's equations and the boundary conditions. It is essential to consider two distinct possible states of polarization of the electromagnetic wave i.e. transverse magnetic wave and transverse electric wave. In transverse magnetic wave (TM-wave), magnetic-field is perpendicular to the plane of incidence. On the other hand in transverse electric wave (TE-wave), the electric-field is perpendicular to the plane of incidence. SPR excitation is possible only with p-polarization or TM-wave.

1.3.3.1 TM-wave or *p*-Polarization

Because we are looking for field of traveling electromagnetic waves, a suitable procedure to represent the two fields in two different medium is as expressed as below [20]:

$$\boldsymbol{E_i = \left(E_{x,i}, 0, E_{z,i}\right). e^{j\left(k_{x,i}\, x + k_{z,i}\, z\right) - j\omega t}} \qquad (\mathbf{1.12})$$

$$\boldsymbol{H_i = \left(0, H_{y,i}, 0\right). e^{j\left(k_{x,i} x + k_{z,i} z\right) - j\omega t}} \qquad (\mathbf{1.13})$$

In the above equation i = 1, 2.The relation of wave vector components results from the Maxwell's electromagnetic theory and boundary conditions may be written as below [20],

$$\boldsymbol{k_x^2 + k_{z,i}^2 = \varepsilon_i k_0^2} \qquad (\mathbf{1.14})$$

$$\boldsymbol{k_{x,1} = k_{x,2} = k_x = \beta} \qquad (\mathbf{1.15})$$

In the above equation k_0 represents the wave vector and β represents the propagation constant. Making use of Maxwell's Equation (1.2) and (1.4), we have the modified expression as given below,

$$\boldsymbol{j k_{z,i} H_{y,i} = \omega D_{x,i} = \omega \varepsilon_0 \varepsilon_i E_{x,i}} \qquad (\mathbf{1.16})$$

According to boundary conditions, E and H components be parallel to interface while D component be transverse to the interface. For continuity condition i.e. $E_{x,1} = E_{x,2}$, $H_{y,1} = H_{y,2}$ *and* $D_{z,1} = D_{z,2}$. The combination of Equation (1.16) with boundary conditions, as defined above results in the equation as expressed below [20]

$$\boldsymbol{\frac{k_{z,2}}{\varepsilon_2} - \frac{k_{z,1}}{\varepsilon_1} = 0} \qquad (\mathbf{1.17})$$

By making use of Equation (1.14), dispersion relation of the surface plasmon wave is attained and is expressed as given below [20],

$$\boldsymbol{\beta = \frac{\omega}{c}\sqrt{\frac{\varepsilon_1 \varepsilon_2}{\varepsilon_1 + \varepsilon_2}} = \beta' + j\beta''} \qquad (\mathbf{1.18})$$

Here β represents the propagation constant. The relation given in Equation 1.18 is known as dispersion relation and is crucial to explain the propagating length of the SPs and the confining of EM-field in the two media. SPW is an exponentially decaying wave both in metal as well as in dielectric medium. The dielectric constant of metal ε_1 is a complex number, the propagation constant of the SPW, β will also be a complex number.

$$\boldsymbol{\beta}' = \frac{\boldsymbol{\omega}}{\boldsymbol{c}}\left(\frac{\boldsymbol{\varepsilon_1}'\boldsymbol{\varepsilon_2}}{\boldsymbol{\varepsilon_1}' + \boldsymbol{\varepsilon_2}}\right)^{\mathbf{1/2}} \tag{1.19}$$

$$\boldsymbol{\beta}'' = \frac{\boldsymbol{\omega}}{\boldsymbol{c}}\left(\frac{\boldsymbol{\varepsilon_1}'\boldsymbol{\varepsilon_2}}{\boldsymbol{\varepsilon_1}' + \boldsymbol{\varepsilon_2}}\right)^{\mathbf{1/2}} \frac{\boldsymbol{\varepsilon_1}''}{\mathbf{2}(\boldsymbol{\varepsilon_1}')^{\mathbf{2}}} \tag{1.20}$$

Here $\varepsilon_1 = \varepsilon_1' + i\varepsilon_1''$ represents dielectric constant of metal and ε_1' and ε_1'' representing the real and imaginary parts. In addition to this, β' and β'' represents the real and imaginary parts of the SPW propagation constant. The wave vector normal component is obtained by substitution Equation (1.18) in Equation (1.14), and is expressed as given below [20],

$$\boldsymbol{k_{i,z}} = \frac{\boldsymbol{\omega}}{\boldsymbol{c}}\sqrt{\frac{\boldsymbol{\varepsilon_i^2}}{\boldsymbol{\varepsilon_1} + \boldsymbol{\varepsilon_2}}} \tag{1.21}$$

Now in both medium, the wave vector normal component in Equation (1.21) needs to be purely imaginary, for examining the EM wave propagation along the interface. This will result in exponentially decaying solutions of the field [21]. It is clear to see that aforesaid condition is satisfied only if $\varepsilon_1 < 0$ and $\varepsilon_2 > 0$ or vice versa. It means that this is possible only if one of the two medium has a dielectric function in negative value. Both Equation (1.18) and Equation (1.21) relations are essential to explain the propagating length of the SPs and the confining of the EM fields in the two medium. The confinement of the electromagnetic field in two different medium is termed as skin depth. Basically skin depth is defined as the depth normal to the interface at which the evanescent wave field amplitude falls to the value 1/*e* [22] [13]. The skin depth into the dielectric, $\boldsymbol{L_{dielectric}}$ and metallic medium, $\boldsymbol{L_{metal}}$ are expressed as given below [22] [13],

$$\boldsymbol{L_{dielectric}} = \frac{\boldsymbol{\lambda}}{\mathbf{2}\boldsymbol{\pi}}\left(\frac{\boldsymbol{\varepsilon_{metal}} + \boldsymbol{\varepsilon_d}}{\boldsymbol{\varepsilon_d^2}}\right)^{\mathbf{0.5}} \tag{1.22}$$

$$\boldsymbol{L_{metal}} = \frac{\boldsymbol{\lambda}}{\mathbf{2}\boldsymbol{\pi}}\left(\frac{\boldsymbol{\varepsilon_{metal}} + \boldsymbol{\varepsilon_d}}{\boldsymbol{\varepsilon_{metal}^2}}\right)^{\mathbf{0.5}} \tag{1.23}$$

Moreover $L_{interface}$ can be termed as the propagation length along the interface, after which the intensity falls to the value l/e and is expressed as given below [13],

$$\boldsymbol{L_{interface} = \frac{1}{2\beta''}} \qquad (\mathbf{1.24})$$

1.3.3.2 TE-wave or *s*-Polarization

Magnetic field is parallel to the plane of incidence in case of transverse electric wave so the Maxwell's electromagnetic equations and boundary conditions results in modified expression as given below [20],

$$\boldsymbol{k_{z,1} + k_{z,2} = 0} \qquad \textbf{(1.25)}$$

$$\boldsymbol{k_{x,1} = k_{x,2}} \qquad \textbf{(1.26)}$$

Combining Equation (1.25) and Equation (1.26) with Equation (1.14), will lead to the expression as given below [20],

$$\boldsymbol{k_1^2 = \left(\frac{\omega}{c}\right)^2 \varepsilon_1 = k_2^2 = \left(\frac{\omega}{c}\right)^2 \varepsilon_2} \qquad \textbf{(1.27)}$$

From the above Equation (1.27), it is clear to say that this equation has no solution, in other words we can say that TE-wave does not support surface EM waves [22][23].

1.4 Surface Plasmon Resonance (SPR)

Even though it was more than a hundred years ago, when the anomalous dark bands observed in the optical spectrum of light reflected from a metal diffraction grating were first reported by R.W. Woods [24], it was not earlier than many decades later, when U. Fano related this phenomenon to leaky SPW supported by the metal grating [25]. In 1957, Ritchie anticipated both the excitation of SPW in metal films & in bulk plasma oscillations [26]. These predictions were rapidly proved and these waves were named as surface plasmons (SPs). But deep description of surface plasmon resonance technology could not be achieved till 1968 when Otto along with Kretschmann and Raether [27, 28] explained technique of ATR for the excitation of the SPs. The idea was based on prism coupling configuration. After this, theoretical and experimental study of plasmons were get accelerated in the following decades [27-29]. The

practicable usage of SPR technology for sensing purposes was started with the first application [30, 31] in 1983 for studying the bio-molecular relations by Liedberg et al [32]. The direct and real time molecular detection was made possible by using SPR optical sensing technology. From that time, SPR optical phenomenon has been showing a considerable potential in SPR sensor manufacturing. In the physio-chemical and biological applicatons, SPR optical sensing technology is providing fast and accurate results. Surface plasmons (SP) are combined electrons oscillations which are present at the metal-dielectric interface (MDI). The propagation of surface plasmon wave (SPW) at MDI is known the phenomenon of surface plasmon resonance (SPR) [33]. SPR excitation phenomenon is possible only with p-polarized light and equivalence condition of incident light photons frequency, f_{ilp} and natural frequency, f_n of surface electrons. From the solution of Maxwell's equation, it is to be noted SPW is a *p*-polarized in nature and there is exponential decays of field intensity into both metal and dielectric medium and it is depicted in Figure 1.5.

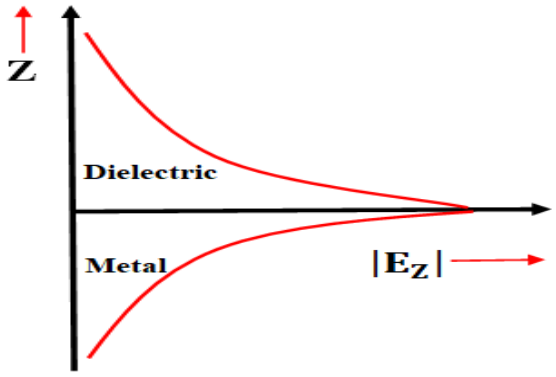

Figure 1.5: Exponential Decay of SPW Field Intensity in Active Metal and Dielectric Medium.

.

According to Maxwell's electromagnetic theory, propagation constant K_{sp} of SPW at the boundary of metal and dielectric media, is expressed by below equation [33]:

$$k_{sp} = \frac{\omega}{c}\sqrt{\frac{\varepsilon_{metal}\varepsilon_{dielectric}}{\varepsilon_{metal}+\varepsilon_{dielectric}}} \qquad (1.28)$$

In the Equation (1.28) ω, c, ε_{metal} & $\varepsilon_{dielectric}$ represents the incident light frequency, velocity of light ($3\times10^{8} m/s$) in vacuum, permittivity of metal layer & dielectric respectively. The ratio $\frac{\omega}{c}$ represents the free space vector (k_0) of TM wave. It is very much evident that plasmon wave is extremely dependent on metal and dielectric permittivity. When light wave propagates through dielectric with frequency ω, then light propagation constant, K_{lp} may be expressed as written below [29]:

$$K_{lp} = \frac{\omega}{c}\sqrt{\varepsilon_{dielectric}} \quad \textbf{(1.29)}$$

Figure 1.6 depicts the relationship between surface plasmon wave propagation constant and light propagation constant. This relation is known as dispersion relation in electromagnetic theory and is represented by two curves. As shown in Figure 1.6, this relation [34] of plasmon wave never meet with light travelling in dielectric media $\varepsilon_{dielectric}$, which means that the applied optical signal is not able to directly excite resonant phenomenon at the interface between dielectric and metal. In order to excite the plasmon resonant phenomenon, incident optical signal momentum in dielectric media has to be increased to match with the momentum of surface plasmon wave.

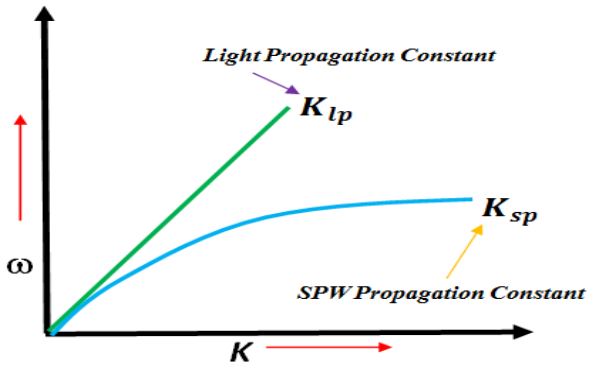

Figure 1.6: Relationship between Surface Plasmon Wave Propagation Constant and Propagation Constant of Light Signal in Dielectric

1.4.1 Otto Configuration

Evanescent waves are the electromagnetic waves whose field intensity decays exponentially into the metal-dielectric-media (MDM). Attenuated total reflection (ATR) procedure was reported by Otto in 1968, in metal-glass prism configuration.

This configuration is known as Otto configuration and it is depicted in Figure 1.7. In Otto configuration, metallic layer is kept at the bottom of the glass prism & very small gap (≅ 200nm) is set between the two. This configuration is demonstrated in Figure 1.7. Evanescent waves are produced when p-polarized light is incident at an incident angle ≥ to the critical angle (θ_c). As a result of total internal reflection (TIR), the evanescent waves are produced at the glass prism-air interface (GPAI). Finally an evanescent wave penetrates deeper into the metal layer which is kept closer to the prism base and excites the Plasmon resonance phenomenon at the metal-air interface [35].

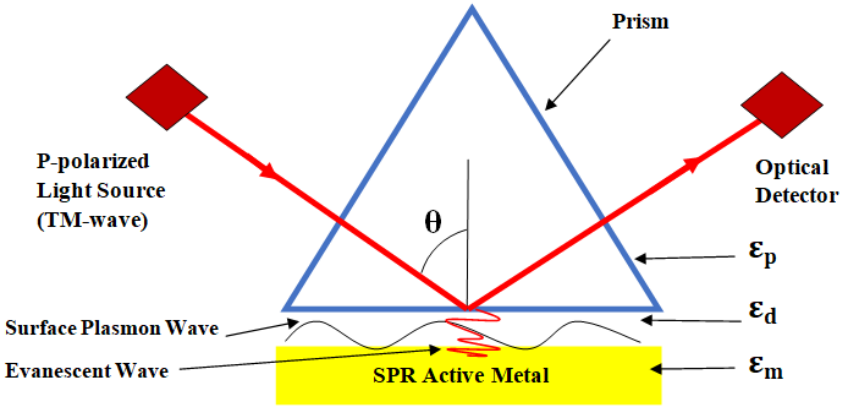

Figure 1.7: Otto Configuration Schematic Representation

Evanescent wave propagation constant at the interface between glass-prism and air (GPAI) can be expressed as [36]:

$$\boldsymbol{K_{evanescent} = \frac{\omega}{c}\sqrt{\varepsilon_{prism}}\, sin\,\theta = k_{prism}\, sin\,\theta} \qquad (\mathbf{1.30})$$

In the above equation ε_{prism}, $\varepsilon_{dielectric}$ denote the prism and dielectric media dielectric constant and $\varepsilon_{prism} > \varepsilon_{dielectric}$, θ denote the light incident angle, k_{prism} denote the light propagation constant in glass prism. Now, for surface plasmon resonance, the phase matched condition required that propagation constant of evanescent waves and surface plasmon waves should be equal and it is expressed [36]:

$$\boldsymbol{K_{evanescent} = K_{plasmon}} \qquad (\mathbf{1.31})$$

However, the drawback of Otto Configuration is that for proper penetration of evanescent wave into the metal sometimes it becomes difficult to maintain small gap spacing between metal and prism. Hence this is the main reason that Otto configuration is not widely used in surface plasmon resonance sensing applications.

1.4.2 Kretschmann Configuration

In Otto configuration a small gap is required to be maintained which is somewhat difficult in some situations therefore Kretschmann and Raether reported a new SPR configuration using prism as shown in Figure 1.8. In this configuration very thin metallic film is attached to the bottom of the glass prism and when a *p*-polarized light is incident then EW is originated at the interface between metal and glass prism. Main problem in maintaining the gap as in Otto configuration, is removed by coating a very thin metallic layer of nobel metal at the base of glass prism. This is depicted in Figure 1.8. In this case the thickness of metallic layer is usually taken as 50*nm*. So upon the incident of TM-wave, evanescent wave will be generated at the metal-glass prism interface. This evanescent wave penetrates deeper in the SPR metal and couples with surface Plasmon wave (SPW). The main advantages of this configuration is that this configuration permits the analyte to be easily attached with the surface of metal and analyte remains in contact with the metal surface more conveniently as compared with Otto configuration. This is the reason that Kretschmann configuration holds positive points for its use in glass prism-based plasmonic biosensors.

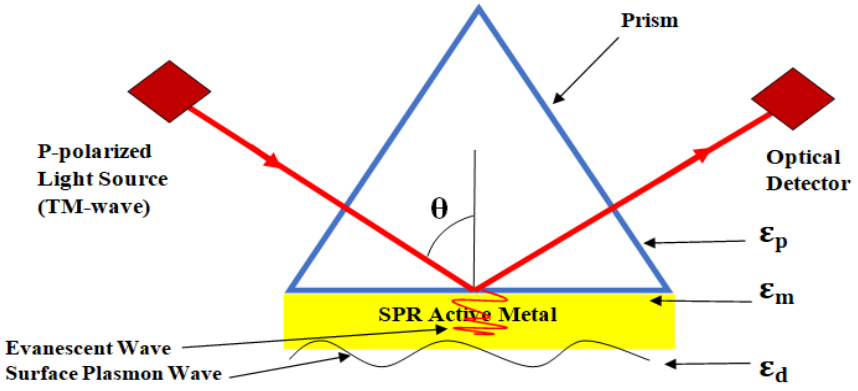

Figure 1.8: Kretschmann Configuration Schematic Representation

1.4.3 Fundamental Concept of SPR and Sensor Characteristics

1.4.3.1 Fundamental Concept of SPR

The fundamental concept behind SPR sensor is to perceive the small change in analyte RI occurring in sensing region. When incident p-polarized light couples with the surface plasmon wave, then free electrons present in the metal gets some part of incident light energy. This results in free electrons oscillation at the interface between dielectric and metal and the reflected light intensity decreases. If there is slight change in the analyte RI or in the dielectric constant at the interface between metal & dielectric, then certain conditions for SPR excitation gets changed. Even a little bit change introduced by biomolecular interaction will results in change in excitation condition of SPR. Also the transferred energy from the incident light photons gets changed with the change in RI. Therefore, RI variations present in the sensing region are identified by observing the change in certain optics properties of the reflected signal [37].

1.4.3.2 Sensor Characteristics

There are certain characteristics of the SPR sensor for evaluating its sensing performance. These characteristics are generally considered for studying the behavior of the SPR sensor. These characteristics are discussed below:

- **Sensitivity:** One of the important key parameters is the sensitivity of the biosensor. This parameter indicates that to a particular RI change near the sensing region how much the sensor is sensitive. Higher the RI sensitivity, lower limit of detection (LOD) can obtained. Sensitivity for angular interrogation bio-sensor S_{aib} can be expressed as the ratio of change of reflectance dip angle with respect to change in the RI of analyte. A slight change in RI by δn_{sense} shifts the resonance curve by $\delta\theta_{RDA}$ angle [38]:

$$\boldsymbol{S_{aib} = \frac{\delta\theta_{RDA}}{\delta n_{sense}}\ (\%RIU)} \qquad \textbf{(1.32)}$$

where $\delta\theta_{RDA}$ indicates a small change in reflectance dip angle and δn_{sense} indicates a slight change in RI of sensing medium. For wavelength interrogation biosensor, the sensitivity can be expressed as [38]:

$$\boldsymbol{S_{wib} = \frac{\delta\lambda_R}{\delta n_{sense}}\left(nm/RIU\right)} \qquad (\mathbf{1.33})$$

where $\delta\lambda_R$ is the change in resonant wavelength, S_{wib} is sensitivity of wavelength interrogated biosensor and it is expressed in *nm/RIU*

- **Linearity:** Linearity is usually a measure of linear relationship between the plasmonic biosensor's output response and measurand over some working limits [39]. In SPR technology based biosensor, linearity defines the linear response of sensor covering definite range of analyte RI. In the linear fit analysis, more the value of R^2 nearer to unity, more linear sensitivity of SPR sensor is. Plasmonic biosensor with linear sensitivity is of utmost importance because they need lesser number of calibration points to give exact sensor calibration response.
- **Resolution:** The smallest change in the RI of the analyte that gives the detectable change in the sensor response is known as resolution of the sensor. The ratio of standard deviation of noise of sensor output to the RI sensitivity is termed as the resolution of plasmonic sensor. The sensor's resolution is having the unit of *RIU*. Thus, if standard deviation (SD) of noise of the sensor output is Ω_{NSO}, and RI sensitivity is S_{n_sense} then resolution can be expressed as given below [40],

$$\boldsymbol{Resolution_{biosens} = \frac{\Omega_{NSO}}{S_{n_{sense}}}} \qquad (\mathbf{1.34})$$

- **Detection Limit:** Minimum value of detectable concentration of analyte is known as detection limit or limit of detection (LOD). This feature which depends on the sensitivity and resolution of the sensor, have significant role in investigating the performance of SPR biosensor. Usually, it is expressed in *nM*

or *mg/mL* units. Also it depends on the bioaffinity of the plasmonic biosensor to the analyte [40].

- **Regenerability:** Regenerability features of plasmonic biosensor can reduces the price of the SPR experiment. Receptors are not mobilized on sensor chip. After the analyte-receptors binding process has occurred, biosensor can be reproduced by separating the analyte target molecules and receptors. Such feature allows the sensor chip to be used again as a fresh sensor chip. However, it is to be taken care of that when the sensor chip is to used multiple times then, the response or output of the sensor might not be reliable or may fluctuate.
- **Stability:** Stability is that characteristics of the sensor which means that over some period, for unchanged value of the measured quantity, the sensor gives the unchanged response, under unchanged operating environment. Moreover stability depends on the optical sensor's robustness.

Chapter 2
Literature Survey

2.1 Introduction

In fiber optic sensing based on SPR, the p-polarized light is used for the excitation of SPs at MDI and there is exponential decay of SPW field strength. It appears at interface between metal and dielectric. Optical light characteristics are processed in electronic circuitry to get the desired detected output. In the recent years SPR based biosensors have been widely used to study the bio-molecular interactions, biological sensing and chemical detections. The interactions which can be studied include any kind of molecules, from organic compounds to proteins. Affinity based SPR biosensors are most widely used to detect the molecular absorption and desorption on surface of optical sensor. They include a bio-recognition element and there is interactions between this element and analyte target biomolecules. Having the distinctive feature such as real-time, label free and non-invasive detection, SPR technology has great potential in the field of optical sensors. We have already discussed in chapter 1, the various fiber optic sensing techniques, type of sensors and their classification based on operating principle, applications. We have also discussed different types of configurations and use of p-polarized (TM-wave) light for the SPWs excitation at the MDI inside sensor structure.

In this chapter, the comprehensive literature survey of multilayer based optical fiber surface plasmon resonance sensor along with different metallic combinations is presented in section 2.2. The comprehensive literature survey of metallic diffraction grating based SPR sensor and nanorod based SPR sensor is presented in section 2.3 and section 2.4 respectively.

2.2 Multilayer with Gold-Graphene Layer Combination based SPR Sensor

Yusser Al Qazwini *et al.* [41] proposed a bimetallic SPR based fiber optic RI sensor having *Ag*-film and TiO_2 thin film on the top. The best possible TiO_2 film thickness in the aforesaid sensor design was investigated numerically. They compared its sensing performance with bimetallic structure consisting of *Ag* and *Au* thin film in the aqueous media using FDTD solution technique. Numerically investigation of *Au/Ag* based structure was performed using FDTD technique. It was found that if *Au* film is replaced by TiO_2 film then TiO_2-*Ag* bimetallic structure significantly enhances the sensing performance in terms of sensitivity and SNR by a factor of 1.7 and 2.6 respectively. The maximum sensitivity exhibited by the *Ag*-60*nm* and TiO_2-30*nm* bimetallic structure is $6400 nm.RIU^{-1}$.

Hyuk Rok Gwon *et al.* [42] numerically investigated the optical sensing characteristics, spectral reflectivity and angular reflectivity of a Kretschmann configuration based sensor. This configuration is extensively employed in biochemical sample sensing systems. For numerical simulation, the Kretschmann based plasmonic sensor with distinct *Au* film thicknesses (30*nm*-70*nm*) was taken. It was concluded that sensor exhibits maximum sensitivity with *Au* film thickness ≈50*nm* and the optimum incidence angle ≈ 42.6°, for Kretschmann wavelength modulation plasmonic sensor.

Hailin Xu *et al.* [43] proposed a sandwich like structure for extremely high sensitivity. They have made the use of multilayer combination of graphene-aluminum-graphene in the sensing region to achieve better sensing performance. The maximum sensitivity exhibited by sensor is $\sim 942/RIU$ at $\lambda_{in} = 633nm$ when number of graphene layers are $N_g = 10$. It was also found that by keeping number of layers fixed, the sensor can be made more sensitive. The proposed SPR biosensor design is 3.4 times more sensitive than the *Al* based sensor without using the graphene layers. These advantages made this design, suitable for detecting different types of bio-chemical species.

Anuj K. Sharma *et al.* [44] proposed a near infrared plasmonic sensor consisting of multilayer structure of ZBLAN fluoride glass-silver-graphene. The substrate material was taken as ZBLAN fluoride glass. The effect of number of graphene layers on the combined sensitivity factor of the plasmonic sensor has been studied. Moreover the combined effect of graphene chemical potential (μ_g) and number of graphene layers (N_g), on biosensor's efficiency has been examined. From the analysis data they found that for single graphene layer, the constant sensing performance of the plasmonic biosensor may be achieved for $\mu_g < 1eV$ and $\mu_g > 0.7eV$.

Chunliu Zhao *et al.* [45] presented a reflective plasmonic sensor based on optical fiber microring. They have used FEM simulation for observing the reflection characteristics of the proposed sensor. From the numerical simulation, it was found that the resonance shift is close to small wavelength region for RI ~ 1.0-1.33 and move toward the long wavelength region for RI~1.33-1.43. The plasmonic sensor presented maximum sensitivity of 2.30×103$nm\text{-}RIU^{-1}$. These advantages made this sensor useful for sensing of gaseous substance.

Anuj K.sharma *et al.* [46] analysed the possibility of various nobel metal combinations which can be utilized in FO SPR sensor. Numerically, they analyzed the performance of the different noble metals like, gold, silver copper and aluminum, concerning with sensitivity, SNR and range of sensing operation. Normalized transmittance characteristics with wavelength for distinct bimetallic arrangements and analyte refractive index (RI) have also been presented.

In addition to these, some research work related to multilayer SPR sensor structure is tabulated as below in Table 2.1

TABLE 2.1: A BRIEF OF CONCLUDED RESULTS OF VARIOUS RESEARCHERS/INVESTIGATORS IN RELATION WITH MULTILAYER SURFACE PLASMON RESONANCE SENSOR

Researcher [Year][ref.]	Parameters Investigated	Design Material Used	Key Findings / Outcomes
Suzuki et al. [2008] [47]	Sensitivity, Full-width half maximum, Reflection Characteristics	Gold (*Au*)	Wavelength interrogated sensor with *Au*-65*nm* layer presented the enhanced sensitivity of $1557 nm.RIU^{-1}$ in RI range of 1.333-1.3469.
Lan et al. [2015] [48]	Sensitivity, SPR angle, FWHM, figure of merit, reflection characteristics	Gold(*Au*), Silver(*Ag*)	Demonstrated experimentally liquid prism based SPR sensor. Maximum sensitivity was found to be 372.73 *%RIU* and 254.55 *%RIU* for *Au*-50*nm* and *Ag*-55*nm* respectively, with diethylene glycol liquid prism.
Xihong Zhao et al. [2015] [49]	Sensitivity, Transmitted Characteristics	Gold(*Au*), SiO_2, TiO_2	Sensitivity was found to be $1.73 \times 10^{-4} RIU$s in intensity interrogation and $1.74 \times 10^{-6} RIUs$ for wavelength interrogation based sensor, using multi-layer modulation.
Dachao Li et al. [2015] [50]	Sensitivity, Full-width half maximum, Sensing length	Gold (*Au*), Chromium (*Cr*)	Experimentally investigated the SRP sensor for glucose sensing and found that fiber optic plasmonic sensor utilizing borate polymer presented high accuracy.

TABLE 2.1: A BRIEF OF CONCLUDED RESULTS OF VARIOUS RESEARCHERS/INVESTIGATORS IN RELATION WITH MULTILAYER SURFACE PLASMON RESONANCE SENSOR (CONT'D)

Researcher [Year][ref.]	Parameters Investigated	Design Material Used	Key Findings / Outcomes
Shukla et. al [2015] [51]	Resonant wavelength, Sensitivity	Platinum(*Pt*)	Theoretically analyzed the sensor and it was found that sensor with *Pt*-layer of 125*nm* thickness possesses enhanced sensitivity.
Yong Zhao et al. [2014] [52]	Reflection spectra, Resonant wavelength, Sensitivity	Silver(*Ag*)	Investigated the sensor for glycerol measurement, with volume concentrations ranging from 0% - 50%. Sensor presented the sensitivity with range from $346.7\times 10^{-9}m/\%$ - $890.7\times 10^{-9}m/\%$.
D.F. Santos et al. [2013] [53]	Transmission coefficient, Electric field distribution.	Gold(*Au*), Tantalum Pentoxide (Ta_2O_5)	Investigated the performance of the sensor using COMSOL, by optimizing residual cladding thickness and thickness of gold (*Au*) & tantalum pentoxide (Ta_2O_5) layer.
Peiling Mao et al. [2015] [54]	Transmittance, fiber modes, sensitivity,residual cladding thickness, depth of resonance dip	Gold(*Au*)	Sensor presented highest sensitivity of $4989nmRIU^{-1}$ for residual fiber thickness of 75μm and *Au*-layer of 50*nm*, in RI range of ~1.33-1.39.

TABLE 2.1: A BRIEF OF CONCLUDED RESULTS OF VARIOUS RESEARCHERS/INVESTIGATORS IN RELATION WITH MULTILAYER SURFACE PLASMON RESONANCE SENSOR (CONT'D)

Researcher [Year][ref.]	Parameters Investigated	Design Material Used	Key Findings / Outcomes
Sarika Singh et al. [2013] [55]	Normalized transmitted power, resonance wavelength, Detection accuracy, sensitivity	Silicon(*Si*), Silver (*Ag*)	Fabricated a SPR glucose sensor and experimentally analysed the sensor for human blood glucose range. It displayed enhanced sensitivity & operating range for sensing of glucose concentration.
Shukla et al. [2015] [56]	Resonant wavelength, sensitivity,	Silver(*Ag*), copper(*Cu*) Zinc oxide (*ZnO*), Gold (*Au*),	Sensor was studied theoretically and it was found that proposed geometry of plasmonic sensor with 40*nm* gold layer & 15*nm*-zinc oxide layer provided the highest sensitivity of 3161*nm/RIU*
Mahua Bera et al. [2009] [57]	Reflectance spectra, Sensitivity, SPR angle, Half width of SPR curve	Gold(*Au*), Magnesium Fluoride(MgF_2)	Proposed geometry of the sensor was simulated with MATLAB and it was found that the sensor is beneficial for the perception of various chemical, biological samples.
Petr Hlubina et al. [2014] [58]	Normalized reflectivity, sensitivity, Sensing length	Gold(*Au*)	Investigated the sensor for measuring ethanol liquid having RI~1.333-1.363. It was also demonstrated that when the fiber SPR sensing length decreases, the RI sensitivity increases.

TABLE 2.1: A BRIEF OF CONCLUDED RESULTS OF VARIOUS RESEARCHERS/INVESTIGATORS IN RELATION WITH MULTILAYER SURFACE PLASMON RESONANCE SENSOR (CONT'D.)

Researcher [Year][ref.]	Parameters Investigated	Design Material Used	Key Findings / Outcomes
Anuj K. Sharma et al. [2018] [59]	Magnetic field distribution, FOM, FWHM, Reflected optical signal	Gold(*Au*), MoS_2 (Molybdenum Disulfide), $MoSe_2$ (Molybdenum selenide)	*Au-ChG-*MoS_2-analyte sensor design exhibited highest FOM in NIR spectral region. The proposed sensor design based on *ChG-Au-2D* material combination provided highly stable sensing of organic compound in infrared spectrum region.
Xiao-Ming Wang et al. [2016] [60]	Transmission spectra, resonance wavelength, sensitivity	Gold (*Au*)	Results concluded that proposed sensor exhibit enhanced sensitivity of $S_n \approx 517.43–6656 nm\text{-}RIU^{-1}$. It was also shown that the correlation coefficient was very high i.e. $R^2=0.9985$, in the RI range from 1.3333 to 1.4.
SK Srivastava et al. [2015] [61]	Resonance wavelength, Reflectance	Silver(*Ag*)	Fabricated the SPR glucose sensor in spectral interrogation scheme, with enhanced sensitivity and stability. Sensor presented the sensitivity$\approx 0.14 \times 10^{-9} m/(mg/dl)$.
W.W. Lama et al. [2005] [62]	Normalized intensity, resonant wavelength	Gold(*Au*), Silver(*Ag*)	Experimentally analysed the sensor. It was found that plasmonic sensor has a detection limit $\cong 8.67\times10^{-6} RIU$, equal to $6.23 mg.dL^{-1}$ of glucose ($C_6H_{12}O_6$) in H_2O.

2.3 Resonant Impact of Metal Diffraction Grating Design on Sensing Performance

SPR technology is accepting continuously flourishing attention from scientific investigators, due to its inherent advantages of real time label free fast detection & enhanced sensitivity. In the last few decades, this technology has made grand evolution in the development of biomedical instrumentation and practicable applications. All of the SPR sensors employ attenuated total reflection technique to give rise to SPW [63]. Metal diffraction grating based application of SPR optical sensor was proposed by Cullen and Lowe [64]. From that time, SPR optical sensors utilizing grating [65], were studied as an alternative to ATR based optical sensing systems [66, 67]. Another advantage is that grating-based sensing systems provide greater miniaturization & integration possibilities, which leads to the developing interest in these types of sensors for lab-on-chip usage [68]. Various investigators have shown the usage of metallic grating in SPR optical sensing system.

R.H. Ritchie *et al.* [69] analyzed the p-polarized light from diffraction gratings having concave shape. The interaction between incident light photon and resonance phenomena on the grating was analysed. The existence of 2^{nd} & higher-order plasmon-grating interaction was observed. In continuation with this, in early 1976, M.C. Hutley *et al.* [70] have shown theoretically and experimentally a phenomenon in which a grating with very shallow grooves absorbs virtually all of the light of a given incident wavelength. The phenomenon represented the principal features of the light absorption at different wavelength, with optimum groove lengths and optimum angle of incidence.

Ashish bijalwan *et al.* [71] proposed a SPR based RI sensor using grating of different metallic combinations for biosensing applications. Numerically simulated the five different designs of the sensor i.e gold grating on gold-sheet, gold grating on silver-sheet, gold grating on aluminum-sheet, *Au-*SiO_2 grating on aluminum-sheet & *Au-*Al_2O_3 grating on aluminum-sheet. It was found that the sensor utilizing gold grating

with silver or aluminum-sheet has enhanced sensitivity with small full width half maximum. But sensor with gold-grating on aluminum-sheet displayed highest sensitivity, S_n ≅284degree/*RIU* and quality factor > 236.67 RIU^{-1}. But because of the oxidation problem of aluminum, Al_2O_3 film has been introduced in the design and *Au*-Al_2O_3 grating/aluminum-sheet design was proposed. With Al_2O_3 thin sheet, sensitivity reduces but at the same time decreases the FWHM of the biosensor and it improves the quality factor. Sensitivity and quality factor has been found to be 270.33°/*RIU* and 267.65 RIU^{-1} respectively. Kouki Ichihashi *et al.* [72] proposed grating based SPR sensor that operates in a differential mode. The differential measurement for two SPR dip corresponding to the $\pm 1^{st}$ diffracted light orders have also been shown. It was found that the angular sensitivity of the grating sensor is 4.8 times higher when compared with conventional G-SPRS and over twice that of a prism-based SPRS. Xiaoliang Sun *et al.* [73] presented a grating based surface plasmon resonance sensor. It was found that for single dip method RI sensitivity reach 493.7*deg/RIU* and for double dip method the sensor possesses maximal sensitivity ≈ 535.9*deg/RIU*. The aforesaid design of the sensor performed well in RI range ~1.32-1.36. SPR sensor utilizing aluminum grating also exhibited enhanced FOM and sensitivity 396.3*deg/RIU* at λ=1.55μm for double dip method. However the sensing performance was little bit degraded after the metal oxidation. In continuation with this, Jianjun Cao *et al.* [74] investigated a wavelength interrogation based grating sensor. Analytical calculations were performed for sensitivity and for observing the effect of parameters such as wavelength of operation λ_{in}, grating period T_0, RI of the sensing sample on sensing. The theoretical analysis concluded that RI sensitivity rises for rise in wavelength for both *Au/Ag*-grating, but it is constant for *Al*-gratings from λ_{in}=500 to λ_{in}=1000*nm*. In addition to these, some research work related to grating based SPR sensor is tabulated as below in Table 2.2.

TABLE 2.2: A BRIEF OF CONCLUDED RESULTS OF VARIOUS RESEARCHERS/INVESTIGATORS IN RELATION WITH METALLIC GRATING SURFACE PLASMON RESONANCE SENSOR

Researcher [Year][ref.]	Parameters Investigated by Researcher	Design Material Used	Key Findings / Outcomes
W. Su et al. [2012] [75]	Sensitivity, SPR curve width, Resonant Angle Shift, Reflectance amplitude	Gold(*Au*), Silver(*Ag*), Aluminum(*Al*)	With numerical simulation *Al*-30*nm* grating based SPR sensor exhibited angular sensitivity of 247.21 *°/RIU*.
Hai-Tao Yan et al. [2013] [76]	RI Sensitivity, Guided modes, Surface plasmon polariton modes	Gold(*Au*)	Proposed metallic grating D-shaped sensor for measuring the RI of pure water & isopropanol. Sensor displayed highest sensitivity ≈917*nm-RIU*$^{-1}$.
Kaiqun Lin [2008] [77]	Sensitivity, SPR curve width, TM Reflective intensity, FWHM, Resonant angle.	Palladium(*Pd*)	Proposed Palladium (*Pd*)-based diffraction grating optical sensor for the detection of hydrogen. Theoretically, the resolution of hydrogen concentration obtained was of the order of 0.001%.

TABLE 2.2: A BRIEF OF CONCLUDED RESULTS OF VARIOUS RESEARCHERS/INVESTIGATORS IN RELATION WITH METALLIC GRATING SURFACE PLASMON RESONANCE SENSOR (CONT'D)

Researcher [Year][ref.]	Parameters Investigated by Researcher	Design Material Used	Key Findings / Outcomes
Tomas Tamulevicius [2011] [78]	Relative reflection coefficient, Angle of incidence	Fused Silica, Photoresist	Proposed a diffraction grating based sensor for RI sensing of liquid (different concentration of sugar-water solution).
K. H. Yoon [2006] [79]	Sensitivity, FWHM,	Gold(*Au*)	Proposed a nano-grating design with sensitivity > 400$nm\text{-}RIU^{-1}$ and sharp reflection resonance peak with FWHM ≅0.03eV. FOM ≅60 for a grating period of 500nm.

2.4 Circular Gold Nanorod Design Based SPR Sensor

The study of nanoparticle-based optical sensors is a tremendously active area of nanoscience research [80]. In the last decade, the use of nanomaterial has a significant effect on bio-sensing system. The distinct properties of noble metal NPs have allowed for the development of new bio-sensing platforms with strong capabilities in the specific recognition of bio-analytes. Furthermore, they also present an improved layer of application for frequently used procedures, such as fluorescence, IR & Raman spectroscopy [81]. In the epoch of nanotechnology, SPR sensor employing nobel metal nanoparticles have a huge potential in the growth of innovative biosensors technology or in the advancement of existing optical bio-sensing methods to for the benefits of public health in medical diagnostics. Nanoparticles have attractive properties which

makes them suitable candidate for the development of a different type of plasmonics bio-sensors for point of care (POC) disease detection. Nanoprobes made by nanoparticles have also shown the interests in the mind of bio- researchers for in-vivo sensing or medical imaging diagnostics. Nanoparticles have remarkable properties such as simplicity in design, large surface area and having different shapes and diameter range between 10^{-9}m to 10^{-7}m. Based on their size and architecture, it is easy to examine distinctive features, like quantum effect in semiconductor nanocrystals technology, effect of plasmonic resonance phenomenon on MNP and paramagnetism effect into magnetic elements. Gold nanoparticles (AuNPs) and Silver nanoparticles (AgNPs) are two most broadly investigated nanomaterials and have huge potential in the discovery of new diagnostics methods for bio-molecular diagnostics, body imaging and remedial treatments [81]. Metal nanoparticles may be utilized single or in conjunction with other types of nanostructures. Metal nano particle sensors give rise to considerable signal intensification, enhanced sensitivity & improved detection of biomolecules and various ions [82]. The huge requirement for sensing extensive collection of biomolecules at extremely small concentrations with high specificity, has stimulated the development of high-tech appliances that includes nanoscale active materials, biological component, and advanced materials, which are jointly termed as nano-biosensors. Noble metals like Au, Ag, Al and Pt nanoparticles have been especially admired and thoroughly studied. Although these noble metal NPs are chemically inactive in their macroscale form but they exhibit exclusive optical properties because of resonance phenomenon at nanoscale [82]. Various researchers have shown the use of nobel metals nanoparticles in SPR technology based optical sensor. Wing-Cheung Law *et al.* [83] demonstrated the use of nobel metal gold nanorods for ultra-sensitive phase-sensitive SPR biosensor using finite element analysis (FEA). Sensitivity enhancement of the sensor was achieved by observing the resonance of *Au* nanorod. The sensitivity of NR conjugated antibody was found to be ~40*pg/ml*, which is 25 -100 times more sensitive. In continuation with this, Dalibor

Ciprian *et al.* [84] presented theoretical analysis of core-shell NPs film based plasmonic sensor using computer model. From the analysis, it was concluded that the overall performance of the optical sensing system increases with the core radius. Kyeong-Seok Lee *et al.* [85] theoretically analysed that plasmonic nanoparticle have a great potential for sensing applications because they have strong scattering or absorption properties. It was found that increase in size and aspect ratio of metal nanorods, increases the sensitivity. But if the metal nanoparticle size is increased too much then it will have negative effect on the sensitivity of the palsmonic biosensor because of the broadening of plasmonic resonance curve. Researchers are continuously working to improve the efficiency and accuracy of plasmonic biosensing. In addition to these, some research work related to metallic NR sensor based on SPR technology is tabulated in Table 2.3.

TABLE 2.3: A BRIEF OF CONCLUDED RESULTS OF VARIOUS RESEARCHERS/INVESTIGATORS IN RELATION WITH METALLIC NR SENSOR BASED ON SPR TECHNOLOGY

Researcher [Year][ref.]	Parameters Investigated by Researcher	Design Material Used	Key Findings / Outcomes
Jie Cao et al. [2012][86]	Wavelength shift, Absorbance, Limit of Detection, Sensitivity	Gold(*Au*)	LSPR based biosensor using *Au* nanorods has been fabricated. Experimental results concluded that AuNR based SPR sensor possesses enhanced RI sensitivity of 509*nm/refractive index unit*.
Shuwen Zeng [2013][87]	Resonant angle, Reflectivity, Electric field distribution	Gold(*Au*), Graphene	Gold (*Au*) nanorod and graphene layer based SPR sensor has been investigated using FEM simulation. It was found that sensitivity of $10^{6^\circ}/RIU$ can be achieved using graphene monolayer and AuNRs.
Chaoying Chen et al. [2015][88]	Propagation modes, resonant wavelength, Sensing length, Transmittance, Electric field distribution	Gold(*Au*)	D-shaped SPR sensor with square AuNR array was simulated using FEM. Sensor has ability to work in RI~1.33-1.39, with enhanced sensitivity of 6266$nm\text{-}RIU^{-1}$ when square AuNR thickness is 70*nm* and spacing ~ 50*nm*.

TABLE 2.3: A BRIEF OF CONCLUDED RESULTS OF VARIOUS RESEARCHERS/INVESTIGATORS IN RELATION WITH METALLIC NR SENSOR BASED ON SPR TECHNOLOGY (CONT'D)

Researcher [Year][ref.]	Parameters Investigated by Researcher	Design Material Used	Key Findings / Outcomes
Ching-An Peng et al. [2014][89]	Sensitivity, Longitudinal plasmonic Wavelength peak shift, TEM analysis	Gold(*Au*), Dextran Sulfate	Presented longitudinal plasmonic detection of glucose using AuNR. TEM analysis showed the red shift and blue shift in wavelength of AuNR coated with dextran sulfate. The degree of wavelength shift of AuNR coated with dextran sulfate has been modulated with glucose, range from 1- 30*mM*.
Hung-Yi Chung et al. [2014][90]	Sensitivity, Phase diff. between *p*- and *s*-waves, Resonant angle	Silver(*Ag*)	Demonstrated the phase-interrogated SPR sensor for glucose detection, with oblique deposited AgNRs. AgNRs were arranged on *Ag* nano-sheet by oblique angle deposition technique. Experimental results concluded that with 10*nm* optimal thick AgNRs sensitivity down to 7.1×10^{-8}*RIU* can be achieved.
Yinquan Yuan et al. [2018][91]	Resonance angle, Sensitivity, Reflection Spectra	Gold(*Au*), SiO_2 nanoparticle (SiNPs)	Highly sensitive and wide range SPR glucose sensor utilizing AuNP & SiNPs was proposed. For different component ratio of NPs, avg. sensitivity was computed as $0.028°/(mg.dL^{-1})$, in glucose conc. range $0 mg.dL^{-1}$–160 $mg.dL^{-1}$.

TABLE 2.3: A BRIEF OF CONCLUDED RESULTS OF VARIOUS RESEARCHERS/INVESTIGATORS IN RELATION WITH METALLIC NR SENSOR BASED ON SPR TECHNOLOGY (CONT'D)

Researcher [Year][ref.]	Parameters Investigated by Researcher	Design Material Used	Key Findings / Outcomes
Arpad Jakab et al. [2011][92]	Resonance wavelength, Plasmonic Nanorod Sensitivity	Gold(*Au*), Silver(*Ag*)	Sensitivity of sensor with AgNRs ≈400*nm-RIU*$^{-1}$. Thin AuNRs have a sensitivity ≈ 170*nm-RIU*$^{-1}$and thick AuNRs have a sensitivity ≈ 250*nm-RIU*$^{-1}$ in the wavelength range of 600-700*nm*.
Liping Song, [2017][93]	Plasmonic Nanorod Sensitivity, Plasmon Wavelength shift	Gold(*Au*), Silica(SiO_2)	Proposed AuNRs based localized SPR sensor with coating of mesoporous silica on AuNRs. This design presented a high stability for localized SPR sensor with sensitivity ≈390*nm-RIU*$^{-1}$.

2.5 Gaps Identified in Present Study

This section lists the common limitations encountered while dealing with optical fiber sensor based on SPR. This would make the reader realize the importance of these drawbacks and elucidate the reasons for making an attempt to get solution to these problems.

According to literature survey, the two parameters of the SPR sensor i.e. resonance angle (θ_{RDA}) and resonant wavelength (λ_{reson}) plays a major role in affecting the sensing performance of the sensor in terms of detection and sensitivity.

- Besides new design and optical platform developments, sometimes noise which originates from the optoelectronic components associated with the SPR experiments, becomes a major issue.

- ❖ Sensitivity, detection accuracy and light transmission efficiency are the major issues presented in surface plasmon resonance sensors.
- ❖ When designing fiber-based SPR sensors for sensing applications, sometime we face a difficult problem of phase matching a plasmon with a core-guided mode.
- ❖ Level of noise in the measurement is another problem in the SPR sensor as it affects the limit of detection.
- ❖ Sometimes there is a very small wavelength or angle shift when the refractive index is being sensed, as the large wavelength or angle shift is responsible for the better sensitivity of the sensor. So this also becomes a major issue in SPR sensing technology.

2.6 Problem Formulation

SPR technology based optical sensing is one of the promising detection techniques. The earliest sensing application of SPR technology was made widely known almost in three decades back. The uses of optical sensors on large scale have some drawbacks. Initially, the SPR technique started with Otto configuration for plasmons excitation at the metal-dielectric interface (MDI). The problem occurring in this configuration shows difficulty in maintaining gap between metal and prism because this gap has to be filled with the analyte (sensing medium). Sometimes it is difficult to maintain the thickness of analyte layer between metal-prism gap. Therefore Kretschman-Raether configuration made its use in optical sensing. This configuration eliminates the problem of maintaining the metal-prism gap.

These prism based plasmonic techniques have some disadvantages such as large, heavy size of prism and number of electronic processing and mobile parts, making it difficult to use at sites which are at remote locations. So, remote measurement is not possible with prism based SPR techniques.

In recent scenario, optical sensing system would be advantageous for modern society if it is cost-effective and be capable of providing in-situ and remote measurements. Kretschman-Raether configuration is implemented in optical fiber to overcome above shortcomings. FOSs have a variety of benefits such as small size, quick response, cheap fabrication, light weight, extremely sensitive and non-reactive to EMI.

Existing SPR based FO sensor are based on the surface plasmons interaction between thin metal and dielectric layer. Normal SPR sensor is not so much sensitive to analyte refractive index variations. Multilayer combination i.e. thin layer of 2D material and gold based SPR sensor provides better sensitivity because graphene material much sensitive to analyte RI fluctuations. Sensing region is created by coating the bare core (unclad core) with metallic layer of suitable thickness. Metallic layer combinations must be carefully chosen.

Now-a-days, numbers of high blood glucose cases are on continuous rise. Therefore glucose sensing is of great significance in biomedical applications. Gold and two-dimensional material graphene based SPR sensor provides greater shift in the TM-reflected light intensity and exhibit better sensitivity in sensing of glucose. This type of optical sensor would be advantageous for the people health and biotechnology domain. Structural optimization of the sensing structure would lead to sensing of wide variety of organic compounds.

Bimetallic diffraction grating design for fiber optic SPR sensor can also be very useful. In recent years, bimetallic diffraction grating based SPR sensor using angular interrogation technique have shown deep interest in field of bio-sensing. They have huge potential to provide excellent sensing platform for analyte refractive index variations. Resonance condition is achieved by the use negative diffraction order. Spectral response and sensitivity is further tuned by metal thickness, choice of metal and angle of incidence. Factors contributing to the analyte RI sensitivity are explored consistently through modeling, design simulating and theoretical explanation.

2.7 Research Objectives

- ❖ To investigate properties of different SPR materials and observe the dependency of resonance wavelength on the properties of the metallic film, length of the sensing region and the refractive index of the medium.
- ❖ To model and design the fiber optic sensor based on SPR and investigates its performance with multi-layer modulation techniques.
- ❖ To analyze the various parameters, e.g. resonance wavelength, angle, phase which are responsible for the improved sensitivity of fiber optic sensor based on SPR.
- ❖ To examine the SPR sensor performance for sensing applications.

2.8 Research Methodology

The research has started with extensive literature survey to achieve the above said objectives. The implementation of the said objectives will be done by using simulation softwares such as COMSOL Multiphysics, OptiFDTD, MATLAB and Origin Pro8 which are available in the Optical Research Laboratory of the department. The research will be carried out as:-

- ❖ Different Nobel metals and geometries of fiber optic sensor based on SPR will be studied and sensor would be investigated in terms of the performance parameters e.g. SPR spectral resonant curve, angular sensitivity and detection accuracy.
- ❖ Designing, characterization and optimization of SPR sensor, made by Step-Index multi-mode PCS (Plastic clad silica) fiber, will be done by using popular COMSOL Multyphysics FEM (Finite-Element Method) and OptiFDTD commercial software package.
- ❖ Mathematical analysis of TM-wave (p-polarized light) propagation inside the SPR structures will be studied.
- ❖ Analysis of parameters is obtained by light source which is used to excite the optical fiber, sensing platform is an optical SPR sensor and observation is

made by using optical spectrum analyzer, spectrometer, optical power meter etc.

- ❖ The sensor will be simulated using the commercial software packages and the parameters will be optimized by performing a large number of iterations to get better performance.

2.9 Major Contribution of Thesis

The major contribution of the research work presented in this thesis was to find out the way to overcome the drawbacks of the FOS based on plasmonic technology as described in the previous sections. The major contribution of this thesis was to design and optimize the multilayer and metallic diffraction grating based SPR sensing structure, and also to obtain better sensing results of fiber optic SPR sensor when correlated with existing and traditional fiber optic surface plasmon resonance sensors. As discussed earlier, for FO SPR sensor based on angular interrogation, the sensitivity is usually expressed in $(^{\circ}/_{RIU})$ and for FO SPR sensor based on wavelength interrogation the sensitivity is expressed in $(nm/_{RIU})$, so for better sensing performance the suitable combination of plasmonic metals, in terms of choice and thickness of metal is required.

Different SPR active metals and their properties have been investigated in order to find the better possible plasmonic metal for multilayer, diffraction grating and nanorod based design of the fiber optic SPR sensor. Usually, the metals whose real part of permittivity functions acquire negative values at operating wavelength, exhibit plasmonic phenomenon.

Suitable multilayer design with enhanced sensitivity, using a novel 2-D material and plasmonic metal gold (*Au*) coated on the core of the fiber and its design performance for Glucose sensing with the help of commercial software COMSOL has been presented. Obtained results demonstrated the sensing performance capability of the sensor design according to the variations in refractive index of the analyte (i.e. glucose) in the sensing region. A suitable approach and design methodology was

developed to estimate the effect of the gold-graphene metal combination on the sensing characteristics of the sensor. Every year as the numbers of glucose cases are following upward trend and glucose sensing is definitely required. The research work discussed here contributes to design a simple and economical bio sensing configuration that may prove beneficial for the general public health. Other than biological sensing analysis, this multilayer sensor configuration can be useful with several advantages in sensing of variety of organic compounds and food processing.

SPR sensor based on metallic diffraction grating presents advanced miniaturization and integration capabilities to greater extent. Grating-based SPR sensors are perfect candidate for compact or integrated SPR biosensors. In literature various researchers have shown the use of diffraction grating in SPR based fiber optic sensor. In the year 2015, Xiaoliang Sun et al. [72] presented a diffraction grating surface plasmon resonance sensor with angular interrogation method for enhancing the sensitivity (*%RIU*). We have presented the resonant impact of *Au/Al* double metal diffraction grating design on the sensing performance of the sensing device and from the results we have achieved the highest sensitivity of the aforesaid design.

Finally, in the last part of the major contribution of research work, we have presented the use of nobel metal NPs in SPR technology based FO sensor. We have analyzed the circular gold (*Au*) nanorod wavelength interrogation based sensor with FEM simulation. Sensitivity was found to be dependent on shape and size of the gold nanorods. From the linear fitting analysis, the R^2- coefficient of determination (COD) = 0.9878 was found to be very high. *Au*-nanord based this suitable design has significant potential in recognizing biological signals.

3.0 Outline of Thesis

Considering the objectives achieved in the present research work, the thesis is organized in six chapters.

- **Chapter 1:** The first chapter devotes to introduce the reader with optical fiber sensing and surface plasmon resonance technology based sensor. An

introduction to types of optical fiber sensing, types of sensors, SPR excitation configurations, SPR sensors and their advantages are given in this chapter.

- **Chapter 2**: This chapter presents the comprehensive literature survey of optical fiber based SPR sensors for refractive index sensing. The motivation for writing the thesis is also given in chapter 2. The state of art work done by various researchers is also acknowledged in this chapter. Thereafter, the research gaps in the present study are pointed out and research objectives with their respective methodology used in this study, are defined in this chapter.
- **Chapter 3:** This chapter describes the proposed design with gold-graphene metallic layer combination for sensing of glucose. Graphene is a 2D material and its unique combination with SPR active metal gold enhances the sensitivity of the sensor.
- **Chapter 4**: This chapter presents the bimetallic diffraction grating design based SPR sensor and its performance investigation using COMSOL multyphysics software. As gold (*Au*) and aluminum (*Al*) are considered to be main active metals, so we have used the bimetallic diffraction grating in the proposed design for enhancing the sensitivity.
- **Chapter 5:** This chapter describes the FEM simulation analysis of circular gold nanorod based fiber optic SPR sensor. Circular design of the AuNR is selected for optimum response.
- **Chapter 6:** This chapter enlists the main conclusions and recommendations. It also presents the scope for future research directions.

Chapter 3
2D material based SPR sensor

3.1 Introduction

This chapter presents the FO SPR sensor employing the unique combination of 2D material and nobel metal gold. As we know that Glucose ($C_6H_{12}O_6$) is a compound having 6C-12H-6O atoms. Its perception is beneficial in several bio-medical utilizations for medical diagnostics. In aforesaid design of the sensor, a combination of 2-dimensional material graphene and *Au* film is utilized in the sensitive region. Unclad fiber core has been enveloped with *Au* film & thin graphene film combination. 2D material based sensor is simulated in angular interrogation method with the help of COMSOL Multiphysics simulation package. Multiple iterations have been performed to examine the sensing capabilities of sensor by considering the parameters in terms of Au film thickness, graphene film thickness, RI of the sensing sample in the sensing region. Simulation results show that 2D material graphene contributes to enhanced SPR sensor sensitivity.

As we have already discussed that SPR is optical phenomenon involving the interactions between light photons and SPW. Different configurations for SPW excitation have been described previously. In year 1902, this phenomenon was first observed by R.W. Wood [94]. In the forties of last century, SPW were observed at the interface between metal and dielectric (MDI) [25]. From that time, SPR technology based multi-layer and diffraction gratings sensors [69-70, 95] have huge potential in biochemical science and to some level it covers civil engineering too. Owing to its numerous advantages, plasmonic technology has emerged as powerful detection technique since last three decades [96]. Prism based RI sensors now a days are being replaced by optical fiber SPR sensors because of the problem of integration and bulky size. FO sensors are ultimate for insensitive surrounding such as intense heat, moist,

fluctuating temperatures, high oscillations & unbalanced environments [97]. Moreover FOS are not bulky & having low maintenance cost [98]. In the literature numerous researchers have shown the use of different multilayer configuration, applied on the fiber core for enhancing the performance of the SPR sensor. Zhao *et al.* [49] have shown the use multilayer based SPR sensor. Shukla *et al.* [51] theoretically discussed extremely sensitive plasmonic sensor utilizing fiber core covered with active metal platinum (*Pt*). Results concluded that sensor with 125*nm-Pt* layer exhibited extremely high sensitivity of $175x10^{-7}$*m-RIU*$^{-1}$. Further Suzuki *et al.* [47] have discussed the influence of *Au* layer thickness on the sensitivity of the sensor. They found that 65*nm-Au* active metal layer is enough for observing the reflectance dip in the resonance curve and sensor has enhanced sensitivity of 1557*nm.RIU*$^{-1}$ *w*ith RI ~1.333-1.3469. Mao *et al.* [54] also presented a multilayer D-shaped SPR sensor with MMF having the Au active metal in the sensing region. Proposed sensor has enhanced RI sensitivity ≈4989*nm.RIU*$^{-1}$. Wang *et al.* [60] reported a miniature and ultra-modern T-shaped FOS based on SPR. It was analysed from the simulated results that SPR transmittance curve moves in the vicinity of long wavelength region with larger increase in sample RI. Results indicated that the proposed geometry of the sensor possesses resolution ≈ 7.11×10^{-6} refractive index unit & 3.52×10^{-6} refractive index unit for sample RI~1.333 to 1.36 & RI~1.37 to 1.4 respectively. In addition to the above, Sharma *et al.* [46] have reported the scope of distinct active multilayer arrangements to be utilized in FOS based on SPR phenomenon. The effect of distinct metallic combinations on sensing performance of the SPR sensor was observed. None of the above discussed the use of 2-dimensional material along with suitable SPR active metal in sensing region. This chapter presents the 2D material based SPR sensor for sensing of organic compound i.e. glucose. A special combination i.e. 2-dimensional material (graphene) and *Au* metal with optimized parameters, has been used in the design of the sensor. COMSOL FEM simulation technique has been employed for deep understanding of the TM reflectivity curves and field distribution. Graphene has a set of remarkable properties

like high electrical conductivity, σ_g and thermal conductivity, k_g. This is because 2-dimensional material graphene has extremely high electrons mobility of the order of $15 \times 10^3 cm^2.(V.s)^{-1}$. Therefore this material has already attracted the lot of interest of the researchers, to employ this material in optical SPR sensing systems. Moreover scientists are making use of COMSOL [99], [100] to learn the applications that can exploit these qualities. The aforesaid design of the 2D material based SPR sensor provides enhanced sensitivity and show excellent linearity and quality.

3.2 Theory

SPR sensor design is based on Kretschmann's configuration [27]. The general design of 2-dimensional material based SPR sensor is shown in Figure 3.1. Sensing region is made by cutting the cladd from fiber core. Finally core is covered by thin *Au* film and graphene film. The topmost layer of the sensing region is thin analyte layer which is placed upon the *Au*-graphene coating. Sensing response of surface plasmon resonance based sensor can be improved by employing more graphene layers. Graphene provides a good platform at the interface and it eases the process of bio-molecules absorption because of huge surface area [101]. In aforesaid design of the sensor as shown in Figure 3.1, use of graphene thin film on *Au* thin film assists in proper absorption of organic compound. It provides enhanced RI change at *Au*-graphene interface. The coating of thin graphene on the fiber core assists in enhancing the sensor's sensitivity [102]. The suitable optical signal from the high performance light source is made to fall on the input side as shown in Figure 3.1 and output light signal is observed at fiber output end.

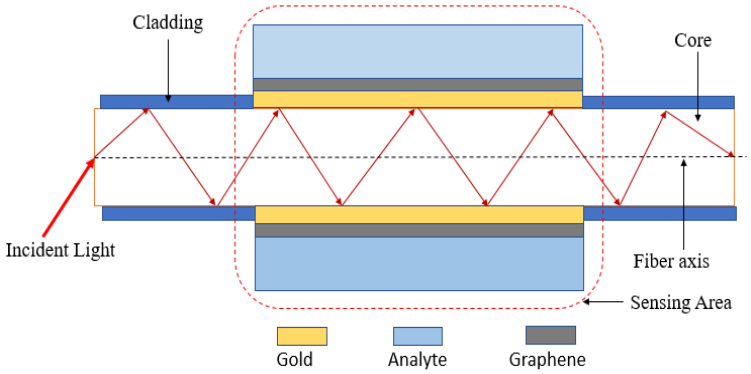

Figure 3.1: Sensor structure with 2D Material (Graphene) and SPR active metal *Au*

Sellmeier equation for the dielectric medium such as fiber may be used. The general expression of Sellmeier equation is given as below [103],

$$\boldsymbol{n^2(\lambda)} \quad \boldsymbol{= 1 + \sum_{z=1}^{3} \frac{B_z \lambda^2}{\lambda^2 - C_z^2}}, \qquad (\mathbf{3.1})$$

where terms B_z, C_z denotes the Sellmeier coefficients [104] and may be calculated for various profiles of core-cladding doping. To find the refractive index, n_{metal} and complex dielectric constant, ε_{metal} for different active metals layers, we have used the Drude model [105]. The well known expression of Drude model is given by the equation as below [105],

$$\boldsymbol{\varepsilon_{metal}(\lambda) = 1 - \frac{\lambda^2 \lambda_{collision}}{\lambda_{plasma}^2 (\lambda_{collision} + i\lambda)}} \qquad (\mathbf{3.2})$$

$$\boldsymbol{n_{metal}(\lambda) + ik_{metal}(\lambda) = \sqrt{\varepsilon_{metal}(\lambda)}}, \qquad (\mathbf{3.3})$$

In the above equation, n_{metal} represents the real part of RI and k_{metal} represents imaginary part of RI of the active metal & ε_{metal} denotes the complex dielectric constant of active metal. Plasma and collision wavelength are denoted by λ_{plasma} and $\lambda_{collision}$ respectively. The plasma and collision wavelength are adopted from ref. [106] for different plasmonic metals i.e. silver, gold, copper, aluminum and oxide metal and are listed in Table 3.1 [106].

Table 3.1: Plasma wavelength (λ_{plasma}) and collision wavelength ($\lambda_{collision}$) of SPR active metals and oxide metal

Active Metal and Oxide metal	**λ_{plasma} (units in meter)**	**$\lambda_{collision}$ (units in meter)**
Gold	1.6826×10^{-7}	8.9342×10^{-6}
Silver	1.4541×10^{-7}	17.6140×10^{-6}
Copper	1.3617×10^{-7}	40.852×10^{-6}
Aluminum	1.0657×10^{-7}	2.4511×10^{-5}
Indium Tin Oxide	5.6497×10^{-7}	11.21076×10^{-6}

3.3 COMSOL 2-dimensional Modeling

COMSOL software is a multiphysics simulation tool [107]. It is also known as finite element analysis (FEA) simulation software. We have used wave optics module of COMSOL multyphysics 5.2a commercial software package for simulation of the design. Different TM reflectance curve and field distribution curves have been represented by this software. With this software package, we have simulated a SPR sensor consisting of multilayer arrangement of 2-dimensional material graphene and *Au* metal which are overlaid on the fiber core. Sensor is simulated in infrared range of electromagnetic spectrum. IR spectrum window covers the electromagnetic waves whose wavelength is from 700*nm* to 1*mm*. In general, Infrared electromagnetic waves fall between visible wave and radio wave region of the spectrum. There are different modules in COMSOL for carrying out the simulation; wave optics module has been used for simulating the sensor design. As the name suggests, finite element method, in COMSOL FEM the whole optical sensor design is divided into finite number of different domains or elements and then for proper light propagation each element have to meshed. For this design of the sensor, we have taken the mesh element size as "*lambda/5/n_domain*", here *lambda* represents the wavelength of operation and "*n_domain*" is the RI of the domain [108]. Next important thing is that until and unless meshing is not proper, light will not propagate through the fiber core. If we use free triangular mesh for the multilayer sensor to be designed then it is computationally

expensive and it will put more burden on the computer simulation memory. Therefore we have made the use of mapped mesh approach for meshing the multilayer optical arrangement. The design consists of two numeric ports, one act as input port for light source and other act as output port for detection purpose. For studying the mode analysis it is essential to apply boundary mode analysis for both numeric type ports. TM reflectance curve is examined at the output with different angle of incident to check the amount of resonance shift.

3.4 Results and Discussions

Sensing area or sensing region is a multilayer stack and it is comprised of fiber core, *Au*-metal, graphene, and analyte. The topmost layer of the sensing region is the analyte. Organic compound glucose is used as analyte and sensor performance is examined for various glucose RI values. If ε_{sense} and n_{sense} being the dielectric constant and RI of the sensing sample respectively, then we may write, $\varepsilon_{sense} = n_{sense}^2$. SPR resonant condition for excitation of SPW can be expressed as given below [34]:

$$\frac{2\pi}{\lambda} n_1 \sin\theta_{in} = Re\left(k_{splasmon}\right), \qquad (3.4)$$

where $k_{splasmon} = \frac{\omega}{\bar{c}} \sqrt{\frac{\varepsilon_{metal}\varepsilon_{sense}}{\varepsilon_{metal}+\varepsilon_{sense}}} = \frac{2\pi}{\lambda} \sqrt{\frac{\varepsilon_{metal} n_{sense}^2}{\varepsilon_{metal}+n_{sense}^2}}$ (3.5)

is the SPW propagation constant and $\bar{c}$ represents the light speed in vacuum. The light propagation constant is represented by left side part of Equation (3.4). The slight variations in RI δn_{sense}, shifts the resonant angle, θ_R. With a small shift in resonant angle θ_R, angular sensitivity is to be computed for the sensor. When the EM-field propagates in the fiber core, then in the sensing area the EM-field penetrates deeper into active metal and interaction takes place between the two at metal-dielectric interface (MDI). When there is no external charge and current, then EM-field in a fiber

is expressed by Maxwell's field equations (1.2-1.5), and modified as written below [109]:

$$\vec{\nabla} \times \vec{E}(c,t) = -\frac{\partial \vec{B}(c,t)}{\partial t}, \quad (3.6)$$

$$\vec{\nabla} \times \vec{H}(c,t) = -\vec{J}(c,t) + \frac{\partial \vec{D}(c,t)}{\partial t}, \quad (3.7)$$

$$\vec{\nabla} \cdot \vec{D}(c,t) = -\rho \vec{B}(c,t), \quad (3.8)$$

$$\vec{\nabla} \cdot \vec{B}(c,t) = 0, \quad (3.9)$$

In the above equations, $\vec{E}$ represent the electric field strength, $\vec{H}$ represent magnetic field strength, $\vec{D}$ represent the dielectric field strength and $\vec{B}$ represent the magnetic induction field strength in above Equations (3.6-3.9).The symbols $\vec{J}$ and ρ represent the current and charge density respectively. Symbol *c* represents the spatial reference coordinate. For SPR sensor structural model for simulation, the wave propagation takes place in *z*-direction and we may express it as given below [109]:

$$H(x,y,z,t) = H(x,y)e^{j(\omega t - \beta z)} \quad (3.10)$$

In the above equation, ω represents the angular frequency and $\beta = \beta' + j\beta''$ represents the propagation constant of SPW. Now let us start with Maxwell's equations where the E-field and H-field are having harmonic oscillations in time with some frequency ω. The value of ϵ and μ is constant and no current or free charges exists. The fields then become $\vec{E}(t) = \vec{E}e^{-i\omega t}$ and $\vec{H}(t) = \vec{H}e^{-i\omega t}$. Then we may write as [109]:

$$\vec{\nabla}.(\varepsilon \vec{E}) = 0 \quad (3.11)$$

$$\vec{\nabla}.(\mu \vec{H}) = 0 \quad (3.12)$$

$$\vec{\nabla} \times \vec{E} = i\omega\mu\vec{H} \quad (3.13)$$

$$\vec{\nabla} \times \vec{H} = -i\omega\varepsilon\vec{E} \quad (3.14)$$

Taking the curl of Eq. (3.14) and inserting Eq. (3.13), we get equation as given below:

$$\vec{\nabla} \times \left(\vec{\nabla} \times \vec{H}\right) = \omega^2 \mu \varepsilon \vec{H} \qquad \textbf{(3.15)}$$

$$\vec{\nabla} \times \left(\vec{\nabla} \times \boldsymbol{H}\right) - \omega^2 \mu \varepsilon \vec{H} = \mathbf{0} \qquad (\mathbf{3.16})$$

Assuming that μ is not spatially dependent, then equation (3.16) may be expressed as [109]:

$$\vec{\nabla}\left(\vec{\nabla}.\boldsymbol{H}\right) - \vec{\nabla}^2 \vec{H} = {k_0}^2 \vec{H} \qquad (\mathbf{3.17})$$

If k_0 be the spatially dependant wave number then with ${k_0}^2 = \omega^2 \mu \varepsilon$, we may write the above equation as:

$$\vec{\nabla} \times \left(\vec{\nabla} \times \vec{H}\right) - {k_0}^2 \vec{H} = \mathbf{0} \qquad (\mathbf{3.18})$$

An eigen value equation for the magnetic field H, which is solved for the eigen value $\lambda = -j\beta$, is derived from Helmholtz equation and is given as [110]:

$$\vec{\nabla} \times \left(n^{-2} \vec{\nabla} \times \vec{H}\right) - k_0^2 \vec{H} = \mathbf{0} \qquad (\mathbf{3.19})$$

The Helmholtz relationship is an approximation of the wave equation that develops from Maxwell's field equations**.** In SPR material, the RI is generally a complex number. Therefore the real part of the RI, slow down the wave and therefore wavelength decreases. Also RI is having value greater than 1. On the other hand, RI imaginary part causes an exponential attenuation of the EM wave. Now, SPR excitation is possible only by TM-wave or p-polarization. In transverse magnetic wave, the magnetic wave vector is always perpendicular to the direction of propagation. Figures (3.2a-3.2d) depicts the magnetic field distribution and the evanescent waves at the MDI interface for different RI of glucose i.e.1.3337, 1.3447, 1.3508 & 1.3603. All these figures depict the surface magnetic field strength, z-component (*A/m*) as wave propagation is considered to be in z-direction. The maximal and minimal values of surface magnetic field strength are (301.281 & -301.018), (297.911 & -297.586), (293.404 & -292.906) and (544.938 & -543.935) for different RI values of 1.3337, 1.3447, 1.3508, and 1.3603 respectively.

(a)

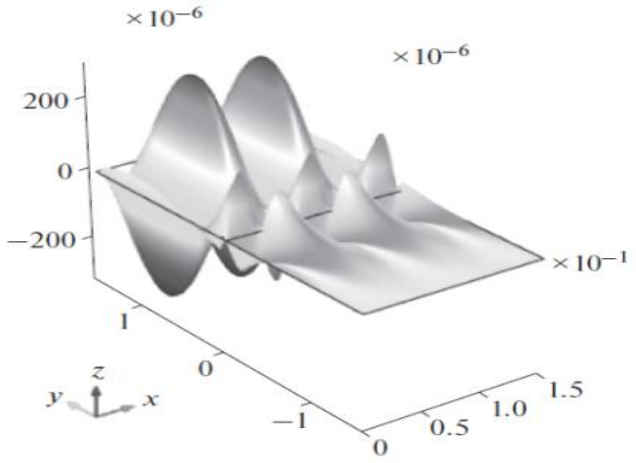
×10−6
×10−6
200
0
−200
×10−1
1
0
−1
z
y
x
0
0.5
1.0
1.5

(b)

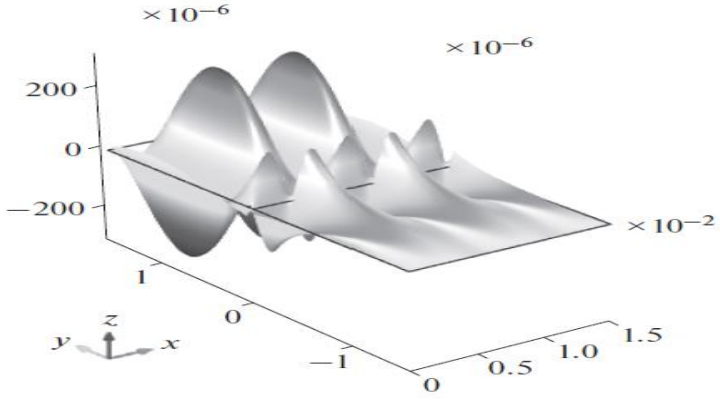
×10−6
×10−6
200
0
−200
×10−2
1
0
−1
z
y
x
0
0.5
1.0
1.5

(c)

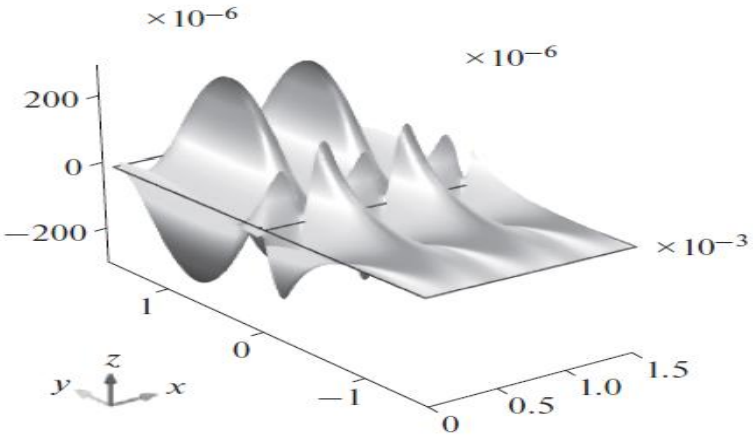
×10−6
×10−6
200
0
−200
×10−3
1
0
−1
z
y
x
0
0.5
1.0
1.5

(d)

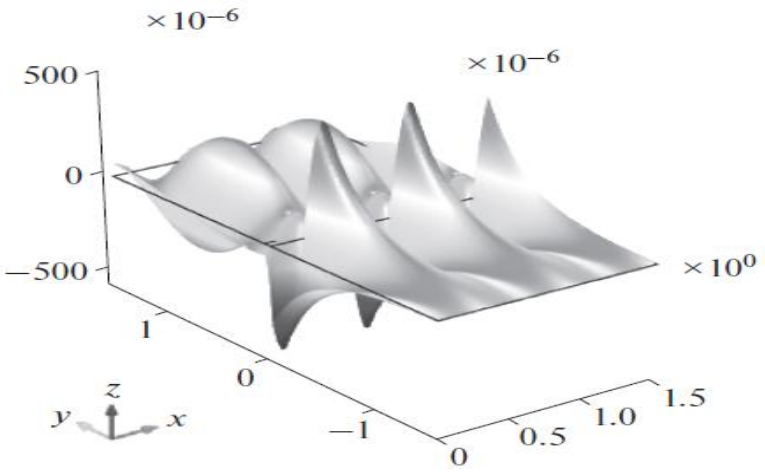

Figure 3.2: Surface Magnetic Field Distribution for Different RI values of Glucose (a) 1.3337, (b) 1.3447, (c) 1.3508 and (d) 1.3603

Well-known angular interrogated technique has-been employed to investigate the behavior of SPR in terms of RI sensitivity. For this both SPR curve width and SPR reflectance shift has to be included. The enhanced sensitivity of the 2D material based SPR sensor has been linked to both the field enhancement at the sensing interface. In addition to this magnetic field has a direct effect on the polarization of the transmitted light signal passing through a dielectric media. The plasmonic sensor is based on the interaction of magnetic field with the optical properties of SPR active materials which are included in the SPR sensing design. Finally, the plasmonic phenomenon results in sensitivity enhancement and is also utilized to modulate the resonance conditions. The magnetic field intensity of SPs is at peak value at the cross point between the metal and dielectric, and slowly decreasing as the depth of dielectric increasing. Based on the field intensity distribution characteristics, it is generally used to evaluate the degree of excitation of SPs at the interface and the resonance intensity of SPR, and estimating whether plasmonic biosensor has enhanced sensing performance.

Figure 3.3(a) depicts the TM Reflectance curve relationship with angle of incident for different RI of glucose i.e. 1.3337 (curve-1), 1.3447 (curve-2), 1.3508 (curve-3),

1.3603 (curve-4) and 1.3702 (curve-5), for A*u* thin film of 60*nm* thickness and graphene thin film of 10*nm* thickness. The RI values of glucose have been adopted from ref. [111]. In addition to this, for better understanding refractive and dispersive optical properties of some other organic substances have also been studied [112]. From the TM reflectance curve it clear that resonant angle shift is increasing with change in RI of glucose.

(a)

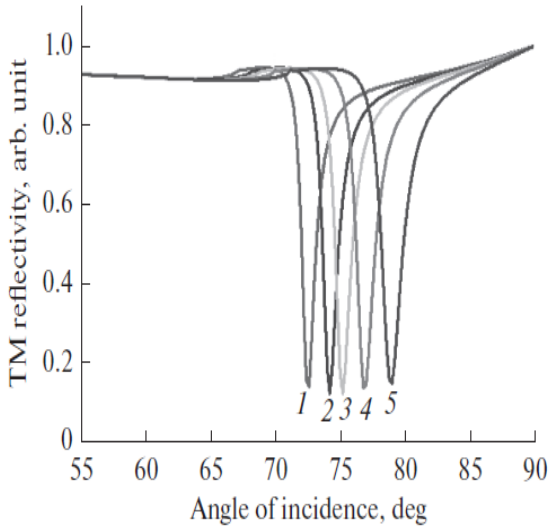

(b)

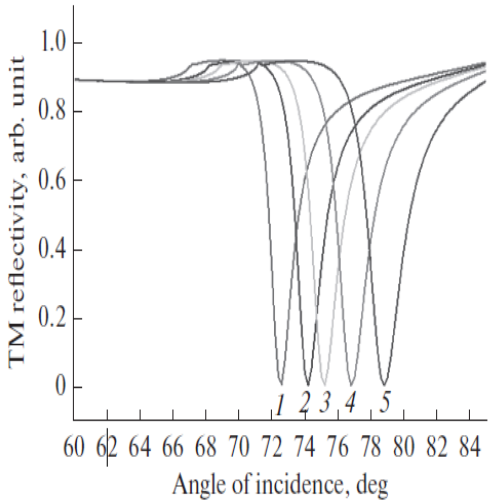

Figure: 3.3 Relationship between TM Reflectance and Angle of incidence (*deg*) for Different RI of Glucose for (a) *Au*-thin film of 60*nm* thickness and graphene-thin film of 10*nm* thickness
(b) *Au*-thin film of 50*nm* thickness and graphene-thin film of 10*nm* thickness.

Similarly, Figure 3.3(b) depicts the TM Reflectivity curve relationship with angle of incidence for different RI of glucose i.e. 1.3337 (curve-1), 1.3447 (curve-2), 1.3508 (curve-3), 1.3603 (curve-4) and 1.3702 (curve-5), for *Au* thin film of 50*nm* thickness and graphene thin film of 10*nm* thickness. In the above Figure 3.3(a-b), TM reflectivity is expressed in arbitrary units and angle of incident is expressed in degree. The SPR curve from 1 to 5 corresponds to various glucose refractive indices 1.3337, 1.3447, 1.3508, 1.3603 and 1.3702 respectively. We observed that a small change in refractive index produces a appreciable shift in resonant angle and it is measurable. From the simulation observation, the computed values of FWHM and angle of resonant, θ_R for various RI values of the sample glucose, are listed in Table 3.2.

Table 3.2: Resonant angle, θ_R (degree) and FWHM (degree) for various RI of sample glucose

Sample RI	***FWHM***	***Resonant Angle,*** θ_R
1.3337	1.04 deg	72.48 deg
1.3447	1.21deg	74.21 deg
1.3508	1.39 deg	75.23 deg
1.3603	1.41 deg	76.87 deg
1.3702	1.73 deg	78.96 deg.

The relationship between full-width half maximum and various refractive indices of glucose for *Au* thin film of 60*nm* thickness and 50*nm* thickness and graphene thin film of 10*nm* fixed thickness is depicted in Figure 3.4.The full width half maximum has been observed to rise with rises in RI of glucose for *Au* thin film of 60*nm* thickness and 50*nm* thickness. A fixed thin film thickness of 10*nm* of 2D material graphene has been chosen for reducing the complexity of aforesaid sensor design.

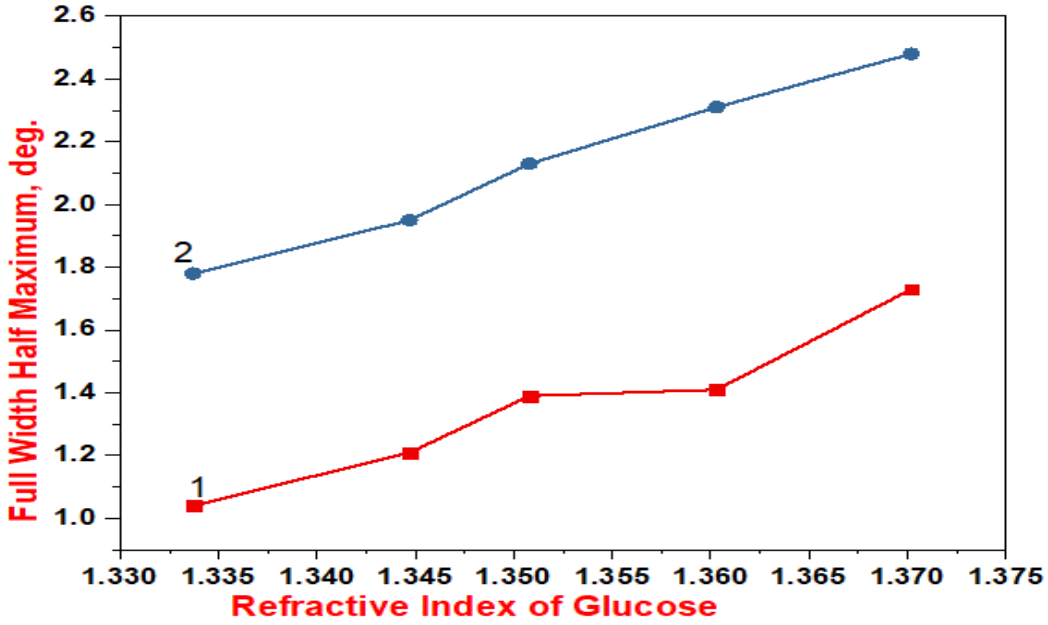

Figure 3.4: The relationship between the full-width half maximum (*deg.*) and various RI values of glucose. Red line (1): *Au*-thin film of 60*nm* thickness and graphene thin film of 10*nm* thickness. Blue Line (2): *Au*-thin film of 50*nm* thickness and graphene thin film of 10*nm* thickness.

Results conclude that the aforesaid design of the 2D material based SPR sensor displayed a larger shift in resonant angle. Figure 3.5 depicts the relationship between resonant angle (θ_R) and RI of glucose. As it is clear from the Figure 3.5 that θ_R rises with rise in refractive index of glucose for both *Au* thin film of 60*nm* thickness and 50*nm* thickness and graphene thin film of 10*nm* thickness. But sensor with 60*nm* thin *Au* film shows abrupt increase in resonant angle as compared with sensor having 50*nm* thin *Au* film. Better shift in resonant angle will ultimately leads to better sensitivity with enhanced performance and accuracy. Simulation observations concludes that sensor with *Au* thin film of 60*nm* thickness and graphene thin film of 10*nm* thickness exhibit enhanced performance with highest sensitivity of $198 degree.RIU^{-1}$ in the RI range from 1.3337 to 1.3702 as depicted in Figure 3.6(a). On the other hand sensor with *Au* thin film of 50*nm* thickness and graphene thin film of 10*nm* thickness has the sensitivity of $192 degree.RIU^{-1}$in the RI range from 1.3337 to 1.3702 as depicted in Figure 3.6(b).

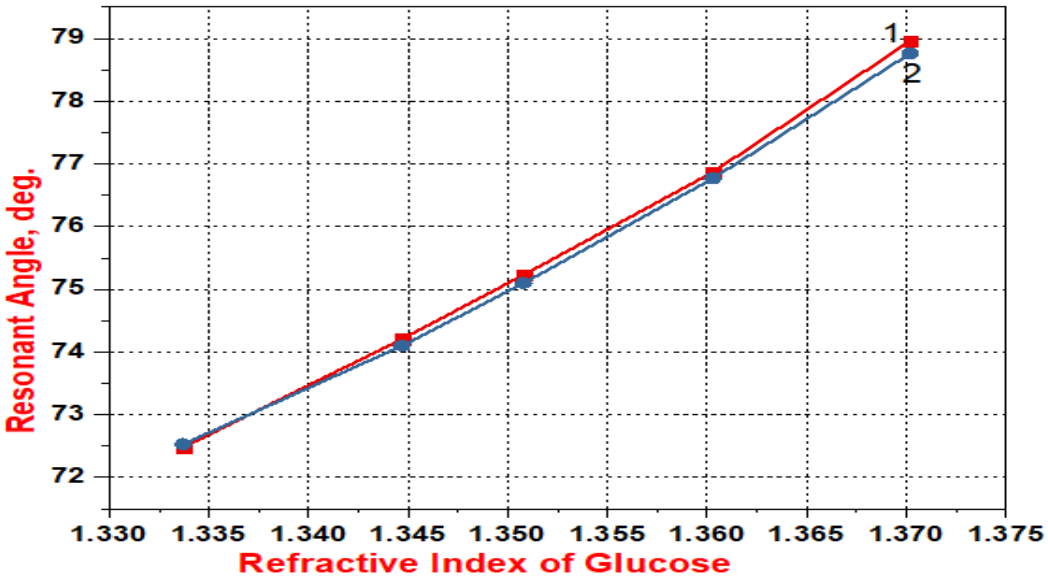

Figure 3.5: Relationship between the SPR Resonant Angle (*deg*) and Various RI of Glucose. Red line (1): *Au* thin film of 60*nm* thickness and Graphene thin film of 10*nm* thickness. Blue line (2): *Au* thin film of 50*nm* thickness and Graphene thin film of 10*nm* thickness.

(a)

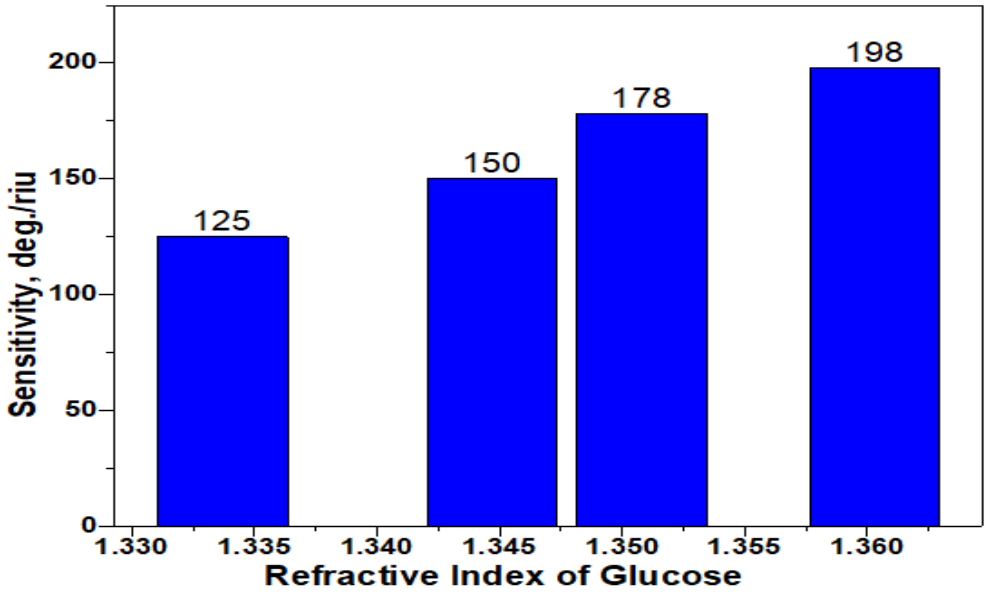

(b)

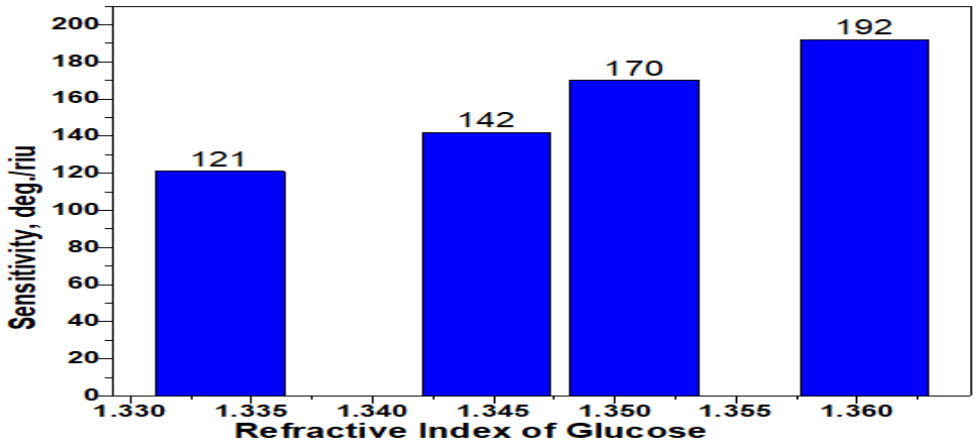

Figure 3.6: Sensitivity (*Deg/RIU*) variation with Various RI Values of Glucose (a) *Au* thin film of 60*nm* thickness and graphene thin film of 10*nm* thickness (b) *Au* thin film of 50*nm* thickness and graphene thin film of 10*nm* thickness.

3.5 Outcomes of the Proposed Sensor Design

In this chapter, the adoption of 2-dimensional material graphene and active metal *Au* for fiber optic SPR sensor design has been discussed. FEM simulation technique is adopted for the aforesaid sensor structure, sensitivity computation and for observing the field distribution. Aforesaid design of two-dimensional material based SPR sensor utilizing *Au* thin film of thickness *60nm* and graphene thin film of *10nm* thickness exhibit highest sensitivity $\approx 198\ degree/RIU$ in glucose RI sensing with range from 1.3337 to 1.3702. The aforesaid design of the sensor has the great potential in biomedical field and it can be useful for glucose sensing in medical diagnostics for the benefit of community health. The 2-dimensioanl material graphene has amazing properties. Further, it improves the sensor performance. Typical TM reflectivity curves are shown using COMSOL commercial software package.

Chapter 4
Bimetallic Diffraction Grating based SPR sensor

4.1 Introduction

This chapter presents the resonant impact of metal diffraction grating on the performance of SPR sensor. The bimetallic diffraction grating consists of gratings of metals like gold, silver, aluminum etc. The sensor can be used for sensing variety of organic compounds like glucose, sucrose etc. High sensitivity is attained if *-ve* order of diffraction of metal grating is used to excite the SPs. Therefore, SPWs are excited by -1^{st} order of diffraction. Using numerical simulation sensing performance is estimated in terms of sensor sensitivity, reflectance amplitude, width of the SPR curve & shift in resonant angle. These factors are considered for the bio-sensing performance analysis. Results shows that bimetallic diffraction grating based surface plasmon resonance sensor proves to be best for sensing applications and provides maximum sensitivity in angular interrogation with good linearity.

In the last three decade, SPR technology has got strong positive points because of its real-time, label free bio-molecular detection. Prism based RI sensors got replacement with diffraction grating based sensor because of the drawbacks of Prism RI sensors such as angle control accuracy, heavy weight and integration problems. In some applications, contrasts grating based optical sensors are used [113]. But diffraction grating design-based SPR sensors have different concept from the operating point of view and are different from others [110]. They have advantage of high sensitivity as compared to others sensors. The conventional SPR sensor have only coating of different SPR active material leading to surface plasmon waves but in the bimetallic diffraction grating design-based sensor, light wave is made to fall on metallic grating and with incidence plane perpendicular to the grating grooves. The incident light wave

at the grating surface is partly reflected and partly divided into sequence of diffraction waves with particular diffracted orders. High sensitivity is obtained if negative diffraction order of metallic grating is used to excite the surface plasmons. Bimetallic diffraction grating-based SPR sensors exhibit a sharper reflectivity dip and perform better in sensitivity and resolution. Also aluminum grating based SPR sensors are more affordable too. In literature, many researchers have shown their interest in metallic diffraction grating based sensor and investigated the sensors for achieving enhanced sensitivity. Wei Su *et al.* [75] designed a metallic based diffraction grating sensor which exhibits best sensitivity when aluminum noble metal is used. Rigorous coupled wave analysis technique has been employed for sensitivity evaluation of the optimized sensor. With angular interrogation method, the sensitivity of *Al*-diffraction grating based designed sensor was found to be $245 degree\text{-}RIU^{-1}$. Hu *et al.* [65] have also shown the performance of bi-metallic (*Al-Au*) based diffraction grating refractive index sensor. Accordingly, the full width and half maximum and TM reflectivity dip were considered as the main influencing factor on the outcome of the sensor. Further the performance was estimated based on the quality parameter χ, which relates the reflectance characteristics and angular shift with the distinct RIs value of sensing sample. With optimized parameters, the angular sensitivity and quality factor was found to be $187^{o}/RIU$ and $201 RIU^{-1}$ respectively. Li *et al.* [114] have experimentally shown the diffraction grating based refractive index sensor. They have also made the use of a polymer photo-resist for holding the thin gold plates with lithography process. With simple and best output nanofabrication, the RI biosensor exhibited excellent figure-of-merit (FOM). A brief comparison between PSPR based RI sensor (which are prism based) and LSPR RI sensor which are nanoparticles based, has also been illustrated. Yan *et al.* [76] have fabricated the metallic diffraction grating based SPR D structure FO sensor for measuring the RI of pure water and isopropanol. Metallic gratings with suitable thickness and grating constant have been created on the 20*nm* *Au*-layer which is deposited on the side of the fiber. With optimized values of the

grating constant and residual cladding, the D-shaped SPR sensor exhibited enhanced sensitivity of 917$nm.RIU^{-1}$. Lin *et al.* [77] presented *Pd*-based (Palladium) diffraction grating optical sensor for the detection of hydrogen. Distinct parameters like grating period, *Pd*-layer thickness and values of gold sub-wavelength grating have been taken into consideration for measuring the performance. An estimate of H_2-concentration value of 0.001% was exhibited by metallic diffraction grating based H_2 sensor. This chapter presents the bimetallic diffraction grating design sensor. The different SPR active metal combination like aluminum & gold, are used to get enhanced sensitivity in grating based [78-79] surface plasmon sensor. The aforesaid design based grating sensor exhibits the enhanced sensitivity and linearity response in sample sensing.

4.2 Theoretical Explanation

When a p-polarized light at a suitable wavelength, is launched in to the one end of the fiber then under the case of phase match, the surface plasmon waves (SPW) [66] are produced at the interface between metal and dielectric. The excitation of SPs at MDI leads to transference of energy to SPs & it diminishes the intensity of the reflected light. When the normalized reflected light intensity, which is generally the observed output signal, is measured with respect to incident angle (*deg*.) then the dip is detected at resonant angle θ_{RDA} owing to effective transference of signal energy to SPs. This angle is denoted by θ_{RDA}. θ_{RDA} is the reflectance dip angle. The method is known as angular interrogation. The measurement of reflected light intensity with respect to wavelength is known as wavelength interrogation method and resonant wavelength λ_{reso} is observed. SPR sensor sensitivity depends on how much resonance dip angle or resonant wavelength λ_{reso} shifts with a change in refractive index of the sensing medium. If the shift is large, the sensitivity is large.

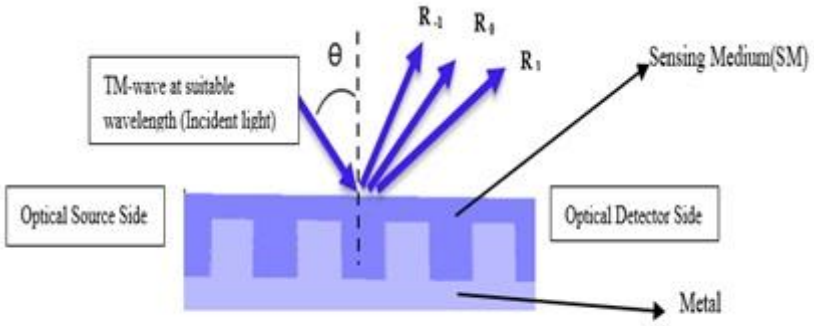

Figure 4.1: General Design of Multiple Metallic Grating based SPR Sensor.

Figure 4.1 shows the general structure design of the multiple metallic grating based refractive index SPR sensor. Here, a TM-wave, at a certain angle of incidence is made to fall on the rectangular gratings [66] and finally at the optical detector side, the reflected wave is observed. The length of the sensing region is 4*mm*. Figure 4.2 shows the metallic grating unit cell and in this figure T represents grating period, w represents grating width and d represents grating depth and ratio, $f = w/T$ represents duty cycle.

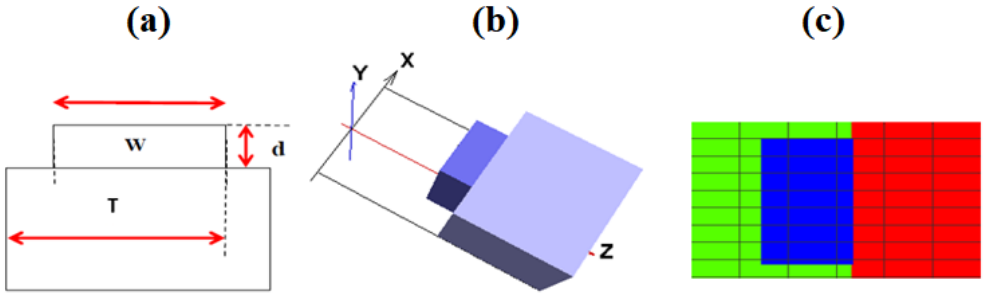

Figure 4.2: Metallic Grating unit cell (a) Schematic (b) 3D Layout (c) 2D Ref_Index_Re(y).

By using such types of gratings with suitable dimensions, we can design the complete grating-based sensor as shown in Figure 4.1 and can be used for refractive index sensing of various compounds.

4.3 Grating Results and Discussions

When a TM-wave, at a certain angle of incidence is made to fall on the rectangular gratings then on the grating surface, the TM wave is split up into a series of diffracted waves. We can express the matched conditions of the wave vector as [75],

$$\boldsymbol{k_0 n_{sense}\, sin[\theta_{RDA}] + m\frac{2\pi}{T} = \pm k_0 \sqrt{\frac{\varepsilon_m n_{sense}^2}{\varepsilon_m + n_{sense}^2}}} \qquad (\mathbf{4.1})$$

In above Equation, ε_m represents the permittivity of the metal and $\varepsilon_m = \varepsilon_{mr} + i\varepsilon_{mi}$, T represents the grating period, θ_{RDA} represents the reflectance dip angle, k_0 represents the free space wave vector of TM-wave, n_{sense} represents the RI of the analyte, integer *m* computes the diffracted waves ordering. No diffraction [66] occurs for integer of order $m = 0$; means there is direct transmission of light through the grating. For first positive diffracted order ($m = +1$), light colors with increasing wavelengths (from blue to red) are diffracted at increasing angles which corresponds to diffracted waves of order $m>0$. For first negative diffracted order ($m = -1$), light colors are diffracted at decreasing angles which corresponds to diffracted waves of order $m< 0$. The design has been numerically simulated for the different refractive indices of glucose. According to Equation (4.1), if the value of λ remains unchanged, then in angular interrogation method, the sensitivity of the sensor is found to be [75],

$$\boldsymbol{S_{Grating} = \left|\frac{\delta\theta_{RDA}}{\delta n_{sense}}\right| = \left|\frac{1}{n_{sense}} \cdot sec\,\theta_{RDA} \cdot \left\{\pm\left(\frac{\varepsilon_m}{\varepsilon_m + n_{sense}^2}\right)^{1.5} - sin\,\theta_{RDA}\right\}\right|} \qquad (\mathbf{4.2})$$

In Equation (4.2), $S_{Grating}$ is an important sensitivity parameter of the grating-based sensor, ε_m is the permittivity of the metal, n_{sense} is the RI of the analyte. θ_{RDA} is the reflectance dip angle or in other words, it is the angle at which the sharp dip occurs in the TM reflectance intensity. This angle is also known as resonant angle. θ_{RDA} is responsive to changes in the RI of the analyte, n_{sense} . $\delta\theta_{RDA}$ indicate a small change in reflectance dip angle and δn_{sense} indicates a slight change in RI of the analyte. The various values of RI of the sensing medium, n_{sense} are 1.3337, 1.3447, 1.3508, 1.3603

and 1.3702.

Now the condition which has to be satisfied for the effective excitation of plasmon waves is $|\varepsilon_m| =>> n_{sense}^2$. Thus Equation (4.1), gives us the expression for the resonant angle, as given below [75]:

$$\boldsymbol{sin[\theta_{RDA}] = \pm 1 - m\frac{\lambda}{T\, n_{sense}}} \qquad (\mathbf{4.3})$$

In Equation (4.3), T is the period of grating, m is the diffraction order, λ is the wavelength, θ_{RDA} is the reflectance dip angle, n_{sense} is the RI of the sensing medium (analyte). One more required thing for positive and negative order of diffraction is the ratio $\frac{T}{\lambda}$. This ratio has to satisfy the following condition [75][77],

$$\frac{T}{\lambda} > \frac{m}{n_{sense}} \qquad \textit{(Diffracted waves of order } m > 0) \qquad \mathbf{(4.4)}$$

$$\frac{|m|}{2 \cdot n_{sense}} < \frac{T}{\lambda} < \frac{|m|}{n_{sense}} \qquad (Diffracted\ waves\ of\ order\ m < 0) \qquad (\mathbf{4.5})$$

The dielectric constant of the active metal can be find with Lorentz–Drude model & is expressed as given below [115],

$$\boldsymbol{\varepsilon(\omega) = \varepsilon_{r,\infty} + \sum_{n=o}^{z} \frac{f_n \omega_p^2}{\omega_n^2 - \omega^2 + j\omega\Gamma_n}} \qquad (\mathbf{4.6})$$

In Equation (4.6), $\varepsilon_{r,\infty}$ represents the dielectric constant at infinite frequency, ω_p represents the plasmon frequency and ω_n, f_n and Γ_n represents the resonance frequency, strength and damping frequency [116][117] respectively of the *nth* oscillator.

The grating period is greatly dependent on the metallic layer thickness, as a result of the change in the propagation constant of surface plasmon politrons. More significantly, the grating period T and the diffraction order, m dominates the value of sensitivity. Higher sensitivity is achievable for SPR sensors with a larger grating period and lower diffraction order. SPR sensor is simulated for different refractive indices of organic compound, using COMSOL Multiphysics software. Here for SPR

excitation, TM-wave (p-polarized light) is used. Figures (4.3a-4.3d) shows the magnetic field distribution and the surface plasmon waves (evanescent waves) at the interface for various RI of glucose i.e. 1.3337, 1.3447, 1.3508 & 1.3603. All these figures depicts the surface magnetic field distribution, z-component ($A.m^{-1}$) and wave propagation is supposed to be in z-direction.

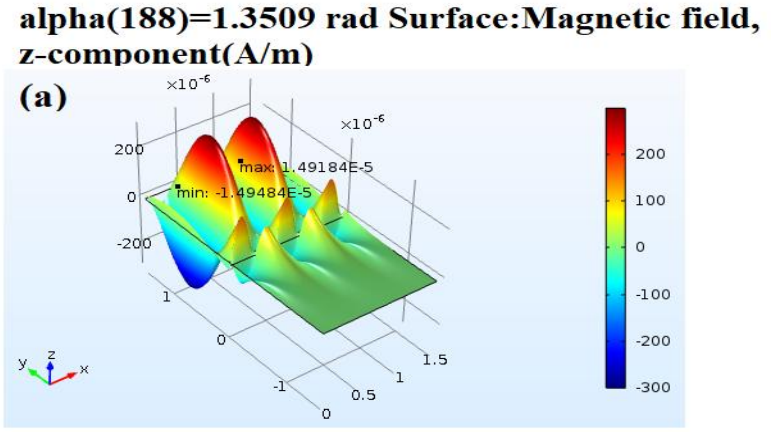

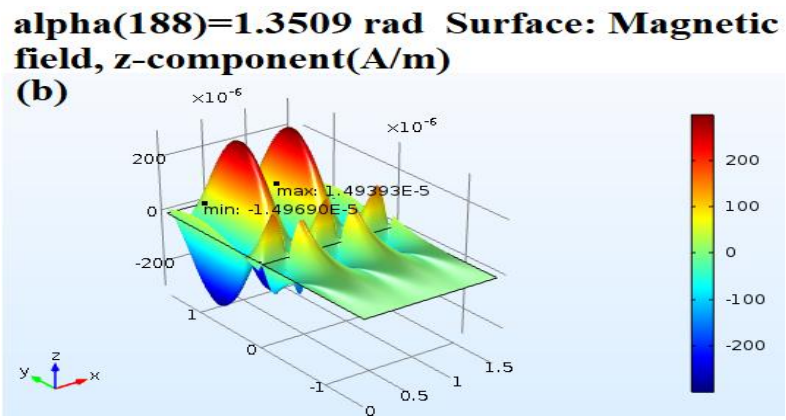

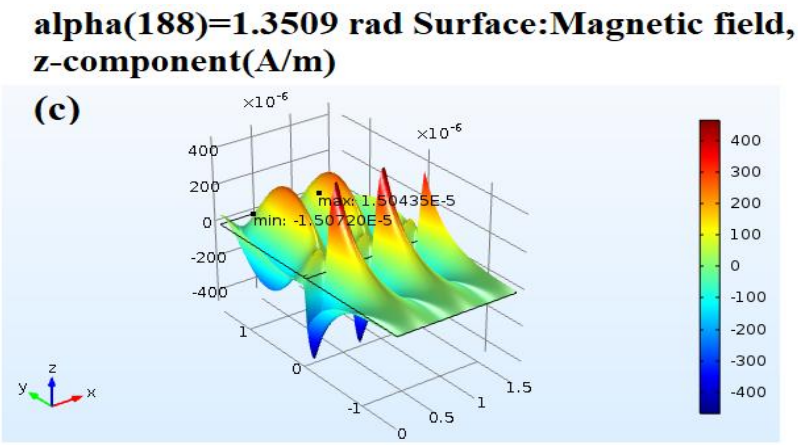

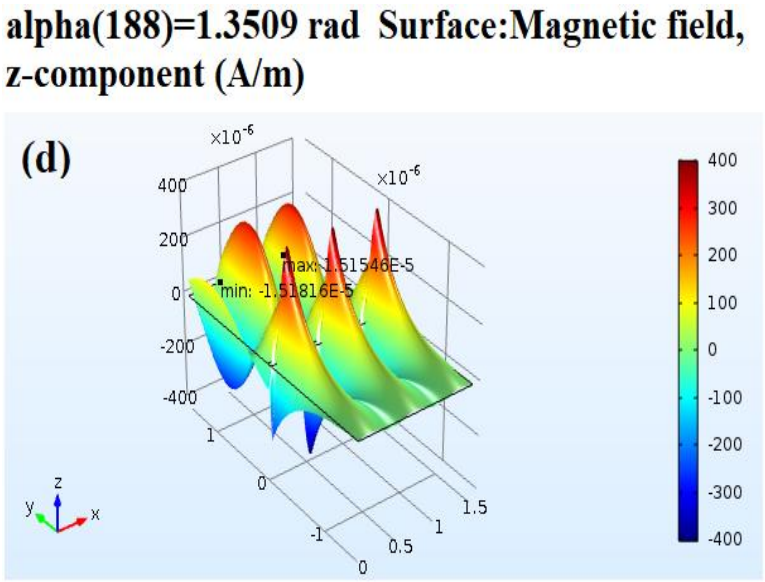

Figure 4.3: Field Distribution for Glucose Refractive Indices (a) 1.3337 (b) 1.3447 (c) 1.3508 and (d) 1.3603 respectively.

In simulation, we have obtained the TM reflectivity variation for *-1st* diffraction order for different bimetallic combinations and it is shown in Figure 4.4 for *Au*=60*nm* and *Al*=20*nm*. The grating depth d, grating width w, and duty cycle, *f* =*w/T* of the metal grating has been taken as 80*nm*, 250*nm* and 0.6, respectively. The wavelength of the incident plane wave light is chosen as 1500*nm*. We have taken the value of grating period, T as 400*nm*. TM reflectivity variation for *-1st* diffraction order by considering the grating depth d, grating width w, and duty cycle, *f* =*w/T* of the metal grating as 60*nm*, 250*nm* and 0.7, respectively for *Au*=50*nm* and *Al*=10*nm* is shown in Figure 4.6. Here the grating period, T has been taken as 350nm.

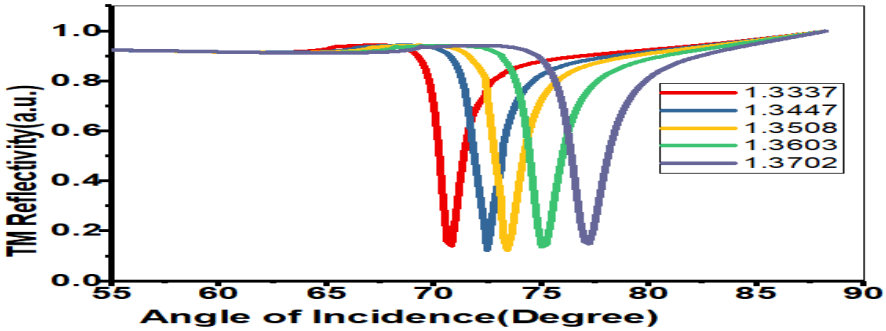

Figure 4.4**:** TM Reflectivity Variation with Angle of Incidence for *-1st* Diffraction Order with *Au*=60*nm* and *Al*=20*nm*.

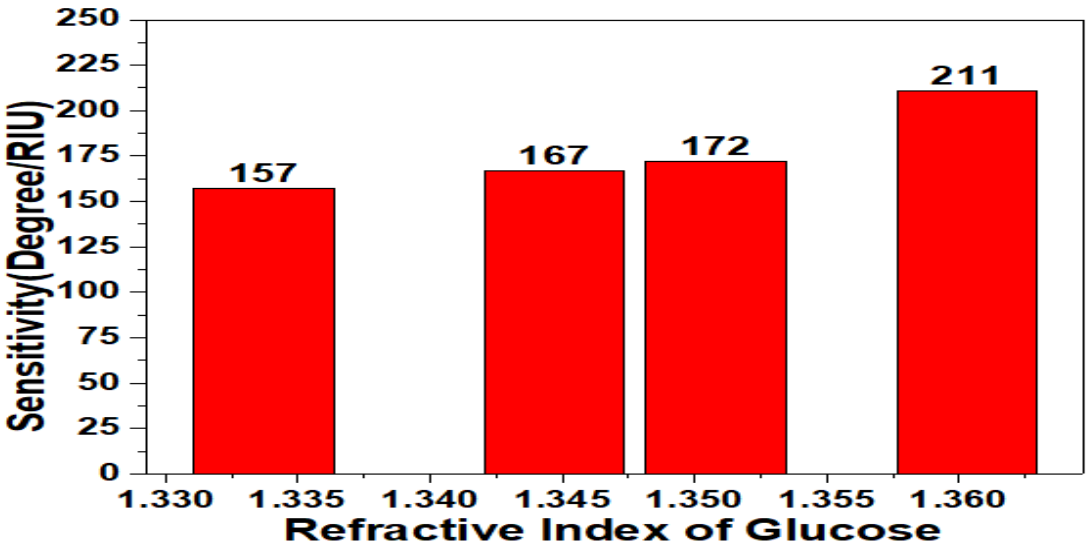

Figure 4.5: Sensitivity Variation with Glucose Refractive Index for *Au*=60*nm* and *Al*=20*nm*.

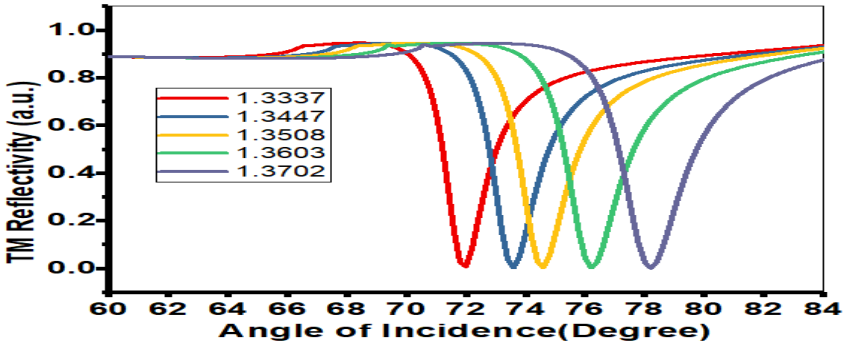

Figure 4.6: TM Reflectivity Variation with Angle of Incidence for *-1st* Diffraction Order with *Au*=50*nm* and *Al*=10*nm*.

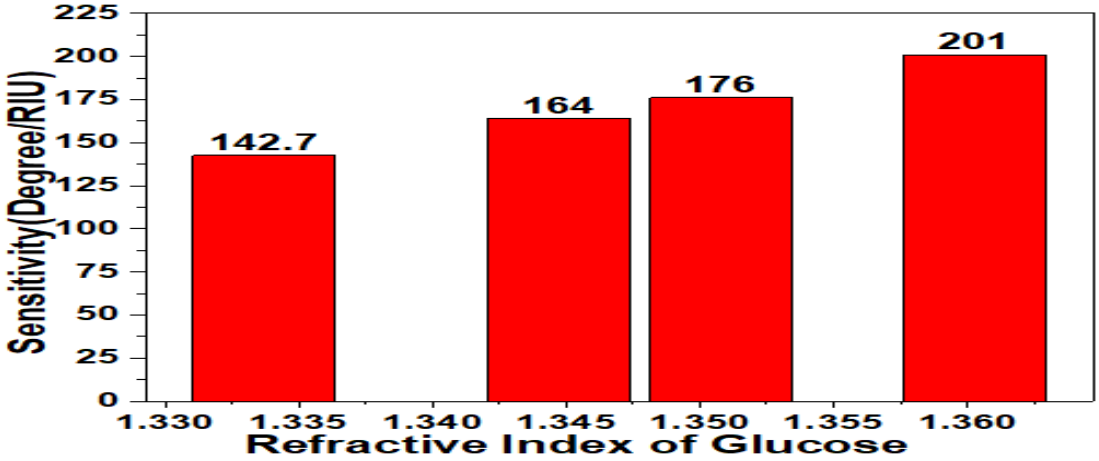

Figure 4.7: Sensitivity Variation with Glucose Refractive Index for *Au*=50*nm* and *Al*=10*nm*.

The calculated sensitivity value and its variation with glucose RI for various cases of metallic combinations is depicted in Figure 4.5 and Figure 4.7. The sensitivity has been found to increase with increase in refractive index of glucose for two best combinations of active metals. But the combination, *Au*=60*nm* and *Al*=20*nm* is most favourable bimetallic combination for the sensor design & it shows the highest sensitivity of 211°*/RIU*.

4.4 Outcomes of the Proposed Sensor Design

In this work, we have reported a bimetallic diffraction grating based SPR sensor which is highly sensitive. The designed sensor is simulated using COMSOL multiphysics software for different refractive index of glucose. We have shown the performance of the sensor for different bi-metallic combinations. The aluminum grating based SPR sensor provides the utmost performance and sensitivity provided by *Al* based sensor is best. But this SPR active metal has poor chemical stability so we have utilized bi-metallic combinations. After performing number of iterations with COMSOL Multiphysics software and taking different thickness of bimetallic combinations, we have found that in the given sample RI range (1.330-1.360), two combinations which provides the enhanced sensitivity are with *Au*=60*nm*, *Al*=20*nm* and *Au*=50*nm*, *Al*=10*nm*. But the bimetallic combination with *Au*=60*nm* & *Al*=20*nm*, exhibits maximum sensitivity of the order of 211°*/RIU*. The sensitivity exhibited by second bimetallic combination (*Au*=50*nm*, *Al*=10*nm*) is less i.e. 201°*/RIU*. The most favourable bimetallic combination for the sensor design is first one. Having the property of bimetallic diffraction grating, the proposed design of the SPR sensor can be realized for sensing variety of organic compounds.

Chapter 5
Optical Fiber Sensor Based on SPR utilizing Circular AuNR array

5.1 Introduction

In the epoch of nanotechnology, SPR sensor utilizing nobel metal nanoparticles have a huge potential in the growth of innovative biosensors technology or in the advancement of existing optical bio-sensing methods to for the benefits of community health in medical diagnostics. Nobel metal nanoparticles have attractive properties which makes them suitable candidate for the development of a different type of plasmonic bio-sensors. In this chapter, FOS based on SPR technology employing Au nanorod array having circular shape, is presented. In nanotechnology domain, usually nanorod dimensional range extends from 1nm to 100 nm. Nanords synthesizing result from the use of metals or semiconductor substances. Usually the standard aspect ratio is 3 to 5. In plasmonic domain, there exist many active metals such Au, Ag, Al and Cu etc, which exhibit plasmonic phenomenon. Therefore the active NPs have the capability to assist the resonant phenomenon at MDI. Apart from the above, NPs do assist in proper scattering and absorbing of wave and peaks of λ_{reso} are highly perceptive to the NPs dimensions, their architecture, and local medium [118]. These properties of nanoparticles [119], have strong contribution in the development of applications based on bio-technology research [120–122] and other scientific technology [123]. Furthermore the essential application of SPR exists in light sensor, characterization of distinct molecules at MDI [124], in instruments involving plasmonic phenomenon [125] and many more. In literature, various investigators have shown the use of nano-particles (NPs) in FO plasmonic sensor. Zeng *et al.* [87] proposed a plasmonic sensor with AuNRs and graphene for enhancing the RI sensitivity. The sensing response of the sensor was measured by carrying out the simulation and optimizing the aspect ratio of AuNR and number of graphene layers.

Sensor structural model was described theoretically by using Fresnel equations. Results concluded that ultimate enhanced sensitivity of $10^6 degree.riu^{-1}$ can be achieved with the aforesaid sensing design. In continuation with this, Cao *et al.* [86] developed a localized plasmonic biosensor employing AuNR that detects anti-human IgG. Multimode fibers (MMF) were used for developing the sensor. Human immunoglobulin G antibody was employed for functionalization of gold NR surface area. The relationship between resonance shift and RI of the sensing sample was recorded. Results concluded that plasmonic biosensor exhibits RI sensitivity of the order of $5.06 \times 10^{-7} nm\text{-}riu^{-1}$ and detection limit as 0.3×10^{-8} for detecting anti-human Immunoglobulin G antibody. Subramaniam Jayabal *et.al* [126] explained the surface modified AuNRs formation for finding poisonous metallic ions. Castellana *et.al* [127] presented a suitable methodology for chemical derivatization of AuNRs for mass spectrometry technique at $\lambda_r \cong 1064nm$. It was concluded that various bi-molecular entities are accurately chemically analysed by exposing the NRs to radiation at aforesaid wavelength. Experimental responses were found to be useful for certain analytical methods which are useful for ionizing the chemical species. Taylor *et.al* [128] have presented the multilayered stack optical AuNRs system for SPR wavelength detuning and readout. With detuning of 60*nm* from SPR wavelength shift, 16-layer readout with enhanced decline in laser power was achieved. In addition to the above, Chen *et.al* [88] presented a D-shaped plasmonic sensor utilizing array of AuNRs in square shape . Experimental results from FEM simulation concluded that enhanced sensitivity, $S_n = 6266 \times 10^{-9} RIU^{-1}$ is possible with thickness of square AuNR=70*nm* and the spacing nearly 50*nm*. The aforesaid sensor design exhibited good response in RI range extending from 1.33 to 1.39. Li *et.al* [129] employed FDTD simulation technique for studying the effect of various modes and configuration on sensor response in AuNR based plasmonic sensor. The FDTD simulated data indicated the presence of blue shift and red shift with longitudinal & transverse SPR, respectively. Ruan *et.al* [130] theoretically calculated the mode field (MFs) of two

types of optical fiber i.e. lead silicate (LS) fiber and Si-nanofiber. Results concluded that Si-nanofiber with 350*nm* diameter exhibits extinction efficiency 1600 times more than SMF, at 1100*nm* wavelength while 400*nm* diameter lead-silicate fiber exhibit extinction efficiency of only 640 times more than SMF. Lee *et.al* [131] presented a LSP enhanced photo-luminescence of $Mo\text{-}S_2$ single film with gold NRs that can be made with huge quantities. Experimental results concluded that the optical signal emission from $Mo\text{-}S_2$ single layer rises when the area density of gold NRs is $\cong 40/\mu m^2$. But it falls when gold NRs density is greater than $40/\mu m^2$. Chau *et.al* [132] explained the AuNR optics properties by using FME technique in a 3-dimensional view model. It was observed that appearance of spatially oscillating patterns due to near-field optical image is efficient for wave propagation of plasmonic mode.

This chapter presents the simulation analysis of sensors with circular AuNRs using FEM simulation technique. The size and shape of NRs does effects the magnetic field intensity and RI sensitivity of the aforesaid sensor. Also nobel metal nanorods are perfect absorbers and scatterers of light signal. The incidence of light signal at suitable wavelength, on the input side results in excitation of plasmonic oscillations at MDI. COMSOL FEM 5.2a commercial software package has been used to observe and study the field distribution at the interface and resonance wavelength. This chapter is arranged into four sections. After introduction part, Section 5.2 describes circular AuNRs based SPR Sensor. Section 5.3 explains the results and discussions concerning the performance of the aforesaid sensor. Finally, the outcomes are made in Section 5.4 of this chapter.

5.2 Circular AuNR based SPR Sensor

Figure 5.1 depicts the fiber optic sensor based on SPR utilizing array of circular AuNRs in sensing region. The cladding is removed from the core from the center of the optical fiber leaving behind the bare core. An array of AuNRs is applied on the fiber core to create sensing region. The sensing length of sensor has been considered as 6*mm*. The AuNRs have got absorption peaks which are highly adjustable in the

whole visible-IR range of the spectrum. At a applicable wavelength, the optical signal from laser light source is made to fall on the input side of the optical fiber. When the optical signal propagates through the fiber core, field interacts with the AuNRs (gold nanorods) due to this interaction plasmonic resonance phenomenon takes place. In the aforesaid AuNRs sensor design, we have used an array of AuNRs and arranged in a way as depicted in Figure 5.1. The *Au* dielectric constant is considered by Drude-Lorentz model [133] and most favourable values of various parameters of plasmonic metals are carefully adopted from ref.[134][116].

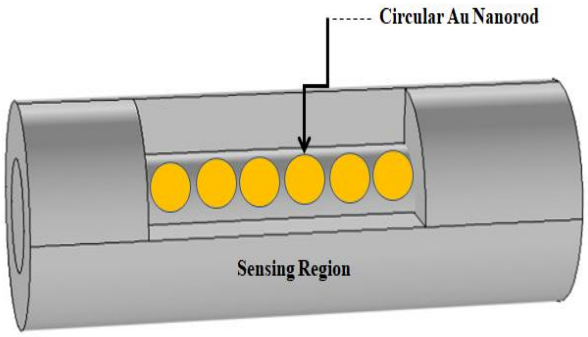

Figure 5.1: Schematic Representation of Circular AuNRs based SPR Sensor

SPW can be resonantly excited by totally internally reflected p-polarized wave or TM-wave for coupling of TM-wave into surface plasmon mode. There is exponential decay in the field strength at the interface. Maxwell's equations have a significant performance in determining the electric and magnetic field in sensing structure. For the aforesaid design simulation, we have used the wave optics module of FEM simulation. From frequency domain study of wave optics module, the Maxwell's equation solutions are attained. The generalized wave equation attained from solutions of Maxwell's equation is expressed as [135]:

$$\boldsymbol{\nabla \times \mu_r^{-1}(\nabla \times E_{scatt}) - \lambda_{wn}^2 \left(\frac{\varepsilon_r \varepsilon_0 \omega - i\sigma}{\omega \varepsilon_0}\right) E_{Scatt} = 0} \qquad (\mathbf{5.1})$$

$$\boldsymbol{E_{scatt}(x, y, z) = \widetilde{E}(x, y) e^{-ik\, z^z}} \qquad (\mathbf{5.2})$$

In the above equation, λ_{wn} represents the wave number, E_{scatt} represents the scattering E-field amplitude, ε_r & μ_r represents the medium relative permittivity and permeability. AuNRs in circular shape has been used in the design of the sensor.

AuNRs are suitable candidate for the enhanced performance of the SPR sensor in terms of RI sensitivity. For the proper propagation of light wave in the fiber core, the meshing of each domain should be perfect. Therefore for carrying out the FEM simulation, we have adopted the user-controlled mesh technique for the aforesaid AuNR based SRP sensor. The maximal element size has been chosen as $lambd0/8$ and minimal element size has been chosen as $3.68 \times 10^{-9} m$. The maximal element growth rate is chosen to be 1.3. Perfectly matched layer scaling parameter is selected as unity in geometry option.

5.3 Results and Discussions

FEM commercial package is adopted for simulating the structural model of AuNR sensor. Nanorod array consisting of 10-circular shaped AuNR is placed around bare core of the optical fiber. The absorption maxima (peak) of AuNRs are adjustable over the visible and IR region of the optical spectrum window. In the aforesaid design of the NRs sensor, we have performed the FEM simulation at 1200*nm* & 1300*nm*. The sensor shows good response in this region. During simulation, the impact of AuNR size on the sensing parameters has been observed. The normalized plot of E-field at 1200*nm* for AuNRs array has been examined, with spacing 200*nm* and various radius values. For distinct NRs size, maximal and minimal values of the surface magnetic field (z-component) have been examined at two distinct wavelengths. Considering the fact that electromagnetic wave is being propagating in z-direction therefore maximal and minimal magnetic field has been examined in z-direction. Figure 5.2(a) illustrates normalized plot of surface E-field for 20*nm* radius AuNRs and Figure 5.2(b) illustrates the surface magnetic field distribution ($A.m^{-1}$) in case of Au NRs of 20*nm* radius, 200*nm* spacing and wavelength value 1200*nm*. The normalized plot of surface E-field ($V.m^{-1}$) for two AuNRs having 20*nm* radius and 200*nm* spacing is depicted in Figure 5.2(c).

(a)

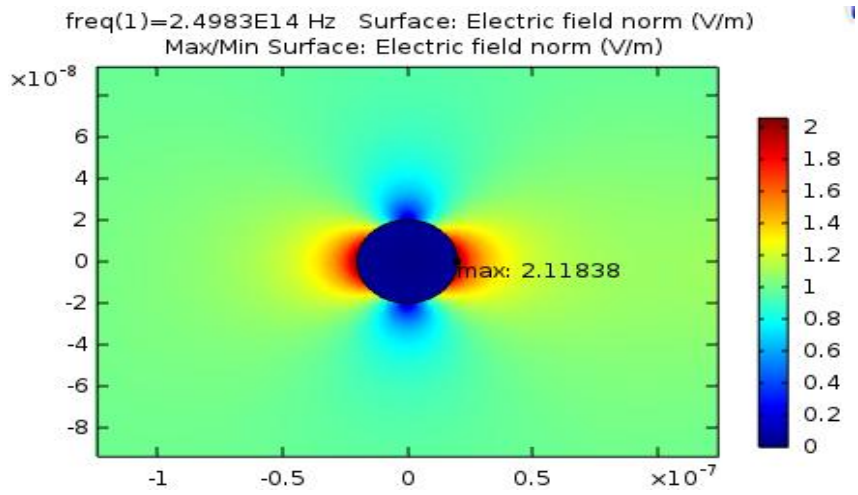

(b)

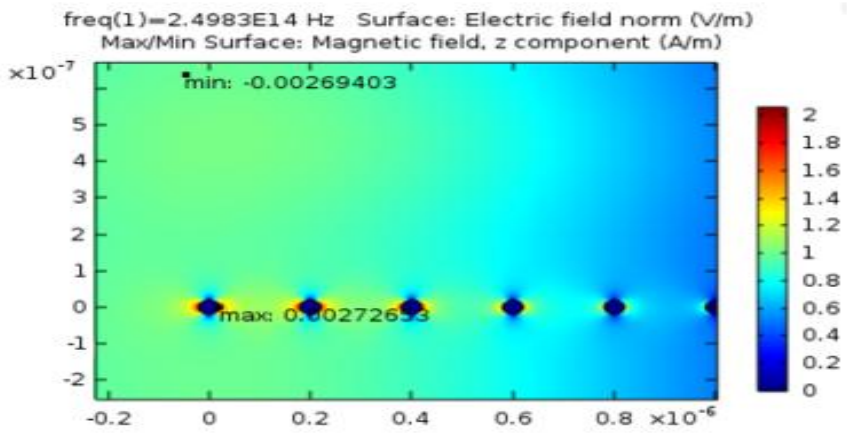

(c)

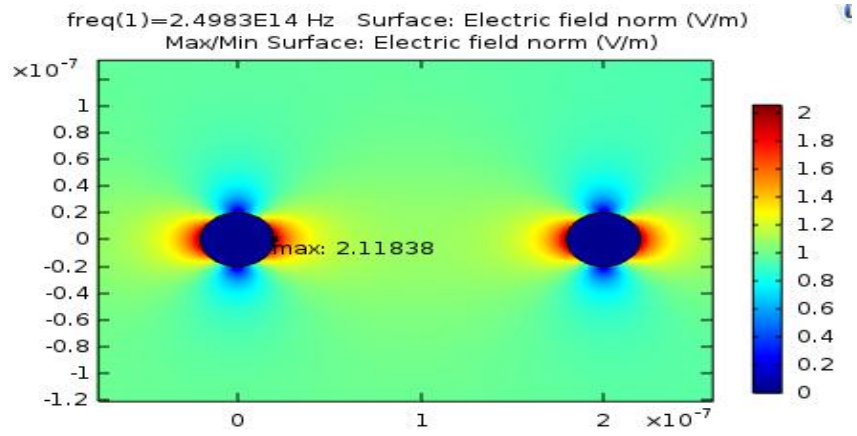

Figure 5.2: (a)Normalized plot of Surface Electric Field for AuNR (*radius=20nm*) (b) Surface Magnetic Field for AuNRs (*radius=20nm and spacing = 200nm*) (c) Normalized plot for Surface Electric Field for 2-AuNRs (*radius=20nm and spacing = 200nm*)

FEM technique of simulation assists in providing vital insights into distinct parameters concerning the sensing performance. With the help of this package, we have examined the maximal and minimal strength of magnetic field. Figure 5.3(a) depicts the relationship between surface magnetic field ($A.m^{-1}$) and AuNRs radius and Figure 5.3(b) depicts the relationship between minimal surface magnetic field ($A.m^{-1}$) and AuNR radii at distinct wavelength 1200*nm* and 1300*nm*. Results from Figure 5.3(a) indicates that at a wavelength of 1200*nm* and 1300*nm*, rise in the AuNRs radius value causes the maximal value of surface magnetic field (*A/m*) to rise.

(a)

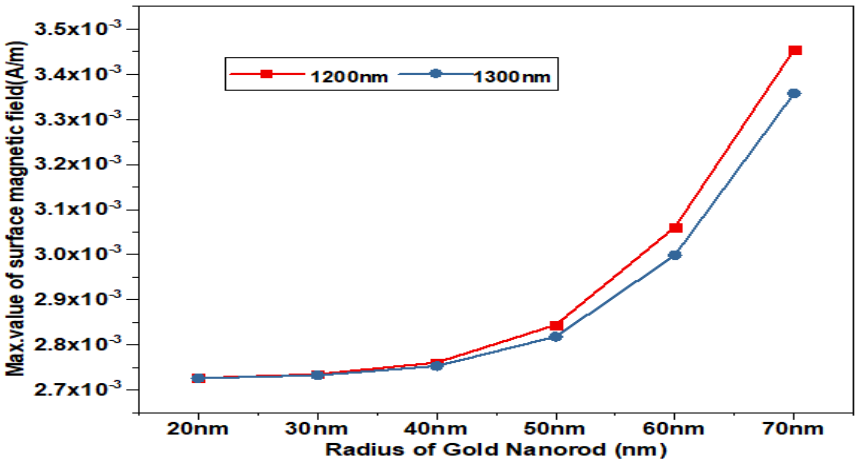

(b)

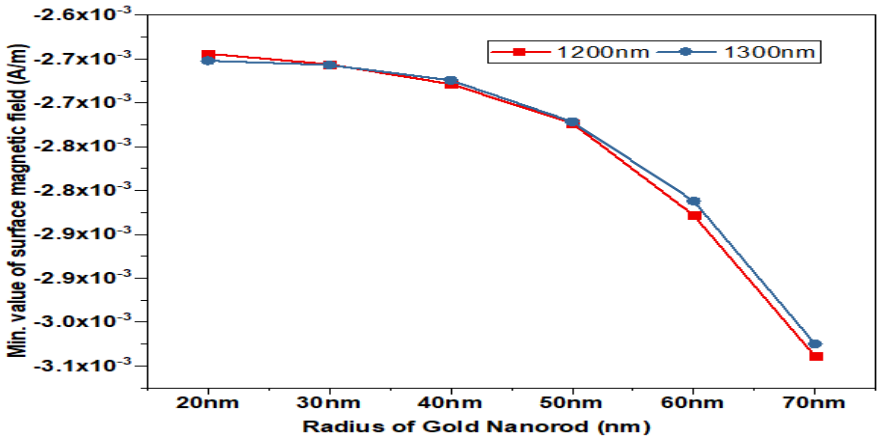

Figure 5.3: (a) Relationship between Maximal Surface Magnetic Field and AuNR radius at 1200*nm*, 1300*nm* (b) Relationship between Minimal Surface Magnetic Field and AuNR radius at 1200*nm*, 1300*nm*

The magnetic field rises abruptly at 1200*nm* as compared with wavelength at 1300*nm*. On the other hand from Figure 5.3(b), we have found that the minimal value of the surface magnetic field decreases with increase in radius of AuNR and this occurs almost to same value for 1200*nm* & 1300*nm*. Figure 5.4(a-c) depicts the plot of electric field norm (*V/m*) with arc length for 20*nm*, 30*nm* and 50*nm* AuNRs radius respectively, at 1300*nm*. We have also attained the polar plot for analyzing the far-field pattern. Figure 5.4(d) depicts the polar plot of far field for 20*nm* AuNR. Figure 5.5(a) depicts the resistive losses ($W.m^{-3}$) relationship with AuNR radius values, for E-field amplitude of E_0=1.$V.m^{-1}$ & E_0= 2$V.m^{-1}$. It has been observed from the results that there is sharp increase in resistive losses with respect to nanorod radius, at a strength of E_0= 2$V.m^{-1}$. The sensor is highly perceptive to sensing sample RI.

(a)

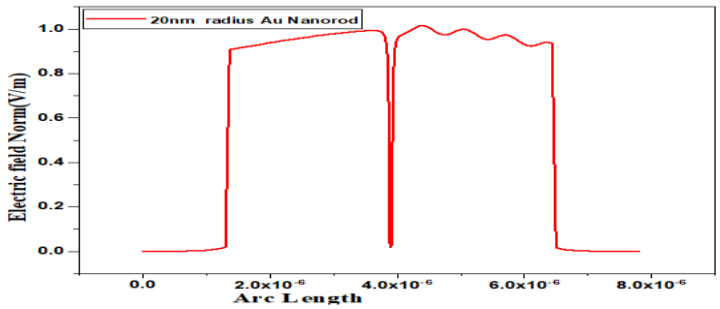

(b)

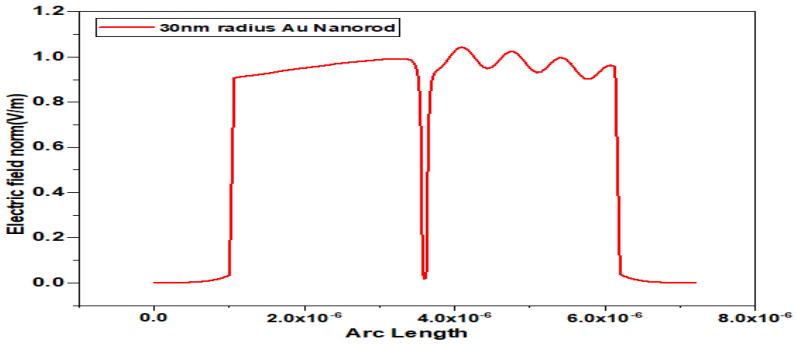

(c)

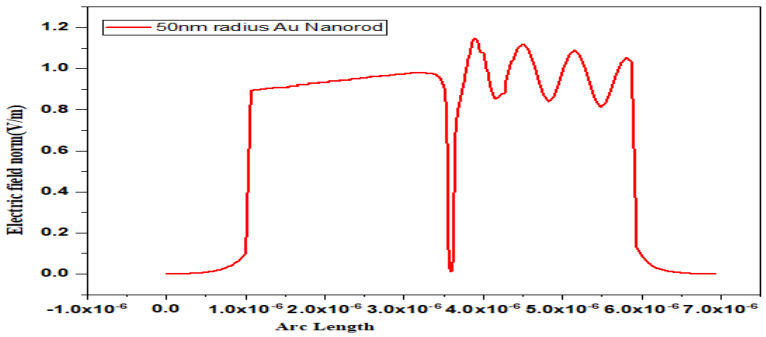

(d)

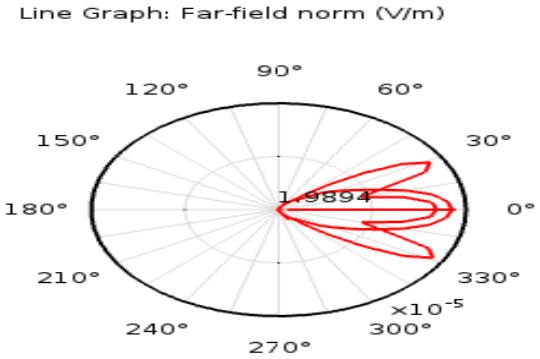

Figure 5.4: Graph of Electric Field norm and Arc length with AuNR (a) radius=20*nm* (b) radius=30*nm* (c) radius=50*nm* (d) Polar Plot showing Far-Field Pattern

Consequently, at a particular wavelength a dip in the reflected light is noticed. This specific wavelength is the resonant wavelength, λ_{reso}. The ratio of change in wavelength to the change in RI is the sensitivity of the sensor. The sensor presents the enhanced sensitivity of $2200 nm.RIU^{-1}$. Figure 5.5(b) depicts the resonant wavelength, λ_{reso} shift with RI of the sensing sample. The resonant wavelength λ_{reso} has been found to rise with rise in RI of the sensing sample. The linear fitting analysis of the data has been achieved & is depicted in Figure 5.5(b) and the extremely high R-square, coefficient of determination ~98.78 %, has been attained. The aforesaid nanorod SPR sensor design may be beneficial for glucose perception. The human body has a special type of protein i.e. hemoglobin A1c and its optimum range covers from 68*mg/dl* to 112*mg/dl.*

(a)

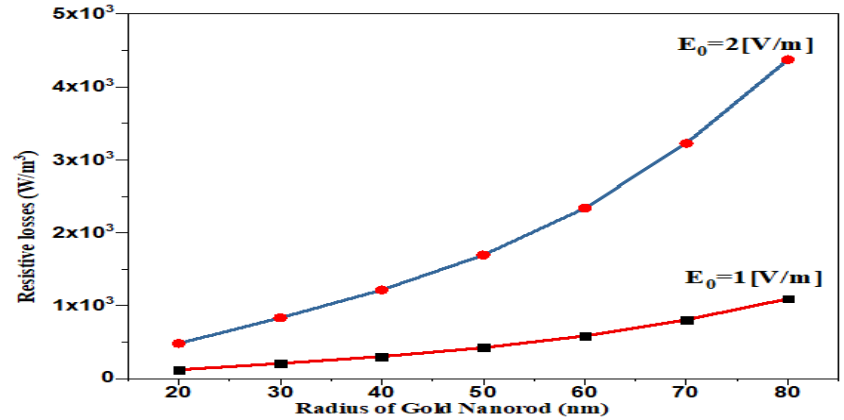

(b)

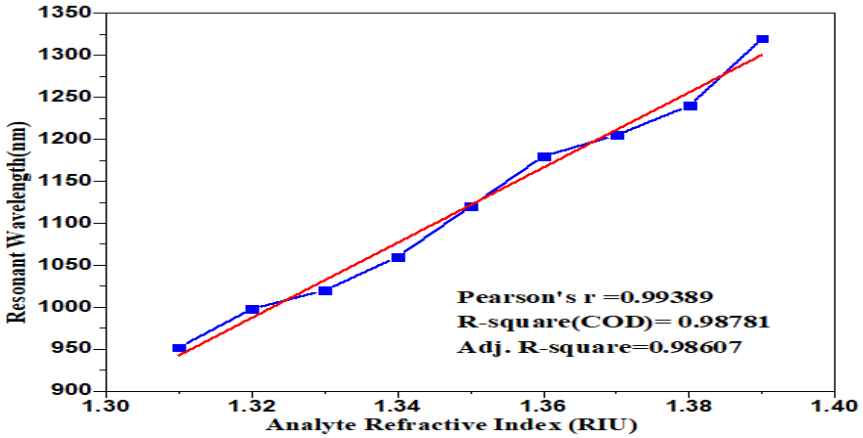

Figure 5.5: (a) Relationship between Resistive Losses and Radius of AuNRs for E-field Strength, E_0=1$V.m^{-1}$ and E_0= 2$V.m^{-1}$ (b) Relationship between Resonant Wavelength, λ_{reso} and Sensing Medium RI.

The glucose level in the human blood and HbA1c level are directly related to each other. More the glucose level in human body, more the HbA1c level is to be detected. Consequently, the sensor can be useful for glucose sensing in diabetes related health problems. To attained good fabrication tolerance, the proposed biosensor structural design required to be optimized and sensor will be simple to fabricate.

5.4 Outcomes of the Proposed Sensor Design

In this chapter we have observed the FEM simulated response of the SPR sensor based on AuNRs array with circular shape. Results conclude that with increase in the radius of AuNR, the surface magnetic field rises for 1200*nm* and 1300*nm*. The maximal value of surface magnetic field for AuNR with radius 70*nm* has been calculated as $3.4\times 10^{-3} ampere\ \ per\ \ meter$ and $3.35747 \times 10^{-3} ampere\, per\, meter$ at the wavelength of 1200*nm* and 1300*nm* respectively. Results indicate that surface magnetic field is accountable for resonant phenomenon and plasmonic oscillations which propagates close to the MDI. It was also found that the resonant wavelength shift increases with increase in RI of the sensing sample. Better the shift in resonant wavelength, more will be the sensitivity. The value of R-square, co-efficient of determination was found to be 98.78 % and it is extremely high. Further results conclude that when the radius of circular AuNR is 60*nm* then the enhanced sensitivity, $S_{AuNR} \approx 2200 nm/RIU$ is presented by aforesaid AuNR based sensor, in RI range ~1.30-1.40. AuNR SPR sensors are beneficial for the perception of many biochemical and organic species and thus expanding their usage for identification of gaseous substances and metallic ions. Moreover, there are certain challenges to model the unique AuNR sensor configuration that may prove beneficial for future research.

Chapter 6
Conclusions, Recommendations and Scope for Future Research

This chapter presents the conclusions, recommendations and scope for future research of the work completed in this thesis. Section 6.1 describes the overall conclusions of the research work carried out in this thesis. Section 6.2 describes the recommendations and section 6.3 presents the possible approach concerning the future research directions.

6.1 Conclusions

This thesis presents the FOS based on surface plasmon resonance technique for refractive index sensing. The association between fiber optic and surface plasmon resonance technology has brought a lot of advancement in refractive index sensing of different biological & physio-chemical species. The main objective and motivation of the research work done in this thesis is to investigate the different properties of SPR active metals in order to select the best suitable metallic combination for fiber optic SPR sensor. A comparative study of different SPR metals has been done in order to achieve better shift of TM reflectivity curve. The selection of suitable material with remarkable properties which are further optimized for SPR sensor has been accomplished. The TM-wave reflectivity curve for different nobel metal thickness has also been investigated. The concept of angular interrogation and wavelength interrogation for different characteristics of FO SPR sensor has been presented.

Accordingly to obtain enhanced performance multilayer structure of 2D material graphene and SPR active metal gold has been simulated using commercial software package COMSOL. The said designed sensor is simulated in angular interrogation mode and resonant angle for analyte refractive index has been observed. The surface magnetic field distribution variation with refractive index has also been presented. It was found that the proposed geometry with gold layer thickness of 60nm in

combination with graphene layer of thickness 10nm provides improved sensing performance and exhibit enhanced sensitivity of $198 degree.RIU^{-1}$ in the sensing of glucose.

Furthermore, a highly sensitive bimetallic diffraction grating based SPR sensor is presented in chapter 4. A combination of two nobel metal gold (Au) and aluminum (Al) has been used to achieve enhanced sensitivity in angular interrogation method. Different properties of SPR active metals and grating period, grating width and the grating depth, has also been investigated. The study showed that diffraction grating based sensor may be beneficial for biosensing domain and it presented enhanced sensitivity if +ve diffraction order of metallic grating is replaced by -ve diffraction order in order to excite the surface plasmons wave. The important feature of the aforesaid design sensor is that it showed enhanced performance against high analyte refractive index. Results showed that the suitable bimetallic grating combination of gold layer of thickness 60nm and aluminum layer of thickness 20nm presents enhanced sensitivity performance of $211 degree.RIU^{-1}$.

Apart from this, circular metallic nanorod array based fiber optic SPR sensor is presented in chapter 5. The effect of size of metallic nanoparticles on the sensor performance has been analysed with COMSOL FEM simulation technique. The variation of resonant wavelength and analyte RI has also been presented. Linear fitting analysis of the simulated data has been done and $R^2(COD)$ found to be 0.98781. Further it was found that this circular gold nanorod based SPR sensor possesses highest sensitivity of $2200 nm.RIU^{-1}$ in wavelength interrogation mode. Further with structural optimization this sensor may be advantageous in achieving label-free optical platform for biosensing applications.

6.2 Recommendations

- It is highly recommended to implement fiber optic sensor based on SPR technology for sensing of organic and inorganic compounds because they provide accurate and fast sensing and reduces detection time. Apart from this,

SPR sensor utilizing 2D material metallic combination can be useful in sensing of various heavy metals ions and in gas sensing for environment monitoring technology.

- Fiber optic sensors based on SPR technology have strong immunity to electromagnetic interference, corrosion resistance, compactness and no electrical leakage. This feature makes the SPR sensor beneficial for many bio-sensing applications and in chemical plants for observing the temperature data.
- In addition to this, research on miniaturization and integration of bio-sensing platform is also under progress. It is greatly recommended to implement the concept of SPR metal nanorod array in fiber optic SPR sensor. This will further ease the technique of analyte detection as well as boost the sensitivity, sensor response and detection accuracy. As the size and shape of the nanoparticle (nanorod) is entirely responsible for sensor's response in terms of sensitivity and accuracy, it will further reduce the cost involved in manufacturing of fiber optic SPR sensor.
- Further it is strongly recommended to implement the multilayer structure approach consisting of novel 2D material and gold in SPR biosensor for glucose sensing in certain biomedical applications. Though highest sensitivity has been achieved by utilizing the aforesaid concept but still further enhancement in the sensitivity and accuracy is still possible with structural optimization and making use of other 2D materials for creating the sensing region.
- SPR sensors based on metallic diffraction grating are also highly recommended for compact and integrated SPR biosensors because of their advanced miniaturization and integration capabilities. This feature will further ease the sensing analysis and provide fast real time information related to a particular disease process.

6.3 Scope for Future Research

Research procedure is a continuous cycle. The research work fulfilled in the thesis can be expanded in several ways. There are some ways where the current thesis research work can expanded, these are described as:

- FO sensors based on SPR technique are bound to find new peaks in near future. The association between fiber optic and surface plasmon resonance technology has contributed to lot of advancements in RI sensing of different physical and biochemical entities. These technological domains have wide research areas in context with FOS based on plasmonic technology.
- The future of plasmonic technology based FO biosensors will be motivated by the requirements of the client, and thus it is essential that the biosensor should be invented and shaped consumers friendly as well as eco-friendly. Recently there have been significant progress in both, the design of fiber optic sensor sensors and strategies for the improvement of the sensing performance of the plasmonic sensors specially RI sensitivity.
- In future, advancement in SPR biosensor's sensing performance can be attained by employing more graphene layers, a suitable plasmonic metal and with optimized parameters, ultimately this will lead to enhanced sensitivity with more accuracy in sensing of glucose. Research work on biosensors can be extended with structural optimization and new simulation technique, for glucose biomarker detection at early stage in diabetes patients. This will further aid the benefits to the community health and medical diagnostics industry.
- Even though the highest refractive index sensitivity has been achieved in this work for the 2D material based fiber optic SPR sensors, further enhancement in RI sensitivity is still possible. In future, this enhancement will make the SPR sensor more useful for sensing wide range of organic and inorganic compounds.
- In future, the use of 2D material graphene and SPR metal, in combination with

other 2D material like transition metal dichalogenide (TMDC) will bring more advancement in palsmonic bio-sensing technology. The work on transition metal dichalogenide monolayer is an emerging research in future.

- Future research in fiber optic SPR sensor will fetch mobile SPR sensing system with which bio-sensing related to certain disease or environment gases will carried out outside the laboratory environment. This mobile sensing platform should permit rapid detection of under observation biological entity. Hereafter, the SPR technology based optical sensing system will requires considerable advancement in miniaturization as well as integration of bio-sensing platform. This will provide the extended benefits to the community health with more ease, fast and accurate medical symptomatic.
- In the era of nanotechnology, metallic nanorod based fiber optic SPR sensors are also getting attention. Future scope of nanorord based fiber optic SPR sensor has to be extended for the identification of other entities i.e temperature, humidity, etc. The technology of localized surface plasmon resonance with metallic nano-particle has shown great potential in SPR bio-sensing applications. But furthermore optimization of the crucial factors and parameters to enhance the bio-sensing capabilities is necessary.

References

[1] Marek Piliarik and Jiří Homola, "Surface plasmon resonance (SPR) sensors: approaching their limits," *Optics Express*, Vol. 17, Issue 19, pp. 16505-16517, 2009.

[2] K. T. V. Grattan, "Recent advances in fiber optic sensors," *Measurement*, Vol. 5, No. 3, pp. 122-134, 1987.

[3] H. Šípová, M. Piliarik, M. Vala, K. Chadt, P. Adam, M. Bocková, K. Hegnerová and J. Homola, "Portable surface plasmon resonance biosensor for detection of nucleic acids," *Procedia Engineering*, Vol. 25, pp. 148- 51, 2011.

[4] K.A. Fidanboylu, H.S. Efendioglu, "Fiber optic sensors and their applications," *In Proc. of 5th International Advanced Technologies Symposium (IATS'09), May 13-15, pp. 1-6, 2009, Karabuk, Turkey.*

[5] Joan R. Casas and Paulo J.S. Cruz, "Fiber Optic Sensors for Bridge Monitoring," *Journal of Bridge Engineering*, Vol. 8, No. 6, pp. 362-373, 2003.

[6] J.W. Berthold, "Historical Review of Microbend Fiber Optic Sensors," *Journal of Light wave Technology*, Vol. 13, Issue 7, pp. 1193-1199, 1995.

[7] MC Connelly, *Fiber Sensors*, Elsevier Ltd., Limerick, 2005.

[8] Eric Udd, Whitten Schulz, John Seim, John Corones and H. Martin Laylor, "Fiber Optic Sensors for Infrastructure Applications," Oregon Department of Transportation, Washington D.C, 1998.

[9] Alexis Méndez, "Overview of fiber optic sensors for NDT applications," *Proc. IV NDT Panamerican Conference*, pp. 1-11, 2007.

[10] David A Krohn, "Fiber Optic Sensors: Fundamental and Applications," *Instrument Society of America*, Research Triangle Park, North Carolina, 1988.

[11] Francis TS Yu and Shizhuo Yin, "*Fiber Optic Sensors*," Marcel Decker, Inc., New York, 2002.

[12] N.D. Lang, “Surface dipole barriers in simple metals,” *Physical Review B*, Vol. 8, Issue 12, pp. 6010-6012, 1973.

[13] Andrei Kolomenski, Alexandre Kolomenskii, John Noel, Siying Peng and Hans Schuessler, “Propagation length of surface plasmons in a metal film with roughness,” *Applied Optics*, Vol. 48, No. 30, pp. 5683-5691, 2009.

[14] Charles Kittel, *Introduction to Solid State Physics*, 7th edition, Wiley, New York, 1996.

[15] Gavin K Brennen, Carlton M Caves, Poul S Jessen and Ivan H Deutsch, “Quantum Logic Gates in Optical Lattices,” *Physical Review Letters*, Vol. 82, No.5, pp. 1060-1063, 1999.

[16] Eugene Hecht, Optics, Addison-Wesley, San Francisco, 2002.

[17] Stefan Alexander Maier, Plasmonics: Fundamentals and Applications. Springer Science + Business Media LLC, 2007.

[18] Paul Drude, “On the electron theory of metals,” *Ann. Phys*, Vol. 1, No. 3, pp. 566-613, 1900.

[19] M. A. Ordal, Robert J. Bell, R. W. Alexander, Jr, L. L. Long, and M. R. Querry, “Optical properties of fourteen metals in the infrared and far infrared: Al, Co, Cu, Au, Fe, Pb, Mo, Ni, Pd, Pt, Ag, Ti, V, and W.,” *Applied Optics*, Vol. 24, No. 24, pp. 4493-4499, 1985.

[20] John Edicson Hernández Sánchez, “Assembly of a surface plasmon resonance (SPR) spectrometer for the characterization of thin organic films,” *Master thesis* presented to Department of Physics, PUC-Rio Scientific Technical Center, Rio de Janeiro, Brazil, pp. 18-25, 2013.

[21] L. Novotny and B. Hecht, “Principles of Nano-optics,” University Press, Cambridge, 2006.

[22] Jiří Homola, Surface plamon resonance based sensors, Springer, Berlin, 2006.

[23] Edward D. Palik, Handbook of optical constants of solids ii, Academic Press, San Diego, CA, 1998.

[24] R.W. Wood, "On a Remarkable Case of Uneven Distribution of Light in a Diffraction Grating Spectrum," *Proc. of the Physical Society of London*, Vol. 18, No. 1, pp. 269, 1902.

[25] U Fano, "The Theory of Anomalous Diffraction Gratings and of Quasi-Stationary Waves on Metallic Surfaces (Sommerfeld’s Waves)," *Journal of the Optical Society of America*, Vol. 31, Issue 3, pp. 213-222, 1941.

[26] R.H. Ritchie, "Plasma Losses by Fast Electrons in Thin Films," *Physical Review*, Vol. 106, Issue5, pp.874-881, 1957.

[27] Andreas Otto, "Excitation of non-radiative surface plasma waves in silver by the method of frustrated total reflection," *Zeitschrift Fur Physik*, Vol. 216, Issue 4, pp. 398-410, 1968.

[28] E. Kretschmann and H. Raether, "Radiative decay of nonradiative surface plasmons excited by light," *Z. Naturforsch*, Vol. 23a, pp. 2135-2136, 1968.

[29] H. Raether, "On the Influence of roughness on the optical properties of surfaces: Plasma resonance emission and the plasmon dispersion relation," *Thin Solid Films*, Vol. 28, Issue 1, pp.119-124, 1975.

[30] I. Pockrand, J.D. Swalen, J.G. Gordon and M.R. Philpott, "Surface-plasmon spectroscopy of organic monolayer assemblies," *Surface Science*, Vol. 74, Issue 1, pp. 237-244, 1978.

[31] J.G. Gordon and S. Ernst, "Surface-plasmons as a porbe of the electrochemical interface," *Surface Science*, Vol. 101, Issue 1-3, pp. 499-506, 1980.

[32] Bo Liedberg, Claes Nylander and Ingemar Lundstrom, "Surface-plasmon resonance for gas-detection and biosensing," *Sensors and Actuators*, Vol. 4, pp. 299-304, 1983.

[33] Jiří Homola, Sinclair S. Yee and Gunter Gauglitz, "Surface plasmon resonance sensors: review," *Sensors and Actuators B-Chemical*, Vol. 54, Issue 1-2, pp. 3-15, 1999.

[34] A.K. Sharma, R. Jha and B.D. Gupta, “Fiber-optic sensors based on surface Plasmon resonance: A comprehensive review,” *IEEE Sensors Journal*, Vol. 7, No. 8, pp.1118-1129, 2007.

[35] R.B.M. Schasfoort and A.J. Tudos, Handbook of surface plasmon resonance, RSC Publication, 2008.

[36] H. Raether, “Surface-Plasmons on Smooth and Rough Surfaces and on Gratings,” *Springer Tracts in Modern Physics*, Verlag, 111, pp. 1-133, 1988.

[37] Rashmi A. Minz, Sudipta S. Pal, R. K. Sinha and Samir K. Monda, “Plasmonic Coating on Chemically Treated Optical Fiber Probe in the Presence of Evanescent Wave: a Novel Approach for Designing Sensitive Plasmonic Sensor,” *Plasmonics*, Vol. 11, Issue 2, pp. 653–658, 2016.

[38] Jiří Homola, “Present and future of surface plasmon resonance biosensors,” *Analytical and Bio-analytical Chemistry*, Vol. 377, Issue 3, pp. 528-539, 2003

[39] Jiří Homola, “Surface plasmon resonance based sensors,” Springer London, Limited, 2006.

[40] Jiří Homola, “Surface plasmon resonance sensor for detection of chemical and biological species,” *Chemical Review*, Vol. 108, Issue 2, pp. 462-493, 2008.

[41] Yusser Al Qazwini, A. S. M. Noor, T. K. Yadav, M. H. Yaacob, S. W. Harun, and M. A. Mahdi, “Performance Evaluation of a Bilayer SPR-Based Fiber Optic RI Sensor with TiO_2 Using FDTD Solutions,” *Photonic Sensors*, Vol. 4, No. 4, pp. 289-294, 2014.

[42] Hyuk Rok Gwon, Seong and Hyuk Lee, “Spectral and Angular Responses of Surface Plasmon Resonance Based on the Kretschmann Prism Configuration,” *Materials Transactions*, Vol. 51, No. 6, pp. 1150-1155, 2010.

[43] Hailin Xu, Leiming Wu, Xiaoyu Dai, Yanxia Gao and Yuanjiang Xiang, “An ultra-high sensitivity surface plasmon resonance sensor based on graphene–aluminum-graphene sandwich-like structure,” *Journal of Applied Physics*, Vol. 120, Issue 5, pp. 053101-1, 053101-6, 2016.

[44] Anuj K. Sharma and Anumol Dominic, “Influence of Chemical Potential on Graphene Based SPR Sensor’s Performance,” *IEEE Photonics Technology Letters,* Vol. 30, No. 1, pp. 95-98, 2018.

[45] Chunliu Zhao, Yanru Wang, Dongning Wang and Zhewen Ding, “Numerical Investigation Into a Surface Plasmon Resonance Sensor Based on Optical Fiber Microring,” *Photonic Sensors,* Vol. 7, No. 2, pp. 105–112, 2017.

[46] Anuj K. Sharma and B. D. Gupta, “On the performance of different bimetallic combinations in surface plasmon resonance based fiber optic sensors,” *Journal of Applied Physics,* Vol. 101, No. 9, pp. 093111-1, 093111-6, 2007.

[47] Hitoshi Suzuki, Mitsunori Sugimoto, Yoshikazu Matsui and Jun Kondoh, “Effects of gold Film Thickness On spectrum profile and sensitivity of a multimode-optical-fiber SPR sensor,” *Sensors and Actuators B:Chemical,* Vol. 132, Issue 1, pp. 26–33, 2008.

[48] Guoqiang Lan, Shugang Liu, Yu Ma, Xueru Zhang, YuxiaoWang and Yinglin Song, “Sensitivity and figure-of-merit enhancements of liquid-prism SPR sensor in the angular interrogation,” *Optics Communications,* Vol. 352, pp. 49–54, 2015.

[49] Xihong Zhao, Yu Chu-Su, Woo-Hu Tsai, Ching-Ho Wang, Tsung-Liang Chuang, Chii-Wann Lin, Yu-Chia Tsao and Mu-Shiang Wu, “Improvement of the sensitivity of the surface Plasmon resonance sensors based on multi-layer modulation techniques,” *Optics Communications,* Vol. 335, pp. 32–36, 2015.

[50] Dachao Li, Jianwei Wu, Peng Wu, Yuan Lin, Yingjuan Sun, Rui Zhu, Jia Yang and Kexin Xu, “Affinity based glucose measurement using fiber optic surface plasmon resonance sensor with surface modification by borate polymer,” *Sensors and Actuators B:chemical,* Vol. 213, pp. 295–304, 2015.

[51] Sarika Shukla, Mahima Rani, Navneet K. Sharma and Vivek Sajal, “Sensitivity enhancement of a surface plasmon resonance based fiber optic sensor utilizing

platinum layer," *Optik -International Journal for Light and Electron Optics*, Vol. 126, No. 23, pp. 4636–4639, 2015.

[52] Yong Zhao, Ze-qun Deng and Qi Wang, "Fiber optic SPR sensor for liquid concentration measurement," *Sensors and actuators B: Chemical*, Vol.192, pp. 229–233, 2014.

[53] D. F. Santos, A. Guerreiro and J. M. Baptista, "Numerical Investigation of a Refractive Index SPR D-Type Optical Fiber Sensor Using COMSOL Multiphysics," *Photonic Sensors*, Vol. 3, No. 1, pp. 61-66, 2013.

[54] Peiling Mao , Yunhan Luo, Xiaolong Chen, Junbin Fang, Hankai Huang, Chaoying Chen, Shuihua Peng, Jun Zhang, Jieyuan Tang, Huihui Lu, Zhe Chen and Jianhui Yu, "Design and Optimization of Multimode Fiber Sensor Based on Surface Plasmon Resonance," *Journal of Optical and Quantum Electronics*, Vol. 47, No. 6, pp. 1495-1502, 2015.

[55] Sarika Singh and Banshi D Gupta, "Fabrication and characterization of a surface plasmon resonance based fiber optic sensor using gel entrapment technique for the detection of low glucose concentration," *Sensors and Actuators B: Chemical*, Vol. 177, pp. 589-595, 2013.

[56] Sarika Shukla, Navneet K. Sharma and Vivek Sajal, "Sensitivity enhancement of a surface plasmon resonance based fiber optic sensor using *ZnO* thin film: a theoretical study," *Sensors and Actuators B: Chemical*, Vol. 206, pp. 463-470, 2015.

[57] Mahua Bera and Mina Ray, "Precise detection and signature of biological/chemical samples based on surface plasmon resonance (SPR)," *Journal of Optics*, Vol. 38, No. 4, pp. 232-248, 2009.

[58] P. Hlubina, M. Kadulova, D. Ciprian and J. Sobota, "Reflection-Based Fiber-Optic Refractive Index Sensor Using Surface Plasmon Resonance*," Journal of the European Optical Society - Rapid Publications*, Vol. 9, pp. 14033, 2014.

[59] Anuj K. Sharma and Baljinder Kaur, “Simulation and analysis of 2D material (MoS_2/$MoSe_2$) based plasmonic sensor for measurement of organic compounds in infrared,” *Optik*, Vol. 157, pp. 161-169, 2018.

[60] Xiao-Ming Wang, Chun-LiuZhao, Yan-RuWang and Shangzhong Jin, “A proposal of T-structure fiber-optic refractive index sensor based on surface Plasmon resonance*,” Optics Communications*, Vol. 369, pp.189-193, 2016.

[61] S.K. Srivastava and I. Abdulhalim, “Spectral Interrogation based SPR Sensor for Blood Glucose Detection with Improved Sensitivity and Stability*,” International Journal of Biosensors and Bioelectronics*, Vol. 6, No. 2, pp. 214-242, 2015.

[62] W.W. Lama, L.H. Chua, C.L. Wong and Y.T. Zhang, “A surface plasmon resonance system for the measurement of glucose in aqueous solution,” *Sensors and Actuators B*, Vol.105, No. 2, pp.138–143, 2005.

[63] Kaiqun Lin, Yonghua Lu, Junxue Chen, Rongsheng Zheng, Pei Wang and Hai Ming, “Surface plasmon resonance hydrogen sensor based on metallic grating with high sensitivity,” *Optics Express*, Vol. 16, No. 23, pp. 18599-18604, 2008.

[64] D.C. Cullen and C.R. Lowe, “A direct surface plasmon polariton immunosensor: preliminary investigation of the non-specific adsorption of serum components to the sensor interface,” *Sensors and Actuators B*, Vol. 1 Issue 1–6, pp. 576–579, 1990.

[65] Changkui Hu, “Surface plasmon resonance sensor based on diffraction grating with high sensitivity and high resolution,” *Optik*, Vol. 122, pp. 1881– 1884, 2011.

[66] M. J. Jory, P. S. Vukusic, and J. R. Sambles, “Development of a prototype gas sensor using surface plasmon resonance on grating,” *Sensors and actuators B*, Vol. 17, pp**.** 203-209, 1994.

[67] C.R. Lawrence, N.J. Geddes, D.N. Furlong and J.R. Sambles, "Surface plasmon resonance studies of immunoreactions utilizing disposable diffraction gratings," *Biosens. Bioelectron*., Vol. 11, Issue 4, pp. 389–400, 1996.

[68] Stefano Rossi, Enrico Gazzola, Pietro Capaldo, Giulia Borile and Filippo Romanato, "Grating-Coupled Surface Plasmon Resonance Optimization for Phase-Interrogation Biosensing in a Microfluidic Chamber," *Sensors*, Vol. 18, Issue *5*, pp. 1621, 2018.

[69] R.H. Ritchie, E.T. Arakawa, J.J. Cowan and R.N. Hamm, **"S**urface-plasmon resonance effect in grating diffraction," *Physical Review Letter*, Vol. 21, Issue 22, pp. 1530-1533, 1968.

[70] M.C. Hutley and D. Mayster, "The total absorption of light by a diffraction grating," *Optics Communications,* Vol. 19, Issue 3, pp. 431- 436, 1976.

[71] Ashish Bijalwan and Vipul Rastogi, "Design Analysis of Refractive Index Sensor with High Quality Factor Using *Au-*Al_2O_3 Grating on Aluminum," *Plasmonics*, Vol. 13, Issue 6, pp. 1995–2000, 2018.

[72] Kouki Ichihashi and Tetsuo Iwata, "Numerical simulation of a metal diffraction grating-based SPR sensor with a water-immersion lens," *Optical Review*, Vol. 24, Issue 6, pp. 668–676, 2017.

[73] Xiaoliang Sun, Xuewen Shu and Changhong Chen, "Grating surface plasmon resonance sensor: angular sensitivity, metal oxidization effect of *Al*-based device in optimal structure," *Applied Optics***,** Vol. 54, Issue 6, pp. 1548-1554, 2015.

[74] Jianjun Cao, Yuan Sun, Yan Kong and Weiying Qian, "The Sensitivity of Grating-Based SPR Sensors with Wavelength Interrogation," *Sensors (Basel)*, Vol. 19, Issue 2, pp. 405, 2019.

[75] W. Su, G. Zheng and X. Li, "Design of a highly sensitive surface plasmon resonance sensor using aluminum-based diffraction grating," *Optics Communication*, Vol. 285, pp.4603–4607, 2012.

[76] Hai-Tao Yan, Qi Liu, Yang Ming, Wei Luo, Ye Chen and Yan-qing Lu, "Metallic Grating on a D-Shaped Fiber for Refractive Index Sensing," *IEEE Photonics Journal*, Vol. 5, Issue 5, pp. 4800706, 2013.

[77] K. Lin, Y. Lu, J. Chen, R. Zheng, P. Wang and H. Ming, "Surface plasmon resonance hydrogen sensor based on metallic grating with high sensitivity," *Optics Express*, Vol. 16, Issue 23, pp. 18599-18604, 2008.

[78] T. Tamulevicius, R. Seperys, M. Andrulevicius and S.Tamulevicius, "Total internal reflection based sub-wavelength grating sensor for the determination of refractive index of liquids," *Journal of Photonics and Nanostructures–Fundamentals and Applications*, Vol.9, Issue 2, pp. 140–148, 2011.

[79] K. H. Yoon and M. L. Shuler, "Design optimization of nano-grating surface Plasmon resonance sensors," *Optics Express*, Vol. 14, Issue 11, pp. 4842-4849, 2006.

[80] James J. Storhoff, Robert Elghanian, Chad A. Mirkin and Robert L. Letsinger, "Sequence-Dependent Stability of DNA-Modified Gold Nanoparticles," *Langmuir*, Vol. 18, Issue 17, pp. 6666-6670, 2002.

[81] Gonçalo Doria, João Conde, Bruno Veigas, Leticia Giestas, Carina Almeida, Maria Assunção, João Rosa and Pedro V. Baptista, "Noble Metal Nanoparticles for Biosensing Applications," *Sensors (Basel)*, Vol. 12, Issue 2, pp. 1657–1687, 2012.

[82] Hedieh Malekzad, Parham Sahandi Zangabad, Hamed Mirshekari, Mahdi Karimi and Michael R. Hamblin, "Noble metal nanoparticles in biosensors: recent studies and applications," *Nanotechnology Review*, Vol. 6, Issue 3, pp. 301–329, 2017.

[83] Wing-Cheung Law, Ken-Tye Yong, Alexander Baev, Rui Hu and Paras N. Prasad, "Nanoparticle enhanced surface plasmon resonance biosensing: Application of gold nanorods," *Optics Express*, Vol. 17, No. 21 , pp. 19041-19046, 2009.

[84] Dalibor Ciprian and Petr Hlubina, “Analysis of nanoparticle-based surface plasmon resonance fiber optic sensor,” *Key Engineering Materials*, Vol. 605, pp. 131-134, 2014.

[85] Kyeong Seok Lee and Mostafa A. El Sayed, “Gold and Silver Nanoparticles in Sensing and Imaging: Sensitivity of Plasmon Response to Size, Shape, and Metal Composition,” *Journal of Physical Chemistry B*, Vol. 110, Issue 39, pp. 19220–19225, 2006.

[86] Jie Cao, Tong Sun and Kenneth T. V. Grattan, “Development of gold nanorod-based localized surface plasmon resonance optical fiber biosensor,” *in Proc. SPIE 8421, OFS 2012 22nd International Conference on optical fiber sensors,* Vol. 8421, 84211X, 2012.

[87] Shuwen Zeng, Mathieu Sylvain Bergont, Aurelien Olivier, Xuan Quyen Dinh, Xia Yu and Ken Tye Yong, “Sensitivity improved surface plasmon resonance sensor based on graphene and gold nanorods,” *in Proc. 2013 IEEE 5th International Nanoelectronics Conference (INEC)*, pp. 414-416, Singapore, 2013.

[88] Chaoying Chen, Yunhan Luo, Peiling Mao, Shuihua Peng, Jun Zhang, Jieyuan Tang, Huihui Lu, Jianhui Yu and Zhe Chen, “Design and optimization of surface plasmon resonance fiber sensor based on square gold nanorod array,” *in Proc. IEEE 2015 International Conference on Numerical Simulation of Optoelectronic Devices*, Taipei, pp.77-78, 2015.

[89] Ching An Peng and Sushil Pachpinde, “Longitudinal Plasmonic Detection of Glucose Using Gold Nanorods,” *Nanomaterials and Nanotechnology*, Vol. 4, Issue 9, pp. 1-5, 2014.

[90] Hung Yi Chung, Chih Chia Chen, Pin Chieh Wu, Ming Lun Tseng, Wen Chi Lin, Chih Wei Chen and Hai Pang Chiang, “Enhanced sensitivity of surface plasmon resonance phase-interrogation biosensor by using oblique deposited silver nanorods,” *Nanoscale Research Letters*, Vol. 9, Issue 1, pp. 476, 2014.

[91] Yinquan Yuan, Na Yuan, Dejing Gong, and Minghong Yang, "A High-Sensitivity and Broad-Range SPR Glucose Sensor Based on Improved Glucose Sensitive Membranes," *Photonic Sensors*, pp. 1-8, 2018.

[92] Arpad Jakab, Christina Rosman, Yuriy Khalavka, Jan Becker, Andreas Trugler, Ulrich Hohenester and Carsten Sonnichsen, "Highly Sensitive Plasmonic Silver Nanorods," *American chemical society Nano*, Vol. 5, No. 9, pp. 6880–6885, 2011.

[93] Liping Song, Lei Zhang, Youju Huang, Liming Chen, Ganggang Zhang, Zheyu Shen, Jiawei Zhang, Zhidong Xiao and Tao Chen, "Amplifying the signal of localized surface plasmon resonance sensing for the sensitive detection of Escherichia coli O157:H7," *Scientific Reports*, Vol. 7, Issue 1, pp. 3288, 2017.

[94] R.W. Wood, "Anomalous diffraction gratings," *Physical Review*, Vol. 48, Issue 12, pp. 928-936, 1935.

[95] R. Petit(Ed.), Electromagnetic theory of gratings, Springer-Verlag, 1980.

[96] A. Alomainy, Y. Hao and F. Pasveer, "Numerical and experimental evaluation of a compact sensor antenna for healthcare devices*," IEEE Transactions on Biomedical Circuits and Systems*, Vol. 1, Issue 4, pp. 242-249, 2007.

[97] V.K. Chaubey, K. K. Dey and P. Khastgir, " Field intensity and power confinement of four layer slab waveguide with various refractive index profiles*" Journal of Optical Communication (Germany)*, Vol. 15, No. 3, pp. 95-100, 1994.

[98] J. Clerk Maxwell, A Treatise on Electricity and Magnetism, *3rd ed.*, Vol. 2. Oxford: Clarendon, pp.68–73, 1892.

[99] E Limiti, G Pelosi, M Pierozzi and S Selleri, "The finite elements method for matched coplanar to rectangular waveguide transitions*," in Proc. 6th International Workshop on Finite Elements for Microwave Engineering*, Chios, Greece, May 30- June 1, 2002.

[100] F Bertazzi, F Cappelluti, F Bonani, M Goano and G Ghione, “A novel coupled physics-based electromagnetic model of semiconductor traveling-wave structures for RF and optoelectronic applications,” *in Proc. 11th GaAs symposium 2003*, pp. 239–242, Munich, Oct. 2003.

[101] A. Verma, A. Prakash and R. Tripathi, “Sensitivity enhancement of surface Plasmon resonance bio-sensor using graphene and air gap,” *Optics Communication*, Vol. 357, pp.106–112, 2015.

[102] H. Fu, S. Zhang, H. Chen and J. Weng, “Graphene enhances the sensitivity of fiber-optic surface plasmon resonance biosensor,” *IEEE Sensors*, Vol. 15, No. 10, pp. 5478-5482, 2015.

[103] A. K. Ghatak and K. Thyagarajan, An introduction to fiber optics, Cambridge, UK: Cambridge University Press, 1999.

[104] A. Méndez and T. F. Morse, Specialty Optical Fibers Handbook, San Diego, California: Academic Press, pp. 39–40, 2007.

[105] Rashmi A. Minz, Sudipta S. Pal, R. K. Sinha and Samir K. Monda, “Plasmonic Coating on Chemically Treated Optical Fiber Probe in the Presence of Evanescent Wave: a Novel Approach for Designing Sensitive Plasmonic Sensor,” *Plasmonics*, Vol. 11, Issue 2, pp. 653–658, 2016.

[106] M. A. Ordal, Robert J. Bell, R. W. Alexander, Jr, L. L. Long and M. R. Querry, “Optical properties of fourteen metals in the infrared and far infrared: Al, Co, Cu, Au, Fe, Pb, Mo, Ni, Pd, Pt, Ag, Ti, V, and W,” *Applied Optics*, Vol. 24, No. 24, pp. 4493-4499, 1985.

[107] Action Nechibvute and Courage Mudzingwa, “Modelling Of Optical Waveguide Using COMSOL Multiphysics,” *International Journal of Engineering Research & Technology*, Vol. 2, Issue 5, pp.1663-1667, 2013.

[108] Waseem Raja, Alessandro Alabastri, Salvatore Tuccio and Remo Proietti Zaccariai, “Surface Plasmon Resonance Sensors: Optimization of Diffraction

Grating and Prism Couplers," *in Proc. of 2013 COMSOL conference,* Rotterdam, Italy, 2013.

[109] Courage Mudzingwa and Action Nechibvute, "Analysis of Single Mode Step Index Fiber using Finite Element Method," *International Journal of Engineering Research & Technology*, Vol. 2, Issue 5, pp. 361-365, 2013.

[110] M.C. Hutley, "Diffraction Gratings," Vol. 6, 1st ed., Academic Press, London, 1982.

[111] Moutzouris, Konstantinos, Papamichael, Myrtia, Betsis, C.Sokratis, Stavrakas, Ilias, Hloupis, George, Triantis and Dimos, "Refractive, dispersive and thermo-optic properties of twelve organic solvents in the visible and near-infrared," *Appl. Phys. B*, Vol. 116, Issue 3, pp. 617–622, 2013.

[112] Adrian E. Flood and Srisuda Puagsa, "Refractive Index, Viscosity, and Solubility at 30 °C, and Density at 25 °C for the System Fructose + Glucose + Ethanol + Water," *Journal of Chemical and Engineering Data*, Vol. 45, No. 5 pp. 902-907, 2000.

[113] H. Kang and M. Kumar, "Two way reflector based on two-dimensional sub-wavelength high index contrast grating on *SOI*," *Optics Communication*, Vol. 366, pp. 266-270, 2016.

[114] G. Li, Y. Shen, G. Xiao and C. Jin, "Double-layered metal grating for high performance refractive index sensing," *Optics Express*, Vol. 23, Issue 7, pp. 8995-9003, 2015.

[115] Bora Ung and Yunlong Sheng, "Interference of surface waves in a metallic nanoslit," *Optics Express*, Vol. 15, Issue 3, pp. 1182-1190, 2007.

[116] Edward D. Palik, Handbook of Optical Constants of Solids, Academic Press: Orlando, FL, 1985.

[117] M. A. Ordal, L. L. Long, R. J. Bell, S. E. Bell, R. W. Alexander, Jr., and C. A. Ward, "Optical properties of the metals Al, Co, Cu, Au, Fe, Pb, Ni, Pd, Pt, Ag,

Ti, and W in the infrared and far infrared," *Applied Optics*, Vol. 22, No. 7, pp. 1099-1120, 1983.

[118] U Kreibig and M Vollmer, Optical Properties of Metal Clusters, Springer, 1995.

[119] Ranjeet Kumar, Chandra Shakher and D.S. Mehta, "Clustering of optically trapped large diameter plasmonic *Au*-NP by laser beam of hybrid-TEM11 mode," *Journal of Nanophotonics*, Vol. 5, Issue 1, pp 053511-17, 2011.

[120] C. Oubre and P. Nordlander, "Optical properties of metallo dielectric nano-structures calculated using the finite difference time domain method," *J. Phys. Chem.*, Vol. 108, No. 46, pp. 17740–17747, 2004.

[121] S. Lal, S. L. Westcott, R. N. Taylor, J. B. Jackson, P. Nordlander and N. J. Halas, "Light interaction between gold Nano shells plasmon resonance and planar optical waveguides," *J. Phys. Chem. B*, Vol. 106, Issue 22, pp. 5609-5612, 2002.

[122] J. K. Lim, K. Imura, T. Nagahara, S. K. Kim and H. Okamoto, "Imaging and dispersion relations of surface plasmon modes in silver nanorods by near-field spectroscopy," *Chem. Phys. Lett.*, Vol. 412, Issue 1-3, pp. 41-45, 2005.

[123] Joel JPC Rodrigues, Nuno M Garcia, Mário M Freire and Pascal Lorenz, "Object-Oriented modeling and simulation of optical burst switching networks," *in Proc. IEEE Global Telecommunications Conference Workshops, GlobeCom Workshops*, pp. 288-292, 2004.

[124] A. J. Haes, S. Zou, G. C. Schatz and R. P. Van Duyne, "A nano scale optical biosensor: the long-range distance dependence of the localized surface plasmon resonance of noble metal nanoparticles," *J. Phys. Chem. B*, Vol. 108, Issue 1, pp. 109–116, 2004.

[125] W. L. Barnes, A. Dereux and T.W. Ebbesen, "Surface plasmon sub-wavelength optics," *Nature*, Vol. 424, pp. 824–830, 2003.

[126] Subramaniam Jayabal, Alagarsamy Pandikumar, Hong Ngee Lim, Ramasamy Ramaraj, Tong Sun and Nay Ming Huang, "A gold nanorod-based localized surface plasmon resonance platform for the detection of environmentally toxic metal ions," *Analyst***,** Vol. 140, Issue 8, pp. 2540-2555, 2015.

[127] Edward T. Castellana, Roberto C. Gamez, Mario E. Gomez and David H. Russell, "Longitudinal Surface Plasmon Resonance Based Gold Nanorod Biosensors for Mass Spectrometry," *Langmuir*, Vol. 26, Issue 8, pp. 6066-6070, 2010.

[128] Adam B. Taylor, Jooho Kim and James W. M. Chon, "Detuned surface plasmon resonance scattering of gold nanorods for continuous wave multilayered optical recording and readout*," Optics express,* Vol. 20, No.5, pp. 5069-81, 2012.

[129] Li Yu Ling, Kan Cai Xia, Wang Chang Shun, Liu Jin Sheng, Xu Hai Ying, Ni Yuan, Xu Wei, Ke, Jun Hua and Shi Da Ning, "Surface Plasmon Resonance Coupling Effect of Assembled Gold Nanorods Based on the FDTD Simulation," *Acta Physico-Chimica Sinica*, Vol. 30, No.10, pp.1827-1836, 2014.

[130] Yinlan Ruan, Shahraam Afshar V, and Tanya M. Monro, "Efficient excitation of surface plasmons in metal nanorods using large longitudinal component of high index nano fibers," *Optics express*, Vol. 19, No.14, pp.13464-13479, 2011.

[131] Kevin C. J. Lee, Yi Huan Chen, Hsiang Yu Lin, Chia Chin Cheng, Pei Ying Chen, Ting Yi Wu, Min Hsiung Shih, Kung Hwa Wei, Lain Jong Li and Chien Wen Chang, "Plasmonic Gold Nanorods Coverage Influence on Enhancement of the Photoluminescence of Two-Dimensional MoS_2 Monolayer," *Scientific Reports*, Vol. 5, Article number: 16374, 2015.

[132] Yuan Fong Chau, Min Wei Chen and Din Ping Tsai, “Three-dimensional analysis of surface plasmon resonance modes on a gold nanorod,” *Applied Optics*, Vol. 48, No. 3, pp. 617-622, 2009.

[133] P. B. Johnson and R. W. Christy, “Optical constants of the noble metals,” *Phys. Rev. B*, Vol. 6, No. 12, pp. 4370-4379, 1972.

[134] D. Rakic, A.B.Djurišic, J. M. Elazar and M. L. Majewski, “Optical properties of metallic films for vertical-cavity optoelectronic devices,” *Applied Optics*, Vol. 37, Issue 22, pp. 5271–5283, 1998.

[135] M. Fliziani and F. Maradei, “Edge element analysis of complex configurations in presence of shields,” *IEEE Transactions on Magnetics*, Vol. 33, No. 2, pp. 1548–1551, 1997.

ISSN 1064-2269, Journal of Communications Technology and Electronics, 2018, Vol. 63, No. 11, pp. 1269–1275. © Pleiades Publishing, Inc., 2018.

ELECTRODYNAMICS AND WAVE PROPAGATION

A Novel Two-Dimensional Material Based Optical Fiber Surface Plasmon Resonance Sensor for Sensing of Organic Compounds in Infrared Spectrum Window[1]

S. Singh[a], *, R. S. Kaler[a], and S. Sharma[b]

[a] *Department of Electronics and Communication Engineering, Thapar Institute of Engineering and Technology, Patiala, 147001 India*

[b] *Department of Bio-technology, Thapar Institute of Engineering and Technology, Patiala, 147001 India*

**e-mail: sarbjit.singh@thapar.edu*

Received June 10, 2018

Abstract—Glucose, sucrose and fructose are typical organic compounds having carbon-hydrogen-oxygen atoms. Their sensing is important in many bio-medical applications. In this paper we present a 2D material-based fiber optic surface plasmon resonance sensor for refractive index sensing of some typical organic compounds. 2D material graphene in combination with active metal gold is used in the sensing region. Fiber core is covered with gold and graphene layer. The sensor is simulated using COMSOL Multiphysics simulation software. To measure the sensing performance of sensor we see the effect of two physical parameters of the sensor, thickness of the Au-metal and graphene layer on the sensing performance. The use of graphene layer enhances the sensitivity of SPR sensor. The angular interrogation method of SPR excitation is used for sensor simulation in COMSOL Multiphysics.

Keywords: glucose, plasmon, near infrared, full width half maximum, organic

DOI: 10.1134/S1064226918110116

INTRODUCTION

Surface plasmon resonance (SPR) is a physics phenomenon in which light photons interacts with a surface plasma wave (SPW). When this physics phenomenon is used in optical fiber along with associated electronics circuitry then the device which is formed, known as optical bio-sensor, exhibits its potential use for the detection of chemical compounds and biomolecular interactions. SPR was first observed in 1902 by R.W. Wood as variances or anomalies in the diffraction efficiency of narrow diffraction gratings of active noble metals [1]. In the forties of last century, these variances or anomalies were found to be related to the excitation of waves guided along the surface of metallic diffraction gratings [2] which later known as surface plasmon wave. Since then, deep research in surface plasmon resonance-based diffraction gratings sensors [3–6] find wide variety of applications in bio-medical field, chemical field and to the little bit extent, in civil field too. Due to its numerous advantages like real-time, label-free molecular detection, this bio-sensing SPR technology has gained the utmost importance across the globe since last three decades. Initially the prism-based refractive index sensors were used but due their bulky size and the problems of integration, now days they are replaced by optical sensor based on metallic diffraction gratings (MDG). Optical fiber sensors are supreme for insensitive conditions like extreme heat, wet, high vibrations, temperatures and unstable environments. Also, they are light in weight and their maintenance cost is low [7]. In the literature various types of SPR materials combinations, coated on the core of fiber, have been investigated for observing the resonance effect on the sensing characteristics of SPR sensor. Zhao et al. [8] investigated the use of multi-layer modulation technique in SPR optical fiber sensor. They have shown that using multiple metal layer modulation procedure, sensitivity can be drastically enhanced. The sensitivity was found to be 1.73×10^{-4} RIUs in intensity interrogation and 1.74×10^{-6} RIUs in wavelength interrogation method of SPR sensing. Shukla et al. [9] theoretically analyzed highly sensitive SPR-based fiber optic sensor with platinum (Pt) layer which is coated on the core of the optical fiber. Sensitivity of the sensor was found to increases enhances linearly with the increase in the refractive index of the medium, for all thicknesses of platinum layers. It was found that using 125 nm thick platinum layer, sensor provides maximum sensitivity of 17.500 nm/RIU. Suzuki et al. [10] investigated the effects of gold layer thickness and spectrum profile on sensor performance. They investigated that sensor

[1] The article is published in the original.

Journal of
Nanoelectronics and Optoelectronics
Vol. 14, pp. 1–6, 2019
www.aspbs.com/jno

ARTICLE

Resonance Effect of Bimetallic Diffraction Grating on the Sensing Characteristics of Surface Plasmon Resonance Sensor with COMSOL Multiphysics

Sarbjit Singh[1,*], R. S. Kaler[1], and Siddharth Sharma[2]

In this article, we present the resonance effect of bimetallic diffraction grating on the performance of surface plasmon resonance sensor. The bimetallic diffraction grating consists of gratings of metals like gold, silver, aluminum etc. The sensor can be used for sensing variety of organic compounds like glucose, sucrose etc. High sensitivity is obtained if negative diffraction order of metallic grating is used to excite the surface plasmon. Therefore, surface plasmon waves are excited by −1st diffraction order. Using numerical simulation sensing performance is evaluated in terms of sensitivity, full-width half maximum, reflectance amplitude, width of the surface plasmon resonance curve and shift in resonant angle. These factors are considered for the bio-sensing performance analysis. Our results shows that bimetallic diffraction grating based surface plasmon resonance sensor proves to be best for sensing applications and provides maximum sensitivity in angular interrogation with good linearity.

Keywords: Surface Plasmon Resonance, Sensor, Grating, Refractive Index.

1. INTRODUCTION

Surface plasmon resonance is a physics phenomenon in which light photons interacts with a surface plasma wave (SPW). When this physics phenomenon is used in optical fiber along with required electronics circuitry then the device formed is known as optical bio-sensor. This device exhibits its potential use for the detection of organic compounds, chemical compounds and bio-molecular interactions. Surface plasmon resonance was first observed in 1902 by R. W. Wood as variances or anomalies in the diffraction efficiency of narrow diffraction gratings of active noble metals [1]. In the forties of last century, these variances or anomalies were found to be related to the excitation of waves guided along the surface of metallic diffraction gratings [2] which later known as surface plasmon wave. Since then, deep research in surface plasmon resonance-based diffraction gratings sensors [3–6] find wide variety of applications in bio-medical field, chemical field and to the little bit extent, in civil field too. Due to its numerous advantages like real-time, label-free molecular detection, this bio-sensing SPR technology has gained the utmost importance across the globe since last three decades. Initially the prism-based refractive index sensors were used but they need precise angle control and due their bulky size and problems of integration, now a day, they are replaced by metallic diffraction gratings (MDG) design based sensors. Diffraction grating design-based SPR sensor is different from others. It has advantage of high sensitivity as compared to others sensors. The conventional SPR sensor have only coating of different SPR active material leading to surface plasmon waves but in the bimetallic diffraction grating design-based sensor, an optical wave is incident on a periodically modulated surface of a metallic grating and in the plane of incidence perpendicular to the grating grooves. The incident optical wave at the surface of the metal grating is partially reflected and partially split into series of diffracted waves (diffraction orders). High sensitivity is obtained if negative diffraction order of metallic grating is used to excite the surface plasmons. Bimetallic diffraction grating-based SPR sensors exhibits a sharper reflectivity dip and perform better in sensitivity and resolution and if Aluminum (Al) is used as a SPR active metal then grating based SPR sensors

[1]Department of Electronics and Communication Engineering, Thapar Institute of Engineering & Technology, Patiala 147001, India
[2]Department of Bio-Technology, Thapar Institute of Engineering & Technology, Patiala 147001, India
*Author to whom correspondence should be addressed.
Email: opticsresearch99@gmail.com
Received: 2 April 2018
Accepted: 28 November 2018

Optik - International Journal for Light and Electron Optics 183 (2019) 508–512

Contents lists available at ScienceDirect

Optik

journal homepage: www.elsevier.com/locate/ijleo

Original research article

FEM simulation analysis of fiber optic surface plasmon resonance sensor based on array of circular gold nanorod

Sarbjit Singh[a,*], R.S. Kaler[a], Siddharth Sharma[b]

[a] Department of Electronics and Communication Engineering, Thapar Institute of Engineering and Technology, Patiala, 147001, India
[b] Department of Bio-Technology, Thapar Institute of Engineering and Technology, Patiala, 147001, India

ARTICLE INFO

Keywords:
Nanorod
Refractive index
Plasmon
Biosensing
Resonant

ABSTRACT

In this paper, we analyze the SPR fiber optic sensor based on array of 10-gold nanorods which are circular in shape. The proposed structure of the sensor is simulated using COMSOL multyphysics FEM method simulation software. Circular shape of the gold nanorod has been chosen for the optimal performance of the sensor in sensing of the particular refractive index. We simulate the sensor with optimized size of the gold nanorods and fiber parameters for best performance. We have shown that how the size of circular gold nanorod effects the sensitivity of the sensor. The maximum sensitivity exhibited by the sensor is 2200 $nm.\ RIU^{-1}$. From the simulated data, we have found that co-efficient of determination (COD) is very high. Improved sensitivity and high co-efficient of determination are achieved after sensor structural optimization. The proposed sensor structure can be useful in label-free optical platform for bio-sensing applications.

1. Introduction

In the field of nanotechnology, nanorods are one of architecture of nanoscale objects. Usually, the range of their dimension is from 1 to 100 nm. They may be synthesized from metals or semiconducting materials. Standard aspect ratios (length divided by width) are 3-5. In SPR technology, we have number of nobel metals such as gold, silver, aluminum, Cu etc. Therefore the noble metal nanoparticles are known for their ability to support surface plasmon resonance (SPR) along the metal dielectric interface. This makes them strong scatterers and absorbers of visible light, with resonant wavelength peaks that are extremely sensitive to the nanoparticle size, shape, and local environment [1]. These properties, together with advances in nanoparticle technologies, have led to applications in both scientific and technological research [2–4]. Besides fundamental significance, application of SPR has occurred in sensor technology, in the characterization of molecules at a dielectric–metal interface [5], in plasmonic devices [6] etc. In literature, various nano-particle based SPR sensors have been investigated and their light enhancement in the sensor has been analyzed in terms of various performance parameters.

Zeng et al. 2013 [7] proposed a sensing configuration for enhancing light transmission in graphene and gold nanorods based SPR sensor. For sensing performance, Finite element method has been used to optimize the number of grapheme layers and gold nanorod aspect ratio (ratio of the width to the height). Fresnel equations are also described

analytically for the proposed models. They found that improved sensitivity up to 10^6 degree-RIU^{-1} can be obtained by the combinations of graphene monolayer and Au layer, with coupling of localized SPR of gold nanorod (AR = 2). Cao et al. 2012 [8] developed a localized plasmonic sensor based on gold nanorod. The sensor was developed by using multimode fiber and the Au nanorod surface was functionalized with human IgG. This sensor detects the anti-human IgG. The resonant wavelength shift of gold

* Corresponding author.
E-mail address: opticsresearch99@gmail.com (S. Singh).

https://doi.org/10.1016/j.ijleo.2019.02.064
Received 26 November 2018; Received in revised form 2 February 2019; Accepted 15 February 2019